

**ELECTROCHEMICAL REDUCTION OF  
CO<sub>2</sub>**

BY

**MUHAMMAD IRFAN MALIK**

A Thesis Presented to the  
DEANSHIP OF GRADUATE STUDIES

**KING FAHD UNIVERSITY OF PETROLEUM & MINERALS**

DHAHRAN, SAUDI ARABIA

In Partial Fulfillment of the  
Requirements for the Degree of

**MASTER OF SCIENCE**

In

**CHEMICAL ENGINEERING**

**NOVEMBER, 2015**

KING FAHD UNIVERSITY OF PETROLEUM & MINERALS

DHAHRAN- 31261, SAUDI ARABIA

**DEANSHIP OF GRADUATE STUDIES**

This thesis, written by **MUHAMMAD IRFAN MALIK** under the direction his thesis advisor and approved by his thesis committee, has been presented and accepted by the Dean of Graduate Studies, in partial fulfillment of the requirements for the degree of **MASTER OF SCIENCE IN CHEMICAL ENGINEERING.**



Dr. Basim A. Abussaud  
(Advisor)



Dr. Mohammed Ba-Shammakh  
Department Chairman



Dr. Khaled, Mazen Mohammad  
(Member)



Dr. Salam A. Zummo  
Dean of Graduate Studies



Dr. Zuhair Omar Malaibari  
(Member)

16/12/15  
Date

© Muhammad Irfan Malik

2015

## **DEDICATION**

I dedicate my work to my Late Grandmother and her sisters. I also dedicate this work to my teachers, relatives and friends who passed away. May Allah place them in Jannatul Firdous. Ameen |

## ACKNOWLEDGMENTS

I express my gratitude and praise to ALMIGHTY ALLAH, the creator of universe, who is beneficent and merciful, guided us in difficult and congeal circumstance, who endowed us with the will to complete this project. Great respect our Holy Prophet Hazrat Muhammad (PBUH), who taught us to learn till lap of grave.

I am highly thankful to Department of Chemical Engineering, King Fahd University of Petroleum and Minerals (KFUPM), Saudi Arabia for awarding me scholarship to pursue my MS.

I express my sincere thanks to my advisor Dr. Basim Abussaud for supervising my research. Without his technical and moral support I would not have been able to complete my work. My heartiest thanks to my committee members: Dr. Mazen M. Khaled and Dr. Zuhair Omar Malaibari for their useful comments and suggestion. I am thankful to Dr. Shaikh Abdur Razzak and Dr. Umer Mehmood for providing me the laboratory facilities and helped me in simulation work. I would also like to thank Muhammad Yasir Khan for guiding me in my research.

Last but not least, thanks to my grandmother, teachers, parents, brothers, sisters and friends in my country who prayed day and night for my success.

# TABLE OF CONTENTS

<b>ACKNOWLEDGMENTS</b> .....	<b>v</b>
<b>TABLE OF CONTENTS</b> .....	<b>vi</b>
<b>LIST OF TABLES</b> .....	<b>ix</b>
<b>LIST OF FIGURES</b> .....	<b>x</b>
<b>LIST OF ABBREVIATIONS</b> .....	<b>xiii</b>
<b>ABSTRACT</b> .....	<b>xiv</b>
ملخص الرسالة.....	<b>xvi</b>
<b>CHAPTER 1 INTRODUCTION</b> .....	<b>1</b>
<b>CHAPTER 2 LITERATURE REVIEW</b> .....	<b>6</b>
<b>2.1 CO<sub>2</sub> reduction methods</b> .....	<b>6</b>
2.1.1 Hydrogenation of CO <sub>2</sub> /CO .....	6
2.1.2 Electrochemical CO <sub>2</sub> reduction.....	10
2.1.3 Photochemical reduction of CO <sub>2</sub> : .....	19
<b>2.2 A detailed review of electrochemical CO<sub>2</sub> reduction</b> .....	<b>22</b>
<b>2.3 Mechanism of electrochemical CO<sub>2</sub> reduction to hydrocarbon and alcohols</b> .....	<b>31</b>
<b>2.4 Objective</b> .....	<b>41</b>
<b>CHAPTER 3 RESEARCH METHODOLOGY</b> .....	<b>43</b>
<b>3.1 Materials and Preparation</b> .....	<b>43</b>
3.1.1 Impregnation of cupric oxides on carbon nanotubes .....	44
3.1.2 Impregnation of cuprous oxides on carbon nanotubes .....	45
<b>3.2 Material Characterization</b> .....	<b>45</b>

3.2.1	Thermogravimetric Analysis (TGA).....	46
3.2.2	Scanning Electron Microscopy (SEM).....	46
3.2.3	X-ray diffractogram (XRD) .....	47
3.2.4	Transmission Electron Microscopy (TEM) .....	47
3.2.5	Raman Spectroscopy.....	48
<b>3.3</b>	<b>Electrochemical Setup.....</b>	<b>48</b>
3.3.1	Working electrode Preparation.....	50
3.3.2	Design of electrochemical Cell .....	51
3.3.3	Nafion 117 Membrane .....	53
3.3.4	Cupric oxide and cuprous oxide based working electrodes.....	54
<b>3.4</b>	<b>Electrochemical Test .....</b>	<b>55</b>
3.4.1	Linear sweep voltammetry.....	55
3.4.2	Chronoamperometry .....	56
<b>Chapter 4 Results and Discussion .....</b>		<b>58</b>
<b>4.1</b>	<b>Physical Characterization .....</b>	<b>58</b>
4.1.1	SEM and EDX analysis.....	58
4.1.2	Energy dispersive X-ray (EDX) analysis .....	65
4.1.3	X-ray diffraction Analysis (XRD Analysis).....	69
4.1.4	Thermogravimetric analysis (TGA) .....	72
4.1.5	Raman Spectroscopy .....	73
4.1.6	N <sub>2</sub> adsorption isotherms .....	75
4.1.7	Transmission electron microscopy (TEM) .....	76
<b>4.2</b>	<b>Linear sweep voltammetry for carbon nanotubes loaded Cu<sub>2</sub>O based electrocatalyst .....</b>	<b>79</b>
<b>4.3</b>	<b>Linear sweep voltammetry for carbon nanotubes loaded CuO based electrocatalyst .....</b>	<b>81</b>
4.3.1	Comparative analysis of Linear Sweep Voltammetry results based on 30% Copper oxides loading on CNT.....	82
<b>4.4</b>	<b>Faradic Efficiency .....</b>	<b>83</b>
4.4.1	Detailed analysis of Faradic Efficiency results.....	85
<b>4.5</b>	<b>Chronoamperometry Analysis.....</b>	<b>86</b>
<b>CHAPTER 5 Density Functional Theory .....</b>		<b>88</b>
<b>5.1.</b>	<b>Quantum Mechanical Modeling .....</b>	<b>88</b>
<b>5.2.</b>	<b>The Khon-Sham molecular orbital (MO) model .....</b>	<b>89</b>
<b>5.3.</b>	<b>Simulation Method.....</b>	<b>90</b>

<b>Chapter 6 Conclusion &amp; Recommendations .....</b>	<b>93</b>
<b>6.1 Conclusion .....</b>	<b>93</b>
<b>6.2 Recommendations .....</b>	<b>94</b>
<b>References .....</b>	<b>95</b>
<b>Appendix .....</b>	<b>106</b>
<b>Internal standard method of calibration.....</b>	<b>106</b>
<b>Vitae .....</b>	<b>108</b>

## LIST OF TABLES

Table 2-1: Periodic table of elements tested for CO <sub>2</sub> reduction at -2.2 V vs SCE in .05M Potassium bicarbonate solution KHCO <sub>3</sub> at low temperature condition [44] ..	13
Table 2-2: Current efficiency for CO <sub>2</sub> reduction products at -2.2V vs SCE in potassium bicarbonate (.05M KHCO <sub>3</sub> )[44].....	15
Table 2-3: Summery of different electrocatalyst and their role on current density and faradic efficiency .....	38
Table 5-1: Calculated Band gaps for Cu <sub>2</sub> O and Cu <sub>2</sub> O supported CNTs.....	90

# LIST OF FIGURES

Figure 2-1: IR adsorption spectra of adsorb species methoxy and formats on catalyst surface of clean Cu(111) and ZnCu <sup>+</sup> (111) during formation of methanol by hydrogenation at 343k and 1 atm[38] .....	9
Figure 2-2: Development process of hole (h <sup>+</sup> ) and e <sup>-</sup> upon UV irradiation by photo catalyst [51].....	19
Figure 2-3: Time dependence effect on methanol formation for titanium and titanium loaded Cu [57].....	21
Figure 2-4: Structure of Cu <sub>2</sub> O [66].....	29
Figure 3-1: Working electrode.....	49
Figure 3-2: Platinum counter electrode.....	49
Figure 3-3: Reference Ag/AgCl electrode .....	50
Figure 3-4: Poly carbonate made electrochemical cell with two compartments separated by nafion membrane for electrochemical reduction of CO <sub>2</sub> .....	53
Figure 4-1: SEM image of 10% CuO supported CNT catalyst .....	59
Figure 4-2: SEM image of 20% CuO supported CNT catalyst .....	60
Figure 4-3: SEM image of 30% CuO supported CNT catalyst .....	60
Figure 4-4: SEM image of 40% CuO supported CNT catalyst .....	61
Figure 4-5: SEM image of 50% CuO supported CNT catalyst .....	61
Figure 4-6: SEM image of 10% Cu <sub>2</sub> O supported CNT catalyst.....	63
Figure 4-7: SEM image of 20% Cu <sub>2</sub> O supported CNT catalyst.....	63
Figure 4-8: SEM image of 30% Cu <sub>2</sub> O supported CNT catalyst.....	64
Figure 4-9: SEM image of 40% Cu <sub>2</sub> O supported CNT catalyst.....	64

Figure 4-10: SEM image of 50% Cu <sub>2</sub> O supported CNT catalyst .....	65
Figure 4-11: EDX image of 10% Cu <sub>2</sub> O supported CNT catalyst .....	66
Figure 4-12: EDX image of 40% Cu <sub>2</sub> O supported CNT catalyst .....	67
Figure 4-13: EDX image of 20% CuO supported CNT catalyst .....	68
Figure 4-14: EDX image of 50% CuO supported CNT catalyst .....	69
Figure 4-15: XRD pattern for CuO supported CNT catalyst .....	71
Figure 4-16: XRD pattern for Cu <sub>2</sub> O supported CNT catalyst.....	71
Figure 4-17: Thermogravimetric curves for Cu <sub>2</sub> O supported CNT catalysts .....	73
Figure 4-18: Raman spectra of CuO supported CNT catalysts.....	74
Figure 4-19: Raman spectra of Cu <sub>2</sub> O supported CNT catalysts .....	75
Figure 4-20: Adsorption-desorption isotherm for CNT without loading .....	76
Figure 4-21: TEM image of 10% CuO supported CNT catalyst .....	77
Figure 4-22: TEM image of 50% CuO supported CNT catalyst .....	77
Figure 4-23: TEM image of 10% Cu <sub>2</sub> O supported CNT catalyst.....	78
Figure 4-24: TEM image of 50% Cu <sub>2</sub> O supported CNT catalyst.....	78
Figure 4-25: LSV profiles for Cu <sub>2</sub> O supported CNT in CO <sub>2</sub> saturated electrolyte .....	80
Figure 4-26: LSV profiles for CuO supported CNT in CO <sub>2</sub> saturated electrolyte.....	82
Figure 4-27: LSV profiles for CNT loaded with 30% Cu <sub>2</sub> O and CuO in CO <sub>2</sub> saturated electrolyte.....	83
Figure 4-28: Faradic Efficiency of Methanol formation.....	84
Figure 4-29: Current responses for Cu <sub>2</sub> O supported CNTS at constant potential in CO <sub>2</sub> saturated electrolyte .....	87
Figure 5-1: Optimized structure of Cuprous oxide (Cu <sub>2</sub> O) P type semiconductor .....	91

Figure 5-2: Optimized structure of Cu<sub>2</sub>O supported carbon nanotube ..... 92

## LIST OF ABBREVIATIONS

<b>CNTs</b>	:	Carbon nanotubes
<b>Pt</b>	:	Platinum
<b>Ag/AgCl</b>	:	Silver/Silver Chloride
<b>LSV</b>	:	Linear Sweep Voltammetry
<b>DFT</b>	:	Density Functional Theory
<b>SHE</b>	:	Standard Hydrogen Electrode
<b>XRD</b>	:	X-ray-Diffraction
<b>TEM</b>	:	Transmission Electron Microscopy
<b>EDX</b>	:	Energy Dispersive X-ray
<b>TGA</b>	:	Thermo Gravimetric Analysis
<b>SEM</b>	:	Scanning Electron Microscopy
<b>MWCNT</b>	:	Multi walled Carbon Nanotubes
<b>HER</b>	:	Hydrogen Evolution Reaction
<b>CuO</b>	:	Cupric Oxide
<b>Cu<sub>2</sub>O</b>	:	Cuprous Oxide
<b>ACF</b>	:	Activated Carbon Fiber
<b>SCE</b>	:	Standard Calomel Electrode

## ABSTRACT

Full Name : [Muhammad Irfan Malik]  
Thesis Title : [Electrochemical Reduction of CO<sub>2</sub>]  
Major Field : [Chemical Engineering]  
Date of Degree : November, 2015]

Electrochemical reduction of CO<sub>2</sub> was carried out to produce high-value energy fuel with the aim of reducing CO<sub>2</sub> efficiently. However, the primary product of CO<sub>2</sub> reduction was hydrogen evolution at high overpotential. The focus of our study is to reduce CO<sub>2</sub> with high current density in the presence of most effective and stable electrocatalyst at room temperature and pressure. A two - compartment electrochemical cell in the presence of copper oxides based electrocatalyst was used at different loading on the surface of carbon nanotubes. Different parameters such as the percentage of copper oxides loading and the voltage applied was carefully examined. Chronoamperometry analysis and faradic efficiency of methanol formation along with DFT simulation was studied, to investigate best performance catalyst.

Prepared catalyst were characterized by SEM, TEM, EDX, XRD, TGA and Raman spectroscopy to ensure uniform deposition of catalyst on carbon nanotubes. Loading of copper oxides on carbon nanotubes have a significant influence on the performance of the catalyst. Cuprous oxide (Cu<sub>2</sub>O) supported CNTs enhanced surface area, uniformity and stability of electrode. Firm attachment of cuprous oxide (Cu<sub>2</sub>O) sites on defects of carbon nanotubes facilitated electron transferring on working electrode surface, it also favors adsorption of CO<sub>2</sub> due to the involvement of conduction band electrons Catalyst tested with 30 % cuprous oxide (Cu<sub>2</sub>O) loading was efficient and stable among all the catalysts.

30%  $\text{Cu}_2\text{O}$  impregnated carbon nanotubes have the excellent and most desirable performance to reduce  $\text{CO}_2$ .

|

## ملخص الرسالة

الاسم الكامل: محمد عرفان ملك

عنوان الرسالة: الاختزال الكيميائي لثاني أكسيد الكربون

التخصص: هندسة كيميائية

تاريخ الدرجة العلمية: نوفمبر, 2015

لقد تم تنفيذ الاختزال الكيميائي لثاني أكسيد الكربون بهدف انتاج وقود عالي الجودة مع اختزال  $CO_2$  بكفاءة. ولكن المنتج الاساسي مع اختزال  $CO_2$  هو الهيدروجين في فرق الجهد عال. التركيز الاساسي في هذه الدراسة هو اختزال  $CO_2$  مع تيار عال في وجود خلية كهروكيميائية بكفاءة واستقرار عند درجة حرارة وضغط الغرفة. تم استعمال خلية كهروكيميائية محتوى حجرتان باستعمال محفز كهربي من اكاسيد النحاس بنسب مختلفة على سطح انابيب نانو كربون. لقد تم بعناية اختبار كلا من نسبة اكاسيد النحاس و فرق الجهد. تحليل بواسطة Chronoamperometry وكفاءة فراادي للميثانول بالاضافة الى DFT لبحث افضل كفاءة للمحفز. المحفز المحضر قد تم تشخيصه بواسطة SEM, TEM, EDX, XRD, TGA و Raman spectroscopy لتوكيد تجانس تحميل المحفز على سطح انابيب نانو الكربون. تحميل اكاسيد النحاس على انابيب نانو الكربون لها تأثير كبير على عمل المحفز. انابيب نانو الكربون المدعمة باكسيد النحاس ( $Cu_2O$ ) حسنت من مساحة السطح, اتساق واستقرار القطب الكهربي. الارتباط الوثيق لأكسيد النحاس ( $Cu_2O$ ) على defects انابيب نانو الكربون سهلت من انتقال الالكترتون الى سطح القطب الكهربي. ايضا تحبز ادمصاص  $CO_2$  نسبة الى لإلكترونات الفرقة التوصلي للمحفز مع 30% من ( $Cu_2O$ ) مستقرة وفعالة بالمقارنة مع باقي المحفزات. 30% من ( $Cu_2O$ ) المخصب في انابيب نانو الكربون حازت على افضل فعالية لتنفيذ الاختزال الكيميائي لثاني أكسيد الكربون.

# CHAPTER 1

## INTRODUCTION

CO<sub>2</sub> is a major greenhouse gas that moves to our atmosphere from the lithosphere. Prior to commissioning of industrial revolutions in the late 60s, concentration of CO<sub>2</sub> in the atmosphere was 350 ppm. However, with a passage of time human activity promoted industrial growth and severely increased CO<sub>2</sub> concentration to 390 ppm recorded in 2011[1], [2].

In order to cop up with CO<sub>2</sub> emission problems, world scientists realized to meet on platform and to propose strict measurement to mitigate CO<sub>2</sub> emission. It was decided in Kyoto protocol to meet with average rise up temperature of 2°C on Earth [2].

The Scientists believes that average rise up of temperature on earth will rise if CO<sub>2</sub> concentration rises to 550 ppm, which is severely alarming condition and could disrupt our eco-environment system [3]. Many technologies have been introduced to make an efficient conversion of CO<sub>2</sub> to valuable products, but there are many challenges, to make it profitable and energy efficient with excellent promising results.

Many efforts have been carried by scientists for a transformation of fossil fuel to renewable energy sources for transportation and power generation. The biggest challenge for scientists is to meet with socio, environment, and economic targets. Therefore, carbon capturing has been focused by scientists for past many decades. A squeeze of CO<sub>2</sub> and its role played in the production of valuable and economic fuel allows scientists to research

more in this technology to develop more alternative and cost effective measurements for the production of environmental fuel.

Excessively dependent on fossil fuel highlights reservations about availability of fossil fuel in future and thus renewable energy is considered meaningful option to transform dependency of fossil fuel to alternative renewable energy solutions. In this regard, solar and wind energy were considered most viable option to drive clean and renewable energy demand, but the challenges associated with storage and its utilization requires the development of economically viable technology[4], [5].

Use of CO<sub>2</sub> and its transformation to the valuable products has been competitive. The World relied on most economical and abundantly available resources of fossil fuel such as oil for the past 100 years because the technology to supersede oil utilization is not the economically viable option[6]. One of the most beneficial ways to utilize renewable energy is electrochemical conversion of CO<sub>2</sub> to convert electrical energy into chemical energy[4], [5].

From 1900 to 1980 the electrochemical reduction of CO<sub>2</sub> has been carried on the different amalgamated metals of copper, zinc and mercury. On all these metals, formic acid was recorded as major CO<sub>2</sub> reduction product [7]. However, in 1980s Frese was first who got methanol as chiefly available CO<sub>2</sub> reduction product by using metals of ruthenium and molybdenum but encountered with low current density of 1mA-cm<sup>-2</sup>[8], [9]. In the same decade, Hori investigated CO<sub>2</sub> reduction on Cu made foil and recorded valuable hydrocarbons of ethylene and methane with substantial efficiency. This was promising step of Hori to further guide research on copper base materials. Since then, the copper has been center of interest to find a selective catalyst for CO<sub>2</sub> reduction.[10].

Methanol is commercially produced at large scale from synthetic gas. Different other pathways of selective hydrogenation of methane both in liquid and gas phase have been applied to produce methanol. Eventually, capturing of CO<sub>2</sub> from exhaust of industries and reducing them into useful hydrocarbons and alcohols are considered most effective to preserve nature, and ultimately meet with demand of growing focus on renewable resources and its utilization in cost effective and environmentally clean projects [5].

Methanol is extensively used in different chemical and allied industries. Its salient features of high octane number and low emission of greenhouse gases particularly NO<sub>x</sub> and reputation of cleaned automobile fuel place it as the most demanding chemical across the globe. Methanol is used to produce methyl ter- butyl ether (MTBE) which enhances octane number of gasoline. Almost world's 20 to 50 % methanol is used to produce formaldehyde which is further consume in plastic formation [11].

Scientists investigating more ways to convert CO<sub>2</sub> to methanol and to other chemicals. Saudi Arabia has a large chemical industry set up and high demand of methanol to produce formaldehyde, biodiesel and acetic acid. Electrochemical reduction of CO<sub>2</sub> is one of the attractive route for researchers to convert stable CO<sub>2</sub> to valuable products. Variety of reduction products like methanol, formic acid, ethane and CO have been obtained by using both aqueous and non-aqueous electrolytes, but there is a problem of low current density, high overpotential, low product selectivity and transport problems [12].

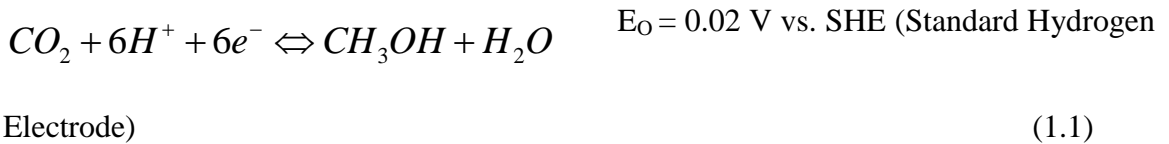
Many electrocatalyst materials essentially metal and its oxides have been developed for good results in terms of high current density, lower overpotential and better hydrocarbons

selectivity. After series of research efforts made by the scientists, they suggested that Cu is the most advantageous electrocatalyst in electrochemical cell which gives promising results with high selectivity of valuable products methane, formaldehyde, and ethane [13].

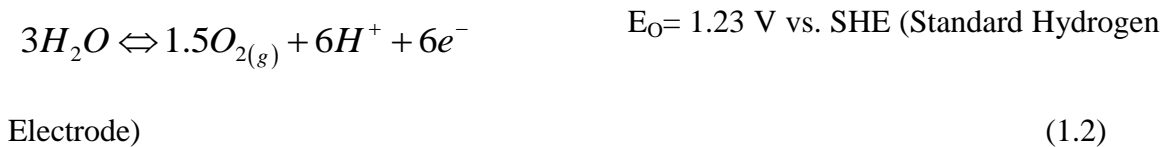
Use of aqueous medium also pushes up hydrogen evolution which adversely affects reduction products and also consumes electrons[14]. Currently, electrochemical conversion of CO<sub>2</sub> is under intensive study. The amount, selectivity and nature of products vary with several factors like catalytic materials, electrode potentials, temperature, electrode material, and electrolyte solutions (aqueous and non-aqueous). Since then, a lot of work has been started to study the behavior of copper lattices and the addition of promoters into oxides of copper [15].

CO<sub>2</sub> reduction potential is only 20mv which is less than the reduction potential of water. That is why, large hydrogen evolution is experienced. Moreover, the excess amount of water in electrolyte produce a large amount of hydrogen gas which consumes a lot of energy and makes the process inefficient [16].

*Cathode :*



*Anode :*





Impregnation of copper on CNTs causes high selectivity of reduction products. It increases the selectivity of alcohols with high chances of C-C chain due to microspores in CNTs.[17].

The most important parameter in CO<sub>2</sub> reduction is electrode materials. Carbon nanotube impregnated with 10%, 20%, 30%, 40%, and 50% copper oxides (CuO, Cu<sub>2</sub>O) on copper foil will increase the selectivity of reduction products and also shifts hydrogen evolution reaction to the more negative potential window. CNT is insoluble in nearly all the solvents which limits its broad spectrum of application. To overcome this difficulty, CNTs are dispersed in 5% nafion solution. Nafion holds hydrophobic and hydrophilic sulfonate groups along with the hydrophobic polymer. CNTs attached with hydrophobic part will disperse in solutions as hydrophilic groups. Nafion is also used in different electrochemical sensors because of its biocompatible nature [18].

Similarly, Sol-Gel system was dispersed in CNTs and synthesized suspensions were used for casting electrode as biosensors [19]–[21]. Addition of modified CNTs to casted electrodes in surfactants/polymers also facilitates diffusion to the electrode surface. Modified SWNT in PVP-Os polymer increased current three -fold [22].

## CHAPTER 2

### LITERATURE REVIEW

#### 2.1 CO<sub>2</sub> reduction methods

Scientists have investigated many methods in past centuries to reduce the CO<sub>2</sub> into desired products like hydrocarbons and alcohols. Initially, hydrogenation of CO<sub>2</sub> at high temperature and pressure was the most attractive route to reduce CO<sub>2</sub>. However, high temperature, pressure and a large amount of consumption of hydrogen made this path costly. Scientists continuously did their efforts to reduce CO<sub>2</sub> at room temperature and pressure and found alternative ways like the solar energy and electrical energy to reduce CO<sub>2</sub> into valuable products. Discovery of most advantageous materials with fewer band gaps, attracts solar and electrical energy to reduce CO<sub>2</sub> into valuable products like formic acid, ethane, methane and methanol [23].

##### 2.1.1 Hydrogenation of CO<sub>2</sub>/CO

Hydrogenation of CO<sub>2</sub> is a two-step process, initially introduced by Franz Fischer and Hans Tropsch in the 1920. In the first step, a mixture of CO<sub>2</sub> and hydrogen is produced by partial oxidation of coal and natural gas. Then in second step process, mixture of CO<sub>2</sub> and hydrogen was converted into valuable products like methanol, formic acid and ethane. Formation of desired products like methanol from synthetic gas (a mixture of CO+H<sub>2</sub>) and traces of CO<sub>2</sub> is defined by stoichiometric number P.

$$P = \frac{\text{mol of } H_2 - \text{mol of } CO_2}{\text{mol of } CO + \text{mol of } CO_2}$$

From above P value, it is clearly shown that mixture of gas, rich with the appropriate ratio of CO<sub>2</sub> and CO would effectively proceed reaction into methanol production. Most optimized value of P for methanol synthesis is reported less than 2, while excess of H<sub>2</sub> leads reaction into undesirable products e.g. ammonia. An adequate mixture of CO/CO<sub>2</sub> would reduce activation energy required for methanol synthesis[24]–[26].

Before World War II, coal was primarily sourced to produce syngas by coal gasification. However, it was not cost effective method and right after World War II, methane was alternatively considered for syngas generation to reduce not only cost but also to reduce impurities in the syngas. Syngas was then directly converted into methanol at high temperature of 300-450°C and at a pressure of (250-350atm). First commercial plant of methanol formation was introduced by BASF(Badische Anilin and Soda Fabrik ) in 1920 [25]. Catalytic hydrogenation of methanol formation is an exothermic reaction. Besides role of water formation as a facilitator to convert mixture of H<sub>2</sub> and CO<sub>2</sub> to CO and H<sub>2</sub>, it may damage active pores site of catalysts and then eventually decrease yield. Many techniques have been employed to reduce this RWGS (reverse water gas shift reaction). In order to obtain higher selectivity, stability and activity on surface catalysts, the catalyst must be synthesized by those materials which reduce this overwhelmed water production and eventually increases methanol formation.[25]

Many catalysts have been tested in past to succeed in dealing with RWGS. Cu, ZnO and different promoters were used as additive to reduce RWGS problem [27].

The role of surface on catalyst particularly affects conversion process in the CO<sub>2</sub> reduction. Therefore, many scientists studied surface characterizations of different metal catalysts and its implication on the CO<sub>2</sub> conversion process and among of all different catalyst tested, it was concluded by scientists that formation of methanol from CO<sub>2</sub> particularly depends upon the surface area of copper made catalysts [28]–[31].

Since then, different forms of copper catalysts were tested and it has been verified that Cu<sup>+</sup> form of copper is most suitable as compared to Cu<sup>0</sup>. When copper was first oxidized into oxides, it shows higher conversion and efficiency to reduce syngas as compared to its pure form [32]. This increase in methanol formation was attributed to high adsorption of methoxy intermediate which forms during the reaction and favors the formation of methanol[29], [33].

Next to active sites, a support plays vital role in formation of methanol. When Cu<sup>+</sup> species loaded on ZnO catalyst, the surprising rise in CO<sub>2</sub> conversion to methanol has been noticed. This rise in methanol synthesis was due to electron pair in ZnO support, which helped to form cation and anion species on the catalyst surface and turns to lead the formation of methanol. ZnO provides an additional active place to adsorb species and transforms intermediate via Cu<sup>+</sup> to form methanol [32], [34].It has been noted that loading of Cu<sup>+</sup> used on ZnO surface did not change surface characteristics of Cu<sup>+</sup>[35].

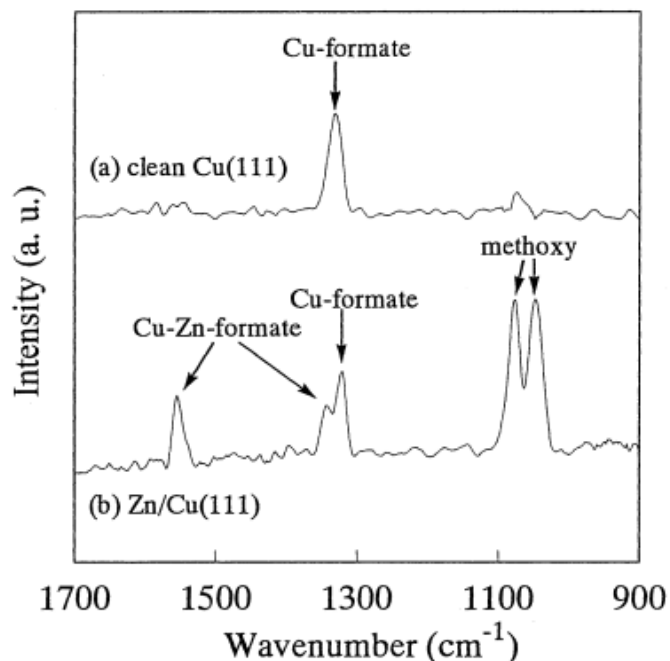


Figure 2-1: IR adsorption spectra of adsorb species methoxy and formates on catalyst surface of clean Cu(111) and ZnCu<sup>+</sup>(111) during formation of methanol by hydrogenation at 343k and 1 atm[35]

Actually, ZnO ensures timely production of methanol and protects the surface of catalyst being poison by sulfur components. As Cu surface is highly sensitive, any impurity in reactant may lead to deactivation of catalyst surface[36].

Other than catalyst surface, operational condition is absolutely necessary for methanol synthesis. Since methanol formation by hydrogenation is an exothermic process, rising reaction temperature will increase particle agglomeration, and also would damage active sites. In addition, high pressure will also lead to damage the surface of the catalyst. That is why, we need catalyst which must be suitable in operational condition of minimum temperature and pressure. If we see thermodynamics, Le Chatlier principle says that

enlargement of temperature will decrease the equilibrium constants and favors high pressure[37].

It is an urgency to shift dependency from non-renewable resources to renewable for generating a high environmentally friendly process for CO<sub>2</sub> reduction. In future, more focus will be on capturing of CO<sub>2</sub> from the exhaust of industries and will be directly converted into methanol. High demand of hydrogen consumption and water intolerance in hydrogenation process, deactivates catalyst surface thus making this process inefficient. To overcome water intolerance in hydrogenation process, electrochemical and photochemical reduction of CO<sub>2</sub> will be used in future to reduce CO<sub>2</sub> at room temperature. These processes takes minimum energy requirement to converts CO<sub>2</sub> into hydrocarbons and alcohols.

### **2.1.2 Electrochemical CO<sub>2</sub> reduction**

Branch of electrochemistry was first studied by Galvani and Volta in late 18<sup>th</sup> century [23]. In electrochemistry, reactions occur at surface of the electrolyte and electrode is driven by external voltage. Electrons are transferred between molecules of electrolyte and anode. It is also termed as oxidation and reduction reactions. Many scientists applied electrochemical techniques and used it as an efficient way to transform raw materials into desired products. One of the principle use of electrochemistry is to reduce CO<sub>2</sub> into valuable hydrocarbons and alcohols. The main advantage of this process is low temperature and pressure which highlight its importance in terms of conservation of energy. Sources of energy supplied to the electrochemical cell are the wind, solar, tidal and many other renewable resources[38].

In this process, water oxidizes at anode surface while reduction of CO<sub>2</sub> takes place at cathode interface. The main challenge in this process is the reduction of water at the cathode. The reduction potential of water at cathode surface is very near to reduction potential of CO<sub>2</sub>. The design of good electrocatalyst which must have higher overpotential for H<sub>2</sub>O reduction is desired and must allow more H<sup>+</sup>(protons) for CO<sub>2</sub> to form methanol [25].

Fisher et al, 1914 have synthesized Cu and Zn electrodes to reduced CO<sub>2</sub> and got formic acid as a product [23]. Similarly up to 1970, different metal and its oxides has been tested to reduce CO<sub>2</sub> to methanol [7].

Different electrolyte solutions that are NaHCO<sub>3</sub>, & K<sub>2</sub>SO<sub>4</sub> were used as a medium along with Pb and Hg electrodes. In these experiments, focus was not only to achieve high electrons transfer during reaction but also to control pH of solutions. The only products obtained were H<sub>2</sub> and formic acid. It was noted in these experiments that current efficiency was surprisingly increased to 100% on Hg electrode but after sometime current density declined to lower values [7].

Methanol forms from CO<sub>2</sub> reduction by intermediates instead of direct conversion because direct reduction of CO<sub>2</sub> to methanol was not achieved by scientists. In this process, formaldehyde as intermediate product was converted to methanol. Direct conversion of formic acid to methanol in CO<sub>2</sub> reduction compartment was not possible due to limited potential range[7]

Right after Paik and his team, Udupa et al., analyzed that by selecting appropriate electrolyte solutions we can raise current density to significant values[39].

Frese was first who successfully reduced  $\text{CO}_2$  to methanol by using molybdenum, ruthenium, InP (Indium phosphide) and GaAs (Gallium arsenide) but with low current density and limited faradic efficiency [8], [40]. Faradic efficiency is then investigated and analyzed by Summers et al., and concluded that faradic efficiency is surface characteristic and can be boosted up by cleaning the surface of electrodes [40].

Hori was a pioneer in successful reduction of  $\text{CO}_2$  to hydrocarbons chiefly, methane and ethylene with good current density. He developed copper as an electrocatalyst and applied different electrolyte solutions of  $\text{NaHCO}_3$ ,  $\text{KHCO}_3$ ,  $\text{NaCl}$ ,  $\text{Na}_2\text{SO}_4$  and their mixtures. Many efforts were carried out to effectively apply copper catalysts to study its surface behavior to convert  $\text{CO}_2$  to methanol [10].

Hori observed in his experiments that  $\text{CH}_4$  was formed while using copper as an electrode. Slightly good faradic efficiency was achieved when Cu surface was cleaned by 7% Nitric acid ( $\text{HNO}_3$ ). Hori also recorded CO as a major product on Au and Ag- based electrodes while hydrogen evolution was dominant on Ni and Fe - based electrodes. Pb, In, Sn and Cd produced formats as major products [10].

After remarkable behavior of Cu - based electrodes, Hori reduced  $\text{CO}_2$  over Cu electrode in bicarbonate electrolytes at different temperatures. He conducted experiments at temperature of  $0^\circ\text{C}$  and significantly recorded rise in faradic efficiency up to 65%, He measured the rise in current density up to  $5\text{mA}\cdot\text{cm}^{-2}$  by increasing temperature to  $40^\circ\text{C}$  and 20 % rise in the formation of ethylene was recorded [41].

Similarly, reduction of  $\text{CO}_2$  was also recorded on glassy carbon electrode in which layers of copper were electrodeposited on GCE (glassy carbon electrode). In these experiments,

CO<sub>2</sub> reduction efficiency was raised to 100% at 8mA-cm<sup>-2</sup> and an amazing rise in the formation of CH<sub>4</sub> and ethylene was noted. Then, efficiency was declined to 79% at 25mA-cm<sup>-2</sup>. These were the highest results produced till that date[42].

**Table 2-1: Periodic table of elements tested for CO<sub>2</sub> reduction at -2.2 V vs SCE in .05M Potassium bicarbonate solution KHCO<sub>3</sub> at low temperature condition [41]**

IVB	VB	VIB	VIIIB	VIIIB	VIIIB	VIIIB	IB	IIB	IIIA	IVA
Ti	V	Cr	Mn	Fe	Co	Ni	Cu	Zn	Al	Si
Zr	Nb	Mo	RE	Ru	Rh	Pd	Ag	Cd	In	Sn
Hf	Ta	W		Os	Ir	Pt	Au	Hg	Tl	Pb

<b>Hydrocarbons</b>
<b>CO</b>
<b>H<sub>2</sub></b>
<b>HCOOH</b>

If we conclude up above discussions, heavy transition metals belong to group IIB, IIIB and IVB produced formates, while IB and VIII are somewhat giving good current efficiency for formic acid and CO. Majority of metal and its oxides from group 4 to group 10 produced hydrogen as major product. Copper which comes in between these

two groups has uniqueness in exhibiting good conducting and electron trapping properties with high adsorption energy of CO<sub>2</sub> which eventually gives high efficiency for CO<sub>2</sub> reduction [43]–[45].

Physical treatments of copper affects the current efficiency and increase hydrocarbons formation. Cleaning with HCL has more significance than HNO<sub>3</sub>. Oxidizing copper by oxygen in the air and then foil was treated with HCL to stabilize Cu<sub>2</sub>O formation to protect Cu<sup>+</sup> from converting to Cu<sup>2+</sup> and Cu<sup>0</sup>. Removing oxides on copper foil prevents precipitation of copper which was believed to deactivate catalyst surface and form cuprous chloride ions in electrolyte[9].

Azuma at al., studied the behavior of 32 metals electrodes over CO<sub>2</sub> reduction. Among all tested metal, Cu made electrode showed highest faradic efficiency toward hydrocarbons (Table 2-2)

.

**Table 2-2: Current efficiency for CO<sub>2</sub> reduction products at -2.2V vs SCE in potassium bicarbonate (.05M KHCO<sub>3</sub>)[41]**

<b>Metal</b>	<b>T (°C)</b>	<b>CH<sub>4</sub></b>	<b>CO</b>	<b>C<sub>2</sub>H<sub>4</sub></b>	<b>C<sub>2</sub>H<sub>6</sub></b>	<b>HCOOH</b>	<b>H<sub>2</sub></b>	<b>Sum</b>
Cd	0	0.015	3.7	0.002	0.0006	55.9	35.7	95
Cd	20	0.0073	1.8	0.001	0.4	35.5	63.2	100
In	0	0.001	3	0.0004	0.0006	70	25	98
In`	20	0.05	14.7	0.0046	0.0067	33.3	56.5	105
Sn	0	0.65	1.4	0.088	0.69	28.5	67.5	99
Pb	0	0.39	0.12	0.008	0.0014	16.5	82.9	100
Pb	20	0.06	0.1	0.001	0.0003	9.9	93.3	103
Tl	0	0.2	0.16	0.003	0.001	53.4	46.2	100
Hg	0	0.0004	0.2	t	t	90.2	9.5	100
Hg	20	0.0035	0.64	0.0002	0.0006	87.6	7.9	96
Zn	0	0.23	9.8	t	nm	19.5	68.1	98
Pd	0	0.083	11.6	0.011	0.014	16.1	73.3	101
Pd	20	0.31	3.2	.061	.078	8.6	90.3	103
<b>Metal</b>	<b>T (°C)</b>	<b>CH<sub>4</sub></b>	<b>CO</b>	<b>C<sub>2</sub>H<sub>4</sub></b> 15	<b>C<sub>2</sub>H<sub>6</sub></b>	<b>HCOOH</b>	<b>H<sub>2</sub></b>	<b>Sum</b>

Mn	0	1.5	0.34	0.093	0.29	0.03	90.9	93
Fe	0	0.07	2.2	t	nm	1.1	89.8	93
Co	0	0.13	0.47	0.0057	0.032	0.85	92.9	94
Zr	0	0.49	0.42	0.021	0.055	t	99.9	101
Nb	0	0.16	0.46	0.0088	0.042	0.03	97.3	98
Mo	0	0.01	t	0.0003	0.0002	0.21	99.9	100
Mo	20	0.031	0.02	0.0008	0.0057	0.19	98.6	99
Ru	0	0.043	0.65	t	t	0.08	99.1	100
Rh	0	0.031	2.5	0.0007	0.0036	1.35	99.3	103
Rh	20	0.053	0.66	0.003	0.011	2.4	99.3	103
Hf	0	0.0046	1.14	0.0003	0.001	0.35	99.2	101
Hf	20	0.0073	0.08	0.0006	0.0005	0.21	100.9	101
Ta	0	0.0015	0.09	0.0015	0.0002	t	100.7	101
Ta	20	0.0039	t	0.0039	0.0001	t	102.2	102
W	0	0.015	0.06	0.0043	0.0022	1.3	96.3	98

<b>Metal</b>	<b>T (°C)</b>	<b>CH<sub>4</sub></b>	<b>CO</b>	<b>C<sub>2</sub>H<sub>4</sub></b>	<b>C<sub>2</sub>H<sub>6</sub></b>	<b>HCOOH</b>	<b>H<sub>2</sub></b>	<b>Sum</b>
W	20	0.055	0.21	0.0022	0.01	2.6	96.9	100
Re	0	0.044	t	0.0002	0.0056	2	99	101
Re	20	0.038	t	0.0002	0.0048	1.4	95.3	97
Cr	0	0.74	0.49	0.05	0.18	0.15	92.2	94
Ir	0	.051	0.52	0.0035	0.0072	1	98.8	100
Ir	20	0.086	t	0.0057	0.015	0.58	100.3	101
Ti	0	t	13.5	t	nm	5.2	69.4	83
Ni	0	0.71	21	0.069	0.18	13.7	61.7	97
Ni	20	0.13	0.6	0.01	0.021	0.1	98.8	100
Ag	0	14	40.7	0.0052	0.013	20.5	32.6	95
Ag	20	1.1	30	0.009	0.0027	16	50	98
Au	0	t	16.9	t	nm	10.3	73.4	101
Cu	0	24.7	16.5	6.5	0.015	3	49.3	100
Cu	20	17.8	5.4	12.7	0.039	10.2	52	98

<b>Metal</b>	<b>T (°C)</b>	<b>CH<sub>4</sub></b>	<b>CO</b>	<b>C<sub>2</sub>H<sub>4</sub></b>	<b>C<sub>2</sub>H<sub>6</sub></b>	<b>HCOOH</b>	<b>H<sub>2</sub></b>	<b>Sum</b>
C	0	0.11	t	0.0064	0.007	0.31	92.5	93
Al	0	0.012	T	0.0002	0.0004	0.78	95.7	96
Si	0	0.025	0.08	t	t	1.6	102.2	104
V	0	0.02	1.3	t	nm	2.6	91.9	95

\*nm= Not measured.

\*t=Traces.

### 2.1.3 Photochemical reduction of CO<sub>2</sub>:

Conversion of CO<sub>2</sub> to methanol at high - temperature 400-800K and pressure 2-12 MPa knock scientists to find alternative possible methods of low temperature and pressure to reduce CO<sub>2</sub> [46], [47]. Photochemical reduction of CO<sub>2</sub> in the presence of sun light open new ways to reduce CO<sub>2</sub> under non severe conditions. Many photocatalysts has a low band gap of energy and produce electron and proton upon absorption of sun light. These electrons and protons help to reduce CO<sub>2</sub> into favorable chemicals like formic acid, methane and methanol.[48]

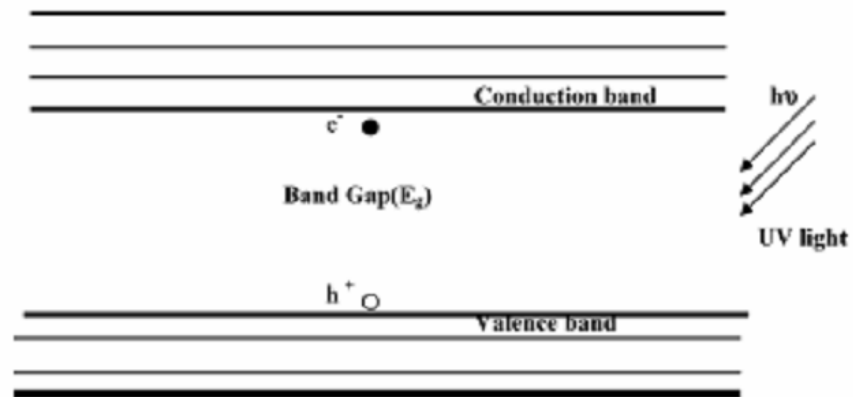


Figure 2-2: Development process of hole (h<sup>+</sup>) and e<sup>-</sup> upon UV irradiation by photo catalyst [48].

First TiO<sub>2</sub> based photochemical cell was introduced in the early seventies as anode while platinum metal was used as cathode. Electrons were excited in unit and thus oxygen was generated on anode and hydrogen produced at cathode side[49].

Different photocatalysts were tested in the 1970. Metals were irradiated but has given only formic acid as a product. Most of the metals produced 2 electrons. However, when

P-gallium phosphide is tested, it goes ahead and produces more than two electrons and ultimately produced formaldehyde and methanol with high over potential[50].

Different surface chemistry of active sites were discussed to investigate better catalyst for CO<sub>2</sub> reduction. During studies, electron hole - pair generation, surface adsorption of intermediate, product separation and then regeneration of active sites were investigated. Ti<sup>+3</sup> ions role in surface adsorption of water has been discussed while TiO<sub>2</sub> and SrTiO<sub>3</sub> were used as catalyst to produce methane and other hydrocarbons [51]. Similarly, other metals catalyst SiC, GaP, ZnO and TiO<sub>2</sub> were tested and behavior of hydrocarbons formation and methanol were studied [52].

One of the main challenge in CO<sub>2</sub> reduction is to convert CO<sub>2</sub> to methanol. We need 6e<sup>-</sup> to reduce C<sup>+4</sup> of CO<sub>2</sub> into C<sup>-2</sup> of methanol. As main drivers in methanol synthesis is CO<sub>2</sub> and H<sup>+</sup>, these radicals produced by absorption of light which transfer electron from valence band to conduction band. Those semiconductors which have low band gap would efficiently reduce intermediate species. Due to low band gap of TiO<sub>2</sub> (3.2 eV), it is considered best photo catalyst for CO<sub>2</sub> reduction. However, despite low band gap of TiO<sub>2</sub>, low production efficiency was achieved for methanol formation. When TiO<sub>2</sub> suspension mixed with copper, this not only provides active surface for CO<sub>2</sub> reduction but at same time it stables Ti<sup>+3</sup> active sites. Similarly, methanol formation was doubled with addition of bicarbonate [53].

Titanium and Cu loaded titanium were studied to investigate methanol formation. Cu was loaded on titanium at different percentage from 1 to 6%. Titanium loaded with 2% Cu had best possible performance by giving methanol 118μmol/g of catalyst on 254nmUV

irradiation. Titanium surface was loaded with several oxidation states of copper and it was concluded that Cu (I) species actively reduced CO<sub>2</sub> to methanol. Cu (I) actually catch electron and protects recombination of hole pairs which created during irradiation[54].

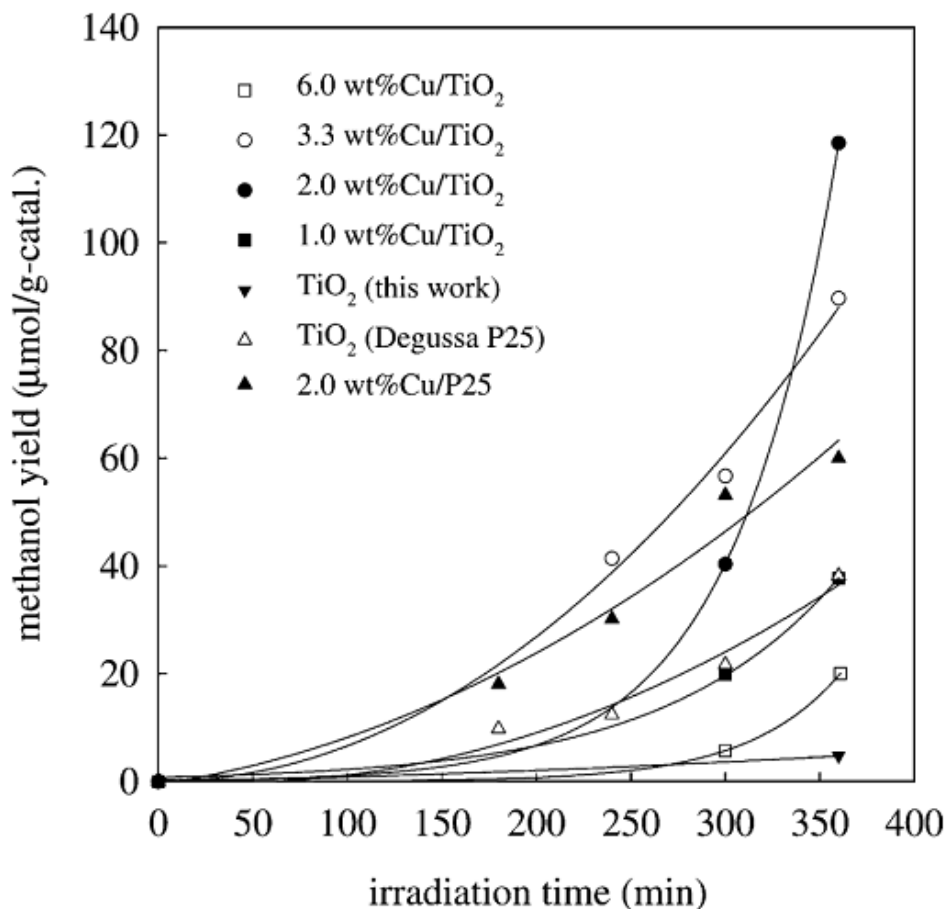


Figure 2-3: Time dependence effect on methanol formation for titanium and titanium loaded Cu [54].

Cu<sub>2</sub>O loaded TiO<sub>2</sub> serves as a best catalyst for methanol generation, but electron hole-pair recombination limit selectivity and efficiency of the process. If we want best photocatalyst for CO<sub>2</sub> reduction, we need the large surface area of support to absorb UV light and provides sufficient energy to conduct reaction [46].

## 2.2 A detailed review of electrochemical CO<sub>2</sub> reduction

In 1983 Hori was studying the electrochemical reduction of CO<sub>2</sub> to investigate selective materials for high valuable hydrocarbons fuel. After series of experiments, he concluded that Cu electrode has high selectivity towards hydrocarbons and alcohols. While using other metals, Ni, Au, Ag, Zn, Pd and Ga electrodes produced CO as the major product. Similarly, HCOO<sup>-</sup> and H<sub>2</sub> formed on Ti, Cd, Sn, In, Hg and Pb made electrodes. Some of metals Fe, Ni, Ti and Fe produced hydrogen as the major product [12].

Hori studied deactivation of copper electrode during reduction of CO<sub>2</sub> and analyzed that rapid disappearance of C<sub>2</sub>H<sub>4</sub> and CH<sub>4</sub> as products was due to Cu deactivation. The presence of Zn<sup>+2</sup>, Fe<sup>+2</sup> and trimethylamine in aqueous KHCO<sub>3</sub> electrolyte damaged electrode surface. Adsorption of Zn<sup>+2</sup>, Fe<sup>+2</sup> formed monolayer coverage on the surface. Prior to Hori experiments, it was assumed that intermediated and end products formed in the cell were adsorbed on electrode surface and deactivate electrode active sites. Hori concluded in his experiments that electrolysis of cell with Pt black electrode removed metal ions and protects surface of Cu. [13]

During CO<sub>2</sub> reduction, initially CO<sub>2</sub> is reduced to CO, which on further reductions reduced to hydrocarbons and alcohols. CH<sub>4</sub> was the major product obtained with high current density in an aqueous medium of KHCO<sub>3</sub> while C<sub>2</sub>H<sub>4</sub> and C<sub>2</sub>H<sub>5</sub>OH were obtained in dilute KHCO<sub>3</sub>. Some of intermediates of acetaldehyde and propionaldehyde formed in the process due to the reduction of ethanol and n- propanol. CO adsorbed as anion on the electrode is intermediate for the production of hydrocarbons and alcohols. Hori tested different kinds electrode made of Pt, Pd, Au, Zn and Ag. These metals were able to

reduce adsorbed CO to alcohols and hydrocarbons. However, Cu was best among all of them which reduced CO<sub>2</sub> efficiently. After Hori experiments, scientists modified Cu made electrode to achieve further high energy efficiency .[15]

Adsorption of hydrogen depends upon the structure of electrodes. In the case of smooth surface, two hydrogen atoms adsorbed on the surface while on rough surface, atomic hydrogen adsorbed on Cu surface likewise on Ni and Fe made electrodes. These rough surfaces favorably adsorb hydrogen to produce space for adsorption [13], [15].

CH<sub>4</sub> and methanol formations on Cu (III) electrode proceeds in different ways. Hydrogenation of carbon of CO leads to the formation of methanol and forms formyl anion which further converted by series reactions with protons to form formaldehyde CH<sub>2</sub>O and methoxy CH<sub>3</sub>O. These intermediates are primary reasons to reduce CO<sub>2</sub> to hydrocarbons and alcohols, the presence of ZnO supports hydrogenation of carbon to enhance intermediates of CH<sub>2</sub>O and CH<sub>3</sub>O responsible for methanol formation while hydrogenation of O in CO held responsible for the formation of CH<sub>4</sub>. Intermediate C-OH formed can have further steps where it deoxygenated to form methane. Both Cu and Cu /ZnO hydrogenate the O of the CO, but Cu/ZnO also has greater ability to hydrogenate C of CO and forms large amounts of formaldehyde and methoxy intermediates. [16]

Hydrogen absorption affects CO<sub>2</sub> reduction. Particularly, in case of the HCOOH which has higher faradic efficiency on Cu/Pd+ H electrode than Cu/Pd electrode. This high faradic efficiency of HCOOH was due to porous structure and cracks present in deposited copper, which result in frequent charging and discharging in pores surface of electrode. This provided the basis for other scientists to open the door for selective materials to reduce CO<sub>2</sub> . [55]

It was investigated by series of activities that Cu is most advantageous electrocatalyst in an electrochemical cell, which gives promising results with high selectivity of valuable hydrocarbons like methane, ethane, and ethylene. Since then, a lot of work started to study the behavior of different copper crystals and the role of promoters into oxide of copper [56].

High current density is essential to obtain a high rate of CO<sub>2</sub> reduction products. Increasing the gas pressure of CO<sub>2</sub> in the aqueous system rises the product rates. High-pressure system with the use of CO<sub>2</sub>-methanol as a medium was also found to increase the rate of reactions. Use of gas diffusion electrodes, result in the high rate of CO<sub>2</sub> reduction. These gas diffusion electrodes contain nano size pore structures to enhance reaction on the surface of the electrode and precedes CO<sub>2</sub> reduction. High porous supported materials like activated carbon fibers with Fe and Ni under high pressure and metal oxides with Cu electrocatalyst were tested and encouraging results were found for both in terms of current density. These experimental results opened doors for a new era of research on electrocatalyst. [57]

Electrochemical reduction of CO<sub>2</sub> on Cu electrodes was carried out at an ambient temperature and pressure in an aqueous solution of 0.1 mol .dm<sup>-3</sup> of KHCO<sub>3</sub>. It was investigated that changing a small amount of electrode potential has severely affected CO<sub>2</sub> reduction products. Faradic efficiency was measured for CO<sub>2</sub> reduction products over variable electrode potential from -1.75 V to small negative potential of -1.35 V. Highest recorded product efficiencies were 32% HCOO<sup>-</sup>, 33%CO, 41% C<sub>2</sub>H<sub>4</sub> and 39% CH<sub>4</sub> at potential of -1.40, -1.52, -1.58 and -1.70 respectively. These variations clearly indicate the dependence of CO<sub>2</sub> reduction products over electrode potential. [57]

Many scientists examined the electrochemical conversion of CO<sub>2</sub> and investigated many factors while reducing CO<sub>2</sub>. Selectivity of CO<sub>2</sub> reduction products increased on hydrogen storing materials Pd with slight modifications of other materials. Using hydrogen storing materials actually suppressed hydrogen evolution and increase production of CH<sub>3</sub>OH, CH<sub>4</sub> and HCOOH. [57]

Similarly, it was investigated that hydrogen adsorption certainly effects CO<sub>2</sub> reduction on Pd electrodes. Cu was used as a modifying material with Pd and Pd+H electrode to enhance CO<sub>2</sub> reduction. The main target in these studies was to measure the effect of hydrogen reactivity on Pd modified electrodes. [58]

Brady and petit studied gaseous reactions of diazomethane on metal surfaces of Cu, Ru, Pd, Fe, and Ni. CH<sub>2</sub>N<sub>2</sub>. H<sub>2</sub> mixture was passed over metal surfaces and formation of C<sub>2</sub>H<sub>4</sub> and N<sub>2</sub> was experienced. It is concluded in these experiments that the formation of CO<sub>2</sub> reduction products was due to adsorbed intermediates CH<sub>2</sub>, which polymerized on the surface with adsorbed hydrogen (metal hydride bond). However, in the case of Cu, chemically adsorbed hydrogen was not readily dissociated and did not initiate polymerization reaction. [58]

NO present in feed does not affects CO<sub>2</sub> reduction products. However, SO<sub>2</sub> significantly affects reduction products. Removal of SO<sub>2</sub> is essential for the production of C<sub>2</sub>H<sub>4</sub> in the product line. Combination of Cu-Rochelle salt and 10 %NaBH<sub>4</sub> solid polymer electrolyte poisoned catalyst because of supporting solvent absence. Major reduction products obtained in these experiments were C<sub>2</sub>H<sub>4</sub>, HCOOH and CO. Recorded current efficiency

for reduced products was 19 and 27%. At the end of these experiments. It was concluded that CO<sub>2</sub> in feed stream must have a concentration of 30%. [59]

Cd, Sn, Pb, In, and Hg electrodes produced formic acid as the main product. However, Zn, Ag, Au and Pd electrodes produced CO. There are some metals Pt, Ni, Fe, Rh, Mo, Ti which have poor performance in reduction of CO<sub>2</sub>, these metals do not reduce CO<sub>2</sub> and as a result high hydrogen evolution was experienced. At end of all these experiments, it was concluded that CO<sub>2</sub> flow rate to electrodes and current density plays vital role in product selectivity of CO<sub>2</sub> reductions. [60]

CO<sub>2</sub> reduction on Au electrode was carried out in an electrochemical cell. The current efficiency was noted to be 90% for CO, and concluded that mainly reduced product were CO and H<sub>2</sub> on Au made electrode. CO formed by using this type of electrolyte was clean and compact. [61]

Many metal oxides (ZnO<sub>2</sub>, ZnO, TiO<sub>2</sub>, Al<sub>2</sub>O<sub>3</sub>, and Nb<sub>2</sub>O<sub>5</sub>) with high- pressure CO<sub>2</sub> gas were analyzed under CO<sub>2</sub> - reagent grade methanol solution, in which tetraethyl ammonium salt was used as supporting electrolyte. These metal oxides without the support of Cu exhibit a very low rate of reduction and mainly hydrogen was produced during these reactions. However, with the support of Cu, an increase in selectivity of CO<sub>2</sub> reduction products was experienced. The smaller addition of Cu 5% has little progress but with an increase in Cu contents upto 50 %, rise in selectivity was experienced with a high rate of products that is 44% HCOOH and 4.4 % CO. Methane and ethylene were also analyzed as products. Among all tested metals, higher current efficiency of hydrocarbons was experienced for Cu/ZrO<sub>2</sub> electrode. [62]

Similarly, electrocatalysts of Ni and Fe were electrochemically tested and analyzed in comparison with activated carbon as support. In the absence of electrocatalyst materials, activated carbon fibers were used as an electrode and the major product found was hydrogen evolution. In the presence of non-activated carbon support with electrocatalyst CF/Ni, CF/Fe, selectivity and rate of products were not encouraging enough but with the support of activated carbon (ACF/Ni, ACF/Fe), surprising rise in terms of partial current density from 5 to 15 mA cm<sup>-2</sup> was recorded at -1.8 V vs. SCE (Standard Calomel Electrode). Similarly, the addition of different carbon black matrix XC-72 and acetylene black (AB) in electrocatalysts of Ni and Fe were also tested as support. Partial current density of CO<sub>2</sub> reduction was continuously increased with an increase in electrode potential while for XC-72 partial current density reached to a maximum at -2.0 V vs SCE and remained same with further increase in electrode potential. Direct relationship with voltage in the case of acetylene black (AB) was due to hydrophobic properties of acetylene black (AB), resulted in higher adsorption of CO<sub>2</sub> on the surface of electrode. [62]

Reduction of CO<sub>2</sub> under CO<sub>2</sub> - methanol medium at ambient temperature and high pressure of 40 atm is also reported in the literature. Different gas phase products like H<sub>2</sub>, C<sub>2</sub>H<sub>4</sub>, and CH<sub>4</sub> were analyzed while HCOOCH<sub>3</sub> and CH<sub>3</sub>OCH<sub>2</sub>OCH<sub>3</sub> were also detected as liquid products. It was reported during experiments that reduction of CO<sub>2</sub> increased with the rise in CO<sub>2</sub> gas pressure and highest value was reported at -1.3V. While at 40 atm, sharp rise in reduction efficiency was achieved. The CO<sub>2</sub> reduction was increased with potential in the negative direction. This behavior was contrary to results showed at 1 atm where the CO<sub>2</sub> reduction was decreasing with the increase of potential in the negative

direction. Increase in current density at 40 atm with potential up to -2.3 V clearly indicates that CO production is not mass transport limited. On other hands,  $\text{HCOOCH}_3$  and hydrogen evolution became diffusion limited at -1.8 and -1.4V. [62]

To further understand the surface characteristics of copper foil, Hori analyzed that  $\text{CO}_2$  efficiently reduced on Cu (111), Cu (100) and Cu (110) in bicarbonate electrolyte at room temperature. Ethylene produced on Cu (100) and Cu (111) produced  $\text{CH}_4$  while Cu (110) formed both of these product [29]. The relationship between surface characteristic of copper was analyzed further. As the copper surface is highly sensitive to oxygen absorbed in the cell, any presence of oxygen would readily adsorb on the copper surface and will deteriorate copper surface. It is noted that presence of oxygen defects on the copper surface will rise selectivity of hydrocarbon.  $\text{Cu}_2\text{O}$  exhibits higher adsorption energy than Cu and thus makes more adsorption of CO and ultimately gives higher selective products[63].

It was also inspected that Cu (I) species in  $\text{Cu}_2\text{O}$  directly reduced  $\text{CO}_2$  to methanol.  $\text{Cu}_2\text{O}$  foil successfully reduced  $\text{CO}_2$  to only methanol, instead of hydrocarbons. [31]

$\text{Cu}_2\text{O}$  foil was also tested and prepared by air oxidized method, anodized method and by thermally oxidized in air. Among all of them, anodized copper based foil has maximum current density of  $33\text{mA}/\text{cm}^{-2}$  at room temperature. [64]

It was reported that  $\text{CO}_2$  reduction potential to methanol was 20mV vs SHE but copper oxides surface reduced  $\text{CO}_2$  to methanol at more positive potential and open large potential window to reduce  $\text{CO}_2$  [65]–[67].

Actually,  $\text{Cu}_2\text{O}$  is P- type semiconductor with a band gap of 2.1eV. Presence of oxygen defects on cuprous oxides and its valence band serve stable surfaces for intermediate adsorption. Oxygen in  $\text{Cu}_2\text{O}$  structure is body centered while  $\text{Cu}^+$  are faced centered [68].

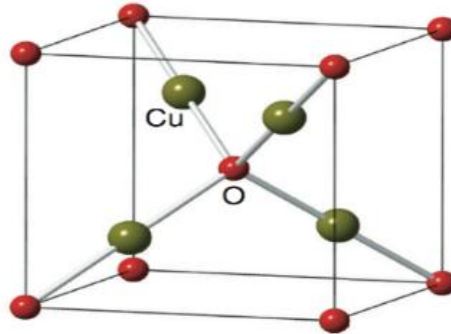
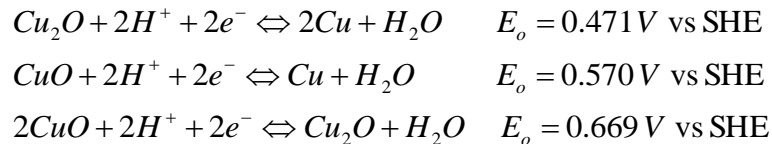


Figure 2-4: Structure of  $\text{Cu}_2\text{O}$  [64].

Reduction of cuprous oxide must take place before  $\text{CO}_2$  reduction. It has been noted that reduction of  $\text{Cu}^+$  to Cu occurs well before than  $\text{Cu}^{+2}$  to Cu. despite that it is difficult to reduce  $\text{Cu}_2\text{O}$  to Cu than  $\text{CuO}$  to Cu[69], [70]



When  $\text{CO}_2$  reduced on copper based electrodes, initially  $\text{CO}_2$  converts into formates and CO and then by further increase in potential up to -1.25 vs SHE, formates and CO converts into ethylene. At the potential of -1.35 vs SHE intermediate converts to form  $\text{CH}_4$ . Another study has been reported on copper (I) halides to investigate effect of Cu (I) species on reduction products. Notable production of  $\text{CH}_4$  and ethylene was recorded. This was because of high adsorption energy of halides for CO than Cu, which not only

supports adsorption but at the same time gives stability to intermediate species, CO adsorption on  $\text{Cu}^+$  cation held perpendicular to the surface [71]–[73]

The scientists made many efforts to use effective support for  $\text{CO}_2$  reduction at low temperature and pressure. Among many tested supports, ZnO is considered an effective support to create cation and anions on the surface of the catalyst and thus gives high production of hydrocarbon products. It helped  $\text{Cu}^{2+}$  to act like  $\text{Cu}^+$  and actively reduced  $\text{CO}_2$ . Presence of ZnO rises faradic efficiency of hydrocarbons products as compared to Cu surfaces. Both in hydrogenation and electrochemical process, ZnO protects deactivation of the surface from impurities and serves as good supports. Optimum percentage of  $\text{Cu}_2\text{O}$  loading on ZnO surface is still not known. Different planes of crystal lattice and loading of ZnO surface are still under study. [74]

Despite that Au is considered an effective catalyst for  $\text{CO}_2$  reduction but when Au tested with the support of  $\text{TiO}_2$ , oxygen defects in Ti shifts electrons chemistry in Au and thus make it suitable for the production of hydrocarbons. Similarly, the role of  $\text{Cu}_2\text{O}$  mechanism and its chemistry due to the presence of oxide defects and whether the copper act as a monolayer in adsorption are still under study. [75]

Above-stated work was done to successfully reduce  $\text{CO}_2$  to methanol, because methanol formation at low pressure and temperature is very important to shift dependence on fossil fuels to renewable energy. It provides safe and easy storage of energy and also serves as an intermediate product in many petrochemical industries. Electrochemical reduction of  $\text{CO}_2$  mitigates environmental degradation and it is an attempt to meet with social and economic targets. Reduction of  $\text{CO}_2$  to methanol by photochemical, electrochemical and

by hydrogenation methods has been done. In all these processes, focus was on the production of methanol with minimum energy input. Need of good electrocatalyst to reduce CO<sub>2</sub> is still under study which should give highly overpotential of hydrogen and opens large window to CO<sub>2</sub> reduction. A lot of studies are required to research on the geometrical structure of catalyst, mechanism of catalyst on a support and kinetic modelling required to solve problems. Extensive kinetic modelling and discussion of experimental data will be a good approach to bring good electrocatalyst in the market. Commercial application of electrochemical reduction of CO<sub>2</sub> will no longer be a dream but it requires human consistency with intelligent approach to make it commercially viable.

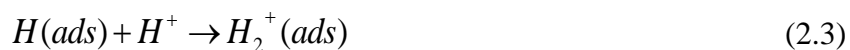
### **2.3 Mechanism of electrochemical CO<sub>2</sub> reduction to hydrocarbon and alcohols**

One of reasons for high selectivity of hydrocarbons products on Cu electrode is CO adsorption. Adsorption energy of CO is less on Cu surface as compared to Ni and Fe. Adsorption is an exothermic process and CO does not adsorb strongly on the surface of Cu as compared to Ni and Fe. Less tightly adsorbed CO has good stretching C-O and thus easily reduces to other hydrocarbons. Order of increase in adsorption energy of CO on the electrode is Cu > Ni > Fe. Five electrons are required to reduce CO in an electrochemical cell along with hydrogen production in parallel reactions [16], [76].

Heyrovsky suggested mechanism for hydrogen evolution on Cu electrode [55]



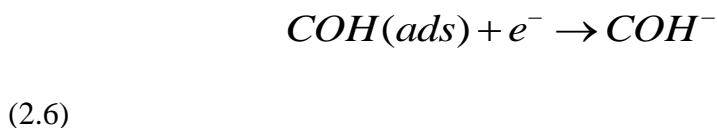
Similarly, Horiuti showed further presence of intermediate species  $H_2^+$  which involved actively in formation of adsorbed hydrogen [77].



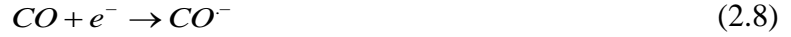
Intermediate species  $H_2^+(ads)$  formed due to combined electron and proton transfer reaction. Almost 90% of Cu surface adsorbed CO at -1.0 V. Remaining surface covered with  $H_2^+(ads)$  or  $H^+ + H(ads)$ , which further reacts and formed hydrocarbons and alcohols [15].



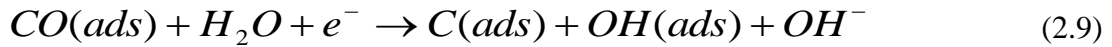
COH (ads) is main intermediate to form  $CH_4$ . Hypothetical intermediates COH (ads) proceeds in following fashion [15].



The rate determining step for formation ethylene is a transfer of an electron to CO [78].



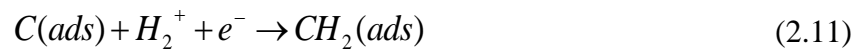
Dissociation of CO to surface carbon atom on Rh electrodes is responsible for the production of hydrocarbons and alcohols. The same approach has been identified in Fisher tropsch reaction where surface carbon holds responsibility for production of hydrocarbons and alcohols. Since Cu was inert in Fisher tropsch reaction, it was assumed that transfer of electron to CO in Cu made electrode converts CO into surface carbon atoms and act as precursor for production of hydrocarbons and alcohols in cell [15], [78].



Splitting of CO is an essential step in the formation of ethylene which does not need any H (ads), H<sub>2</sub><sup>+</sup> (ads) or H<sup>+</sup>. Similarly, the second rate determining step after surface carbon reaction is [15].



Further shifting of C (ads) to CH<sub>2</sub> is



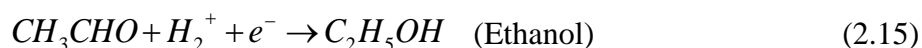
CH<sub>2</sub> is responsible for the formation of CH<sub>4</sub> and C<sub>2</sub>H<sub>4</sub> in product line [15]. CO reacts with CH<sub>2</sub> (ads) which turns to form alcohols followed by the addition of H<sub>2</sub> on RH/TiO<sub>2</sub> catalyst by Takeuchi and Katzer [79].



Further CH<sub>2</sub> - CO(ads) hydrogenation leads to the formation of ethylene [15].



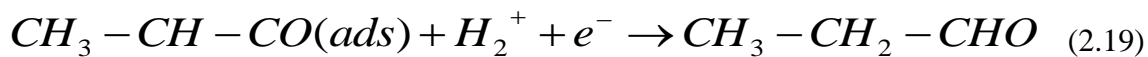
Ethylene form in products further shifts to acetaldehyde by hydrogenation, then ultimately turns to form ethanol [15].



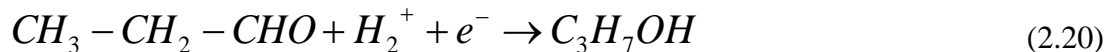
A small quantity of acetaldehyde forms vinyl alcohols, which further hydrogenated to form an intermediate homology series of  $CH_2$  [79].



CO adds up in intermediate



N-propanol is formed [15], [79].



Cu and Cu/ZnO electrodes were electrochemically tested in  $CO_2$  reduction cell to compare the performance of these two electrodes. It has been investigated that  $CH_4$  was

primary product by Cu electrode. However, rise in selectivity for methanol were noted in gas phase reaction by using Cu/ZnO electrodes. Methanol formation was due to support of ZnO which increased coordination between Cu and CO by making Pi bond between them. As a result, improved in hydrogenation of adsorbed carbon was experienced which eventually leads to increase the methoxy generations. Increase in strength of bond formation between adsorbed carbon and Cu makes electrode surface stable to reduce CO<sub>2</sub> efficiently. [80]

These experiments were conducted at -1.4 V vs Ag/AgCl. Products detected were CH<sub>4</sub>, CO and ethylene, along with liquid phase product of methanol, ethanol, propanol, and methyl format. The faradic efficiency of both these electrodes was almost same. Cu with the support of ZnO is commercially a catalyst used in the production of methanol. Large number of elements with ZnO support, tested for increase in CO<sub>2</sub> adsorption over Cu surface. [80]

It was also analyzed that increase in methanol yield is due to Cu (I) species which facilitate adsorption of CO. Cu (I) active site enhanced adsorption of CO and HCO High heat of adsorption of Cu (I) species gives stability to intermediates methoxy (H<sub>3</sub>CO), carbonates CO<sub>3</sub><sup>2-</sup> and formate HCOO<sup>-</sup>. Cu (I) plays a vital role in CO adsorptions and at the same time decrease reduction potential of CO/H<sub>2</sub>. Alkali metals help to promote methanol yield by activating Cu (I) active sites and at a mean time increase Cu (I) concentrations, which enhance the selectivity of methanol. [80]

Electrochemical reduction of CO<sub>2</sub> to methanol over oxidized Cu or Cu (I) electrodes is time dependent, the reaction was limited to a short period of time. However, methanol produced by Cu-ZnO electrode was independent on reaction time and was stable. The

increase in selectivity of hydrocarbons to alcohols depends on the surface of electrode and coordination between surface and CO<sub>2</sub>. Rough surface of Cu has relatively high current density than a flat surface. It was experienced that faradic efficiency of ethylene production over both Cu and Cu/ZnO were same. However, an increase in alcohols yield was due to strong coordination between CO<sub>2</sub> and electrode surface of ZnO. ZnO actually distributes Cu over the surface which turns to increase active sites for hydrogenation reaction, are main reasons behind the increased in current efficiency for methanol. [35], [80]

Pi bonding increased the strength of CO and provided activation energy to the carbon of CO, this increase in activation energy increases the methanol production [81], [82]. According to DFT theory, Zn plays a vital role in selectivity of methanol. Zn lowers the energy needed for hydrogenation reaction of CO and thus increases methanol yield [81]. ZnO worked together with Cu to increase hydrogenation of these intermediates adsorbed products [83]. Comparison of methanol formation on three electrodes of cuprous oxide, anodized Cu electrode and air Oxidized Cu electrode also has been reported in literature. Among them cuprous oxide produced high amount of methanol ranging from 10 to 43  $\mu\text{mol}\cdot\text{cm}^{-2}\cdot\text{h}^{-1}$  while anodized electrodes and air oxidized electrode have 0.9 to 1.5  $\mu\text{mol}\cdot\text{cm}^{-2}\cdot\text{h}^{-1}$  and .08 to 0.9  $\mu\text{mol}\cdot\text{cm}^{-2}\cdot\text{h}^{-1}$  respectively. The rate of formations of methanol started to increase from -1.1V (SCE) and reached to a maximum value at -1.55V (SCE) along with high hydrogen evolution. After -1.55 V (SCE) rate of formation of methanol decreased and increased in CH<sub>4</sub> was experienced, this decrease in methanol formation could be because of reduction of cuprous oxide active sites or could be affected by

methanol oxidation at a counter electrode or by some impurities present in electrolyte [84].

Methanol formation is time dependent and its formation decreased at longer reaction times greater than 30 minutes. The high faradic efficiency of 38% was monitored at -1.1 V (SCE) over cuprous oxide electrode. The primary product was liquid methanol and it was the only liquid product along with high hydrogen evolution and CO formation. The yield of methanol by using cuprous electrode is two orders greater than air oxidized electrode and one order of magnitude bigger than the anodized electrode. Cu (I) species play a vital role in CO<sub>2</sub> to methanol conversion [84]. Carbon atoms in CO molecule hydrogenate due to protons transfer from a solution which leads to formation of CH<sub>4</sub> [85]. Availability of proton transfer from solutions is less than the hydrogenation to adsorb oxygen on the surface in gas phase reactions. Formyl anions formed in both phases by hydrogenation, continuously reacts with electrons and protons to form H<sub>3</sub>CO adsorbate. If last electron and proton transfers to C of H<sub>3</sub>CO, it would form CH<sub>4</sub>. Coordination of H<sup>+</sup> with surface bound oxygen of cuprous oxide electrode favors hydrogenation of O in H<sub>3</sub>CO instead of C which favors methanol formation. This hydrogenation reactions to form methanol instead of CH<sub>4</sub> would be due to stable Cu (I) species in cuprous oxide. [85]

**Table 2-3: Summary of different electrocatalyst and their role on current density and faradic efficiency**

<b>Reference</b>	<b>Electrocatalyst</b>	<b>Current Density (amp-cm<sup>-2</sup>)</b>	<b>Potential</b>	<b>Faradic Efficiency (%)</b>
Nehar. U et al. 2015	Ir/Ru-Oxide	0.003	-1.7	35.5
V. Kumar et al. 2015	Zn-Co oxide	0.06	-2.5	7.5
Y. Liu et al. 2014	Nitrogen-Nano diamond	0.03	-1.5	27
SK. Hossain et al. 2014	CNT-Cu	0.034	-1.7	37
S. Sen et al. 2014	Cu-Nano foams	0.02	-1.5	34
G. Lu et al. 2013	Pd-MWCNTs	0.004	-1.0	35
M. Le at al. 2009	CuO electrodes	0.005	-3.2	41
J. Nakamura et al. 2007	Cu-ZnO	0.0015	-1.8	21
Y. Hori et al. 2005	Pt black	0.0061	-2.7	15
K. Okahwa et al. 2005	Cu/Pd/Pd+H	0.0075	-3.5	9
Y. Hori 1997	Cu based electrodes	0.019	-2.7	21

If we conclude up above discussions, heavy transition metals belong to group IIB, IIIB and IVB produced formates, while IB and VIII are somewhat giving good current efficiency for formic acid and CO. Majority of metal and its oxides from group 4 to group 10 produced hydrogen as major product. Copper which comes in between these two groups has uniqueness in exhibiting good conducting and electron trapping properties with high adsorption energy of CO<sub>2</sub> [43]–[45].

Consumption of higher overpotential with less faradic efficiency of methanol was a major problem in CO<sub>2</sub> reduction. Thermodynamically, it is possible to reduce CO<sub>2</sub> to methanol at -0.02 V vs Ag/AgCl reference electrode. We are looking for a large surface area support which allows less energy to reduce CO<sub>2</sub> into favorable product of methanol. CNT as a potential support can offer a large surface area but at the same time can adsorb more selective intermediate species to increase current density and stability of electrode. Almost all the electrocatalysts tested in past had lower stability to reduce CO<sub>2</sub>.

Numerous properties of CNTs including good compatibility, large surface area, excellent conductivity, modifiable surface, and nanotube structure with ability to form suspensions in solvents, made CNTs a game changer in variety of electrochemical applications [86].

CNTs have tubular structure nanomaterials with high length to diameter ratio which enables them to behave as molecular wire for transferring electron between electrode and CO<sub>2</sub> in electrolyte solution. Tubular shape CNT with high electrocatalyst activity, chemical stability, modifiable surface and unique morphology of these materials drive our confidence ahead to achieve ultimate by clean and desired products [86].

Advantage of CNTs over the other nanomaterials is that they adsorbed water insoluble on hydrophobic and Pi conjugation sidewalls, across which sharing of electron occurs to achieve good conductivity and better electrocatalytic activity [55].

Carbon nanotubes have properties of good electrical conductivity, uniform straight meso, and micro pores structure and also resistant to acid and base medium. Low mass transfer resistances increase residence time in pores for good adsorption which makes them fruitful to be used in the variety of applications as a support [87].

Scientists investigated many uses of carbon nanomaterials. They did a lot of research on nanomaterial and have developed alternate transformations of CO<sub>2</sub> to usable products. However, by reviewing the literature of past three decades, we analyzed some areas where we need to work out. Impregnation of carbon nanomaterials with oxides of copper would direct new path in electrochemical CO<sub>2</sub> reduction. Material morphology reduces CO<sub>2</sub> to obtain a higher selectivity of desired products like methanol.

According to the best of our knowledge, not a single study has been published for reduction of CO<sub>2</sub> using the copper oxide loaded CNTs based electrocatalyst. Based on this conclusion, we set our general objective to investigate most stable support with high performance electrocatalyst for CO<sub>2</sub> reduction.

## 2.4 Objective

The main objectives of this research study are as follows,

1. To prepare the copper oxides supported CNTs based electrocatalyst.
2. To characterize the surface of electrocatalyst with SEM, EDX, TGA, TEM, BET, XRD, Raman spectroscopy and FTIR.
3. To design an efficient two compartment electrochemical cell with minimum contamination.
4. To study the effect of Linear sweep voltammetry, Chronoamperometry and Faradic efficiency of methanol formation.
5. To optimize the electronic geometry of the best performance electrocatalyst and to measure the band gaps by DFT simulation.

The copper oxide based CNT electrodes will enhance the adsorption of the  $\text{CO}^-$ . Higher adsorption energy of  $\text{Cu}_2\text{O}$  with surface bound oxygen facilitates the electron flow with an increase in current density and methanol yield.

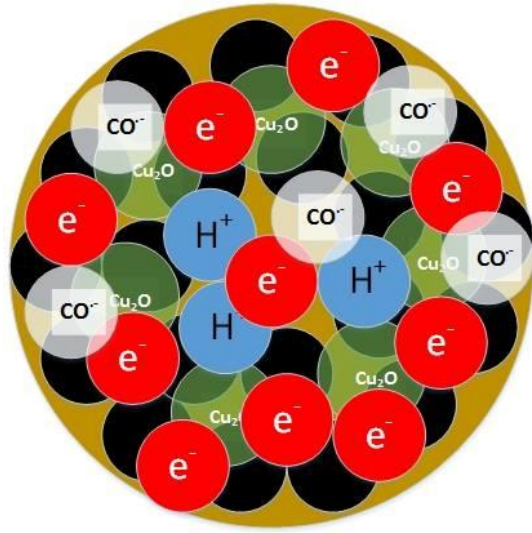


**Figure 2-5: Suggested mechanism of CO<sub>2</sub> adsorption on Copper oxides supported CNTs**

Modified CNTs based copper oxide electrodes serve both in conducting electrons and play active role in catalyst performance which supports electron transfer to CO<sub>2</sub>.

## CHAPTER 3

### RESEARCH METHODOLOGY

Right from beginning, our emphasis was to investigate selective catalyst for CO<sub>2</sub> reduction. After a thorough study of literature, it has been confirmed that suitable metal oxides sites, good support particularly with large surface area and surface morphology of catalyst play a vital role in CO<sub>2</sub> reduction. To achieve the objective of research, we prepared catalysts and performed experiments to reduce CO<sub>2</sub>. In this section, we will discuss detail preparation of catalyst along with characterizations techniques and experimental procedures to achieve our target.

#### 3.1 Materials and Preparation

Carbon nanotubes with specifications of OD (outer diameter) 10-20 nm, length 10-30 micrometer with purity of >95% and specific surface area (SSA) >150 m<sup>2</sup>/g was purchased from Cheap Tubes Corporation. MWCNT was functionalized by treating with HNO<sub>3</sub> in order to attach carboxylic group on surface of carbon nanotubes [88], [89]. Copper salt (copper nitrate pentahydrate, Cupric chloride) along with other chemicals (sodium dodecyl sulfate, sodium hydroxide, hydroxyl ammonium hydrochloride) and solvent (Ethanol) were purchased from Sigma Aldrich. All chemicals were analytical grade and no additional treatment was conducted.

### **3.1.1 Impregnation of cupric oxides on carbon nanotubes**

To prepare desired CuO supported carbon nanotubes, different weight percent of copper nitrate pentahydrate salt ranging from 10 to 50 % and desired quantity of carbon nanotube were taken. Desired quantity of carbon nanotubes was added into ethanol solution beaker and then the mixture was subjected to ultrasonication to homogenize mixture to prevent agglomeration. Mixtures of carbon nanotubes and ethanol were sonicated for 30 minutes with an amplitude of 60% in the full frequency range. Meanwhile copper salt (copper nitrate pentahydrate) was added in ethanol solvent containing carbon nanotubes slurry. The amount of copper salt depends upon wt% of copper oxides needed, i.e. 10%, 20%, 30%, 40%, and 50%. A mixture of carbon nanotubes and copper salt in ethanol solution was sonicated further for 30 minutes with same frequency and amplitude to ensure satisfactory dissemination of copper salt over carbon nanotubes. After sonication, a mixture containing carbon nanotubes and copper salt were placed in an oven for drying at a temperature of 80<sup>0</sup>C for 24 hours in order to evaporate ethanol solvent and to make sure that mixture is completely dried. Finally, dried cake was crushed to powder in a crucible and placed in furnace for calcination at a temperature of 350<sup>0</sup>C for 3 to 4 hours. After calcination, prepared sample was cooled to room temperature and metal oxide supported carbon nanotubes catalyst was put in bag for future application.

### **3.1.2 Impregnation of cuprous oxides on carbon nanotubes**

To prepare cuprous oxide supported carbon nanotubes, carbon nanotubes with specifications of OD (outer diameter) 10-20 nm, length 10-30 micrometer with purity of >95% and specific surface area (SSA) >160 m<sup>2</sup>/g was functionalized and added in deionized water. After addition of carbon nanotubes, the sample was sonicated for 30 minutes using ultrasonic sonicator. Then, the desired amount of copper chloride salt (0.1M CuCl<sub>2</sub> light blue) depending on percentage loading which ranges from 10 to 50% and sodium dodecyl sulfate (SDS) were added into carbon nanotubes solution under vigorous magnetic stirring. After sodium dodecyl sulfate (SDS) was dissolved, mixture was placed in water bath under temperature of 30<sup>0</sup>C. Meanwhile, desired amount of sodium hydroxide (1.0 M NaOH) was added, the blue color of the solution changed to light yellow green which confirms presence of copper(II) hydroxide Cu(OH)<sub>2</sub>. After that, hydroxyl ammonium hydrochloride (0.1M NH<sub>2</sub>OH.HCL) was introduced rapidly in yellow-green solution and as result color of solution become yellow and meanwhile system was subjected to half hour stirring. At the end, CNT supported cuprous oxide mixtures was centrifuged at the speed of 4500 rpm for 5 minutes and washed with ethanol and deionized water until pure catalyst was recovered from solution

### **3.2 Material Characterization**

It was essential to characterize our materials by different characterization techniques. The catalyst was characterized to critically investigate surface morphology, particle size distribution over carbon nanotube, composition and location of impregnation. We investigated very surprising features of our catalyst which have direct connectivity with

results. In this section, we will discuss detail characterization of CuO and Cu<sub>2</sub>O loaded carbon nanotubes.

### **3.2.1 Thermogravimetric Analysis (TGA)**

Thermal analysis of materials was carried out by using TGA (Thermogravimetric analysis) which measures the drop in weight of prepared materials with the function of rise in temperature. It indicates the presence of moisture or volatile material present in the sample with the proximity of both change in mass and phase. TA instruments from (K.U.Leuven SDT Q600) were utilized for TGA analysis. In these experiments, alumina pan was used and experiments were conducted in temperature limit of 25<sup>0</sup>C to 890<sup>0</sup>C with heating rate of 10<sup>0</sup>C per minute. Purging of air with 99.99% purity was done at 100 ml/minute.

### **3.2.2 Scanning Electron Microscopy (SEM)**

Scanning electron microscopy is used for analysis of particle morphology particularly, particle size, surface structure and catalyst composition. Scanning electron microscopy model (JEOL JSM-646OLV) operated at 20 kV to produce energy dispersive X-ray (EDX), was used to identify the composition of the sample. In this technique, sample was coated with platinum 5nm thickness on sputter coating machine. Then, coated samples placed at sample holder under 20kV for the bombardment of an electron on the sample.

### 3.2.3 X-ray diffractogram (XRD)

XRD machine is used to conduct an analysis of crystals lattice and to understand phases of metal oxides. This technique is used for composition and detailed analysis of crystallites. We performed XRD analysis in a range of  $2\Theta = 20^{\circ}$ - $80^{\circ}$ , with the step size of  $.02^{\circ}$ , a higher degree of crystallinity would cause better catalytic performance. In these analysis, powder sample of carbon nanotubes supported catalyst was spread on a glass slide and the sticky tab is used to stick material on glass tab. Glass slide was then put in Rigaku XRD X-ray diffractometer and analysis was carried out with Cu- $K_{\alpha}$  radiations. After diffractogram analysis, crystal size was calculated by using scherrer equation

$$d = \frac{0.9\lambda}{\beta \cos\Theta} \quad (3.1)$$

Where  $\Theta$  is diffraction angle,  $\lambda$  is X-ray wavelength and  $\beta$  is FWHM of the peak. All these analysis was carried by using PDXL software.

### 3.2.4 Transmission Electron Microscopy (TEM)

TEM model (FETEM (JEOL, JEM-2100F) provides more resolution and better magnification images from micro level up to few angstrom  $10^{-10}$  nm. It gives information about composition and structure of materials. TEM has electron source beam which directs to the surface of materials to strike electron which deflects and collected in the chamber. As a results, contrast is developed and different resolution images were

extracted from these deflected electrons. TEM operates at 200kV to produce ultra-resolution images.

TEM samples were prepared by adding 1 milligram of prepared catalyst in 8 ml of ethanol solution and sonicated for half hour then prepared suspension was dropped on specimen holder with a sticky tape to facilitate electron transfer.

### **3.2.5 Raman Spectroscopy**

Raman spectroscopy is used for sample identification and quantification from vibrations of molecules. It is very important to identify the location of impregnated materials on support. Raman spectroscopy used monochromatic laser light and record scattered light frequency from the sample. The comparison is made between the frequency of excited source and scattered light, if both of these frequencies match then this type of scattering is called Rayleigh scattering. However, there are few rays which have different frequency than source due to vibration interaction of molecules. From this difference of frequency level, the location of metal oxides on support surface will be identified.

### **3.3 Electrochemical Setup**

Two electrode compartments H - type electrochemical cell were used in our experiments. Working electrode, counter electrode fabricated by platinum showed in Figure 3-2 and Ag/AgCl reference electrode showed in Figure 3-3 was assembled in the cell. To conduct sufficient flow of electrons, 0.5M sodium bicarbonate solution ( $\text{NaHCO}_3$ ) as an electrolyte was used. The counter electrode was used as an anode while working

electrode was the cathode. Counter electrode has 3 times large surface area than working electrode.



**Figure 3-1: Working electrode**



**Figure 3-2: Platinum counter electrode**

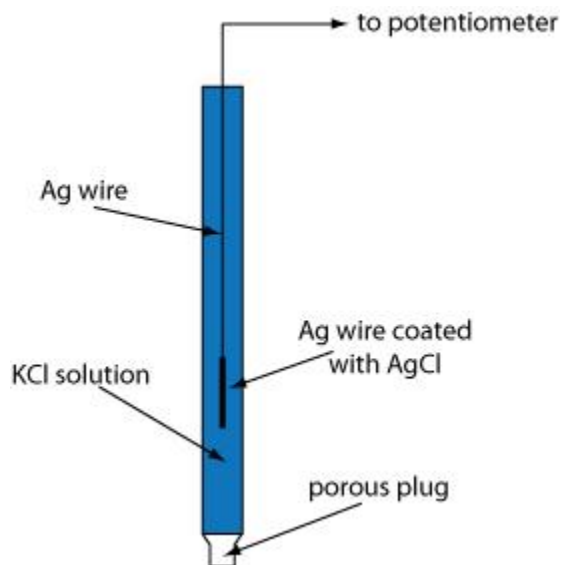


Figure 3-3: Reference Ag/AgCl electrode

0.5 M  $\text{NaHCO}_3$  electrolyte solution was taken in electrochemical cell, and all three electrodes were assembled down in the cell. After that, all the electrodes were properly dipped inside the solution. Before the start of reduction reaction,  $\text{N}_2$  was purged in the system to remove any dissolved oxygen if present in system. Potential was applied in between reference and working electrode. At the same time, current is measured between the counter and working electrode. Electrochemical cell system is showed in Figure 3-4.

### 3.3.1 Working electrode Preparation

$\text{CuO}/\text{Cu}_2\text{O}$  loaded carbon nanotubes along with the addition of 5% Nafion and isopropanol solution were sonicated for half hour. After sonication, suspension of prepared solution was dropped on the surface of the copper foil and was allowed to dry on that foil. Bubbled  $\text{CO}_2$  in 0.5 M  $\text{NaHCO}_3$  electrolyte solution in an electrochemical

cell having two separate compartments. These compartments were separated by Nafion membrane. Three electrodes system, working electrode, platinum (Pt) made counter electrode and reference (Ag/AgCl) electrode assembled in electrochemical cell. All potential measurements in these experiments were measured with respect to reference Ag/AgCl electrode. Polishing of copper electrode was carried out before casting catalyst on the surface of working electrode in order to clean its surface from contamination. Before experiments, nitrogen was purged into the electrolyte to remove any presence of air in the system, then CO<sub>2</sub> with 99.99% purity was purged into the 0.5 M NaHCO<sub>3</sub> electrolyte solution. Linear sweep voltammetry and chronoamperometry was used to investigate activity of copper oxide based modified carbon nanotubes electrodes.

### **3.3.2 Design of electrochemical Cell**

Techniques involving the design of electrochemical cell continued for a long time to analyze thermodynamics and kinetic study in an electrochemical cell. Presently electrochemical cell is used in a variety of electrochemical applications of electrocatalyst, sensors, and corrosion research[90]. Various designs of electrochemical cells have been employed in different applications. Three electrodes system is better than two electrode system because it offers less uncompensated resistance[91].

Electrodes can be assembled in one compartment, or in several. In many compartments we can avoid interactions between reaction and electrode interface, which have great importance to prevent adsorption of impurities on working electrode [91].

In two electrode compartment, products formed at counter electrode could go to block active sites of working electrode. The blockage of these gaseous products is necessary for both quality and accuracy of the electrochemical cell[92].

In order to avoid contaminations, we designed two - compartment electrochemical cell by using Solidworks software tool and introduced Nafion 117 membrane between two compartments.

In these studies, we developed new set up to reduce oxygen diffusion from counter to working electrode compartment. Electrochemical measurements were carried out in two compartment cell made of polycarbonate transparent glass with a reference electrode (Ag/AgCl) and Pt mesh counter electrode. Figure 3-4 shows systematic diagram of polycarbonate transparent cell with modified counter electrode compartment. Working electrode is assembled in working compartment and a reference electrode connected to working electrode compartment with a small hole on top. The incoming gas inlet for CO<sub>2</sub> and N<sub>2</sub> purged through holes located at top of working electrode compartment.

The reference electrode is freely standing in the electrolyte while ion conducted Nafion membrane is held tightly with spacers. The screw fitting was made tight to prevent any leakage of electrode and at same time to efficiently hold Nafion membrane to transfer ions.

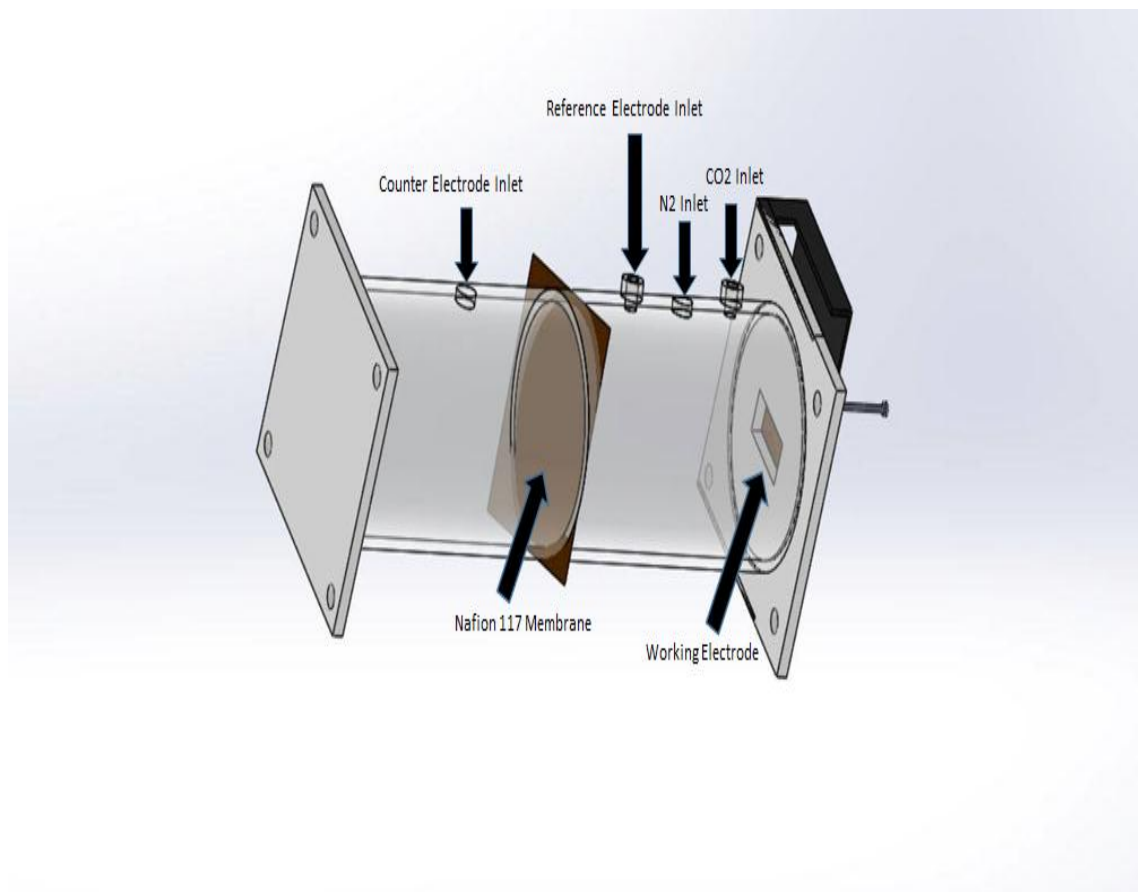


**Figure 3-4: Poly carbonate made electrochemical cell with two compartments separated by nafion membrane for electrochemical reduction of CO<sub>2</sub>**

### 3.3.3 Nafion 117 Membrane

Nafion is a perfluorinated membrane which has sulfate groups located at end of side chains. These chains allow transfer of water molecules with H<sup>+</sup> protons and repel negative ions by sulfate groups. This membrane satisfies the concept of proton transfer and blocked anions which damage the active surface of working electrode[92]. Copper foil easily goes to contamination by oxygen and possess high affinity to adsorb oxygen produced in cell. Nafion is resistant to a variety of chemicals and we achieved excellent separation of oxygen between two compartments. The deposition of organic on surface of

the Nafion may damage membrane ability to transfer protons. We washed Nafion membrane by immersing it into 10% HNO<sub>3</sub> at 80<sup>0</sup>C for two hours. After removing Nafion membrane from acid solution, it was washed with deionized water to remove acid residues. Cleaning procedure would turn back Nafion to its original performance. For every experiment, same cleaning procedure was repeated.

### **3.3.4 Cupric oxide and cuprous oxide based working electrodes**

CuO and Cu<sub>2</sub>O supported carbon nanotubes were loaded on copper foil. It was investigated by Hori that reduction of CO<sub>2</sub> on copper oxide surface selectively reduced CO<sub>2</sub> to desirable hydrocarbon and alcohols. Reduction of CO<sub>2</sub> strongly depends upon operational parameters. Cleaning off the electrode surface can increase the prospect of suitable hydrocarbons [31]. Scientist converted CO<sub>2</sub> to most selective product methanol by using GaAs, and InP, but due to low current density it was not appreciated [20], [31]. Similarly, other metals were investigated for the search of high current density to methanol. Ru and Mo made electrodes that give current density less than 2mA with 60% faradic efficiency [18], [41]

However, highest faradic efficiency larger than 100% was recorded with 33mA by Frese. The faradic efficiency of methanol formation based on 6 e<sup>-</sup> in the reduction reaction. [20], but oxidation state of copper surface is not reported in these experiments. However, it has been concluded in the photochemical reduction of CO<sub>2</sub> that Cu loaded titanium serves as a good catalyst to reduce CO<sub>2</sub> to favorable alcohols like methanol. But the problem was

low quantum efficiency in UV region of spectra. [42], [43]. Role of Cu-based electrodes particularly Cu (I) species significantly and actively enhanced CO<sub>2</sub> reduction [44], [45].

Similarly, other researchers investigated that oxide defects on surface of electrocatalyst kept catalyst stable against hydrogenation reaction and thus play effective role in CO<sub>2</sub> reduction [47], [48].

In this research thesis, we investigated the effect of CuO and Cu<sub>2</sub>O loaded carbon nanotubes on CO<sub>2</sub> reduction. We have investigated optimum electrocatalyst which effectively reduced CO<sub>2</sub> to desired products.

### **3.4 Electrochemical Test**

#### **3.4.1 Linear sweep voltammetry**

Initially, pure copper foil under different conditions of N<sub>2</sub> and CO<sub>2</sub> saturated in 0.5M NaHCO<sub>3</sub> was tested and run the linear sweep voltammetry in potential range of -0.2 to -1.8V. After the inception of given potential, we recorded current vs voltage behavior and measured constructive results. In both cases, under N<sub>2</sub> and CO<sub>2</sub> purging, there was no physical change in working electrodes which basically signify stability of our catalysts. Similarly in N<sub>2</sub> saturated electrolyte, whole current was due to hydrogen evolution reaction while in CO<sub>2</sub> saturated electrolyte we noticed two type of reactions, CO<sub>2</sub> reduction and hydrogen evolution. Both of these reactions competes each other's [17], [93], [94]. Hydrogen evolution consumes electrons and lowers the CO<sub>2</sub> reduction. Under N<sub>2</sub> saturation current density was 0.0044 A-cm<sup>-2</sup>at -1.4 V while under CO<sub>2</sub> saturation

current density was  $0.00628 \text{ A-cm}^{-2}$  at  $-1.4\text{V}$ . Such trends of results were also reported in the literature [17], [95], [96].

Higher current density in  $\text{CO}_2$  saturated electrolyte was due to efficient cleaning of copper foil by sand paper. High current density in  $\text{CO}_2$  saturated system for different electrodes were also reported in the literature [17].

To further note the effect of copper oxide based electrodes, we prepare different loading of cupric oxide and cuprous oxide based electrodes varied from 10 to 50% and tested all these catalyst for a  $\text{CO}_2$  reduction in an electrochemical cell. We measured current vs voltage response for each load of cupric and cuprous oxides loaded carbon nanotubes

### 3.4.2 Chronoamperometry

To investigate the stability of the catalyst, chronoamperometry was done for each percentage of cuprous oxides supported CNTs based electrodes. We conducted chronoamperometry test for fixed potential value for 1200 seconds and decrease in current with each loading of cuprous oxide based electrodes was noted. 30%  $\text{Cu}_2\text{O}$  supported CNTs was the most stable with highest current density catalyst. Decrease in current density for high loaded catalyst was due to agglomerates of particles. These agglomerates can be seen in TEM and SEM images. Chronoamperometry analysis clearly validates that catalyst is effective for long time operation. Similarly, theoretical faradic efficiency of methanol formation was measured by using formula

$$FE = \frac{nFm}{It} \quad (3.2)$$

Where  $n$  is the number of electrons involved in reaction to produce methanol. For methanol  $n$  is 6,  $F$  is faradic constant,  $I$  is current in amperes,  $m$  is a mole of product formed while  $t$  is a time in seconds. Faradic efficiency is the function of potential. Highest faradaic efficiency was recorded at  $-0.8$  V vs Ag/AgCl.

## Chapter 4

### Results and Discussion

In the part of this chapter, the results of different characterization techniques have been discussed. Physical and electrochemical characterizations were conducted to evaluate performance of electrocatalyst. Physical characterizations of CuO and Cu<sub>2</sub>O impregnated CNTs are presented and discussed and later, their catalytic activities to reduce CO<sub>2</sub> to methanol are discussed.

#### 4.1 Physical Characterization

Prepared catalyst was characterized to investigate its surface morphology, phase analysis, quantitative elemental analysis and thermal stability. Surface morphology was analyzed using scanning electron microscope (SEM). Elemental analysis was conducted using energy dispersive X-ray (EDX) spectrum while phase composition and crystallinity of catalyst were studied using X-ray diffraction (XRD) machine. Similarly, thermal stability analysis and defect density of impregnated materials were carried out by Thermogravimetric analysis (TGA) and Raman spectroscopy. All characterization are describe briefly below.

##### 4.1.1 SEM and EDX analysis

To understand the activity of reaction on copper oxides based electrodes, we analyzed surface morphology, structure and composition of the catalyst. It is clearly seen from SEM images that CuO is uniformly and homogeneously impregnated on the surface of

CNT and tubular geometry of carbon nanotubes showed in SEM images confirmed that morphology of carbon nanotubes did not change despite impregnation which indicates the effectiveness of preparation method. CNT threading CuO nanoparticles and strong binding between CNT and CuO is visible in Figure 4-1. However, upon an increase in loading of cupric oxides uniformity of impregnated material improved, as showed in Figure 4-2. Further increase in loading of 30% CuO on CNTs catalyst, uniformity and homogenous deposition of CuO on surface of CNT is further improved. Improved coverage of CuO is clearly visible Figure 4-3, which validates the effectiveness of our method of preparation. However, upon additional increase in loading, CuO particle tends to form agglomerates and eventually increase in particle size is experienced in the image of Figure 4-4 and Figure 4-5. This means that higher loading of CuO more rapidly form agglomerated with CNT and clusters of particles formed in catalyst.

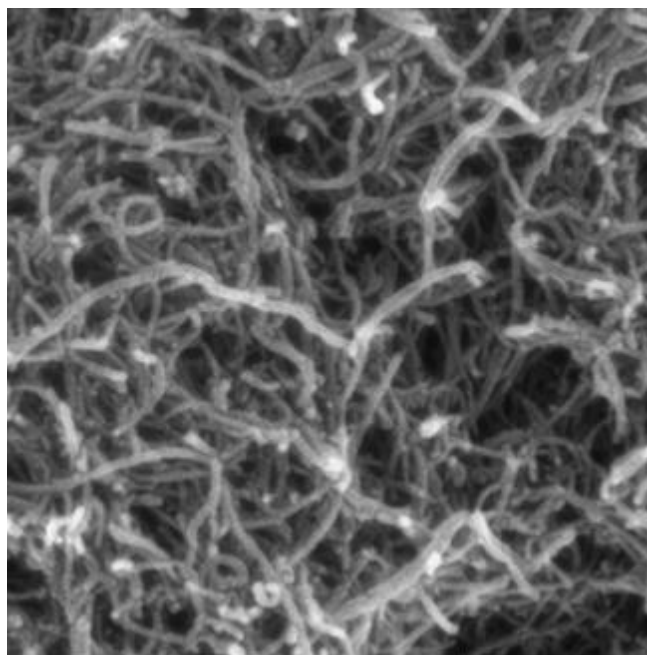


**Figure 4-1: SEM image of 10% CuO supported CNT catalyst**

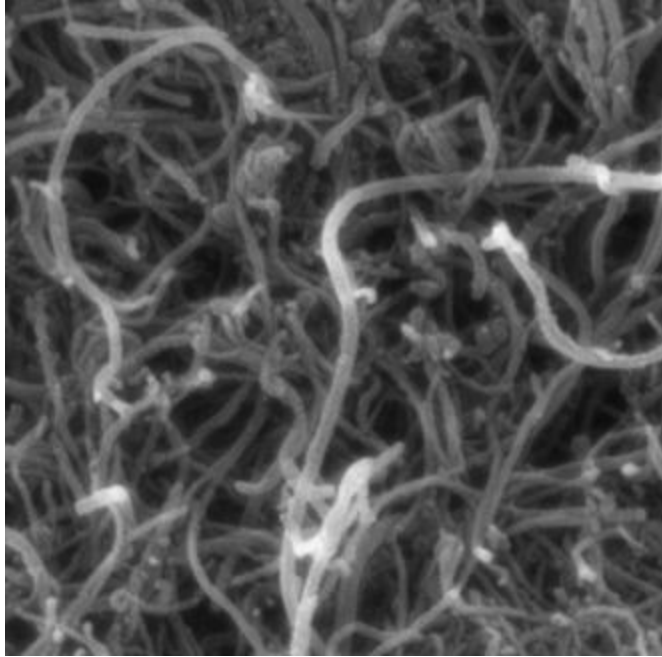


**Figure 4-2: SEM image of 20% CuO supported CNT catalyst**

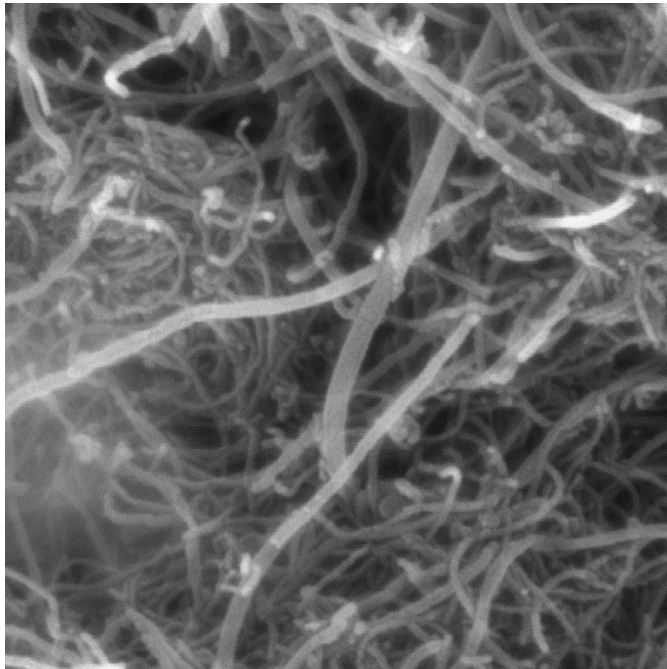


**Figure 4-3: SEM image of 30% CuO supported CNT catalyst**

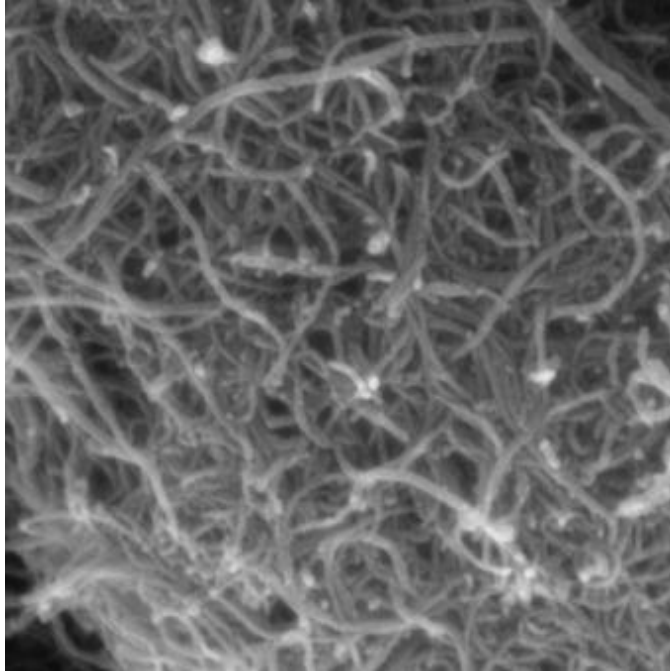


**Figure 4-4: SEM image of 40% CuO supported CNT catalyst**

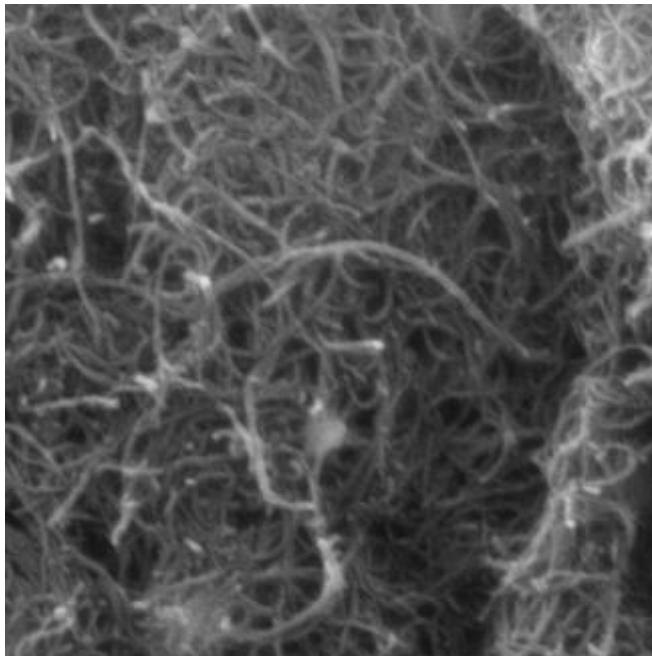


**Figure 4-5: SEM image of 50% CuO supported CNT catalyst**

Faces (100), truncated edges (110) and corners (111) of  $\text{Cu}_2\text{O}$  nanoparticles is clearly visible in SEM images from Figure 4-6 to Figure 4-10. These edges (111) in crystals which are active surface and responsible for water decomposition to produce more protons ( $\text{H}^+$ ) for reduction of  $\text{CO}_2$  and at the same time considered the best catalyst for photochemical application [97]. Similarly, truncated edges (110) which do not actively participate in photocatalyst and electrochemical application can also be seen in images.

CNT threading  $\text{Cu}_2\text{O}$  nanoparticles and strong binding between CNT and  $\text{Cu}_2\text{O}$  is visible in Figure 4-6. Upon an increase in loading of cuprous oxides, uniformity of impregnated material improved, as showed in Figure 4-7. Further increase in loading of 30%  $\text{Cu}_2\text{O}$  on CNTs catalyst, uniformity and homogenous deposition of  $\text{Cu}_2\text{O}$  on surface of CNT is further enhanced. Growing particle size with rise in loading of  $\text{Cu}_2\text{O}$  is clearly visible in images from Figure 4-6 to Figure 4-8. Better coverage of  $\text{Cu}_2\text{O}$  is clearly visible in Figure 4-3 and in Figure 4-8, which validates the effectiveness of our method of preparation. However, upon further increase in loading,  $\text{Cu}_2\text{O}$  particle tends to form agglomerates and eventually sharp increase in particle size is experienced in the image of Figure 4-9 and Figure 4-10. We observed that higher loading of  $\text{Cu}_2\text{O}$  more rapidly form agglomerates with CNT and clusters of particles in the catalyst was noted. Four side pyramidal structure of  $\text{Cu}_2\text{O}$  crystal lattice on CNT surface is visible in Figure 4-10

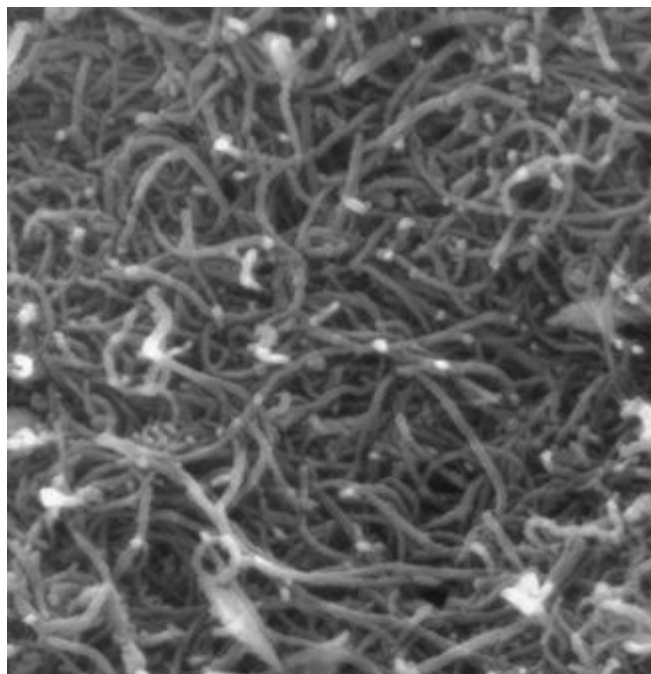


**Figure 4-6: SEM image of 10% Cu<sub>2</sub>O supported CNT catalyst**

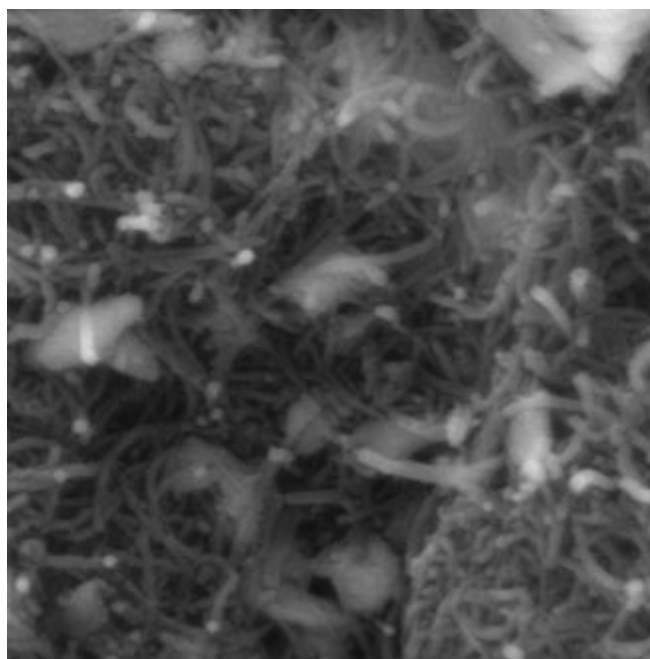


**Figure 4-7: SEM image of 20% Cu<sub>2</sub>O supported CNT catalyst**

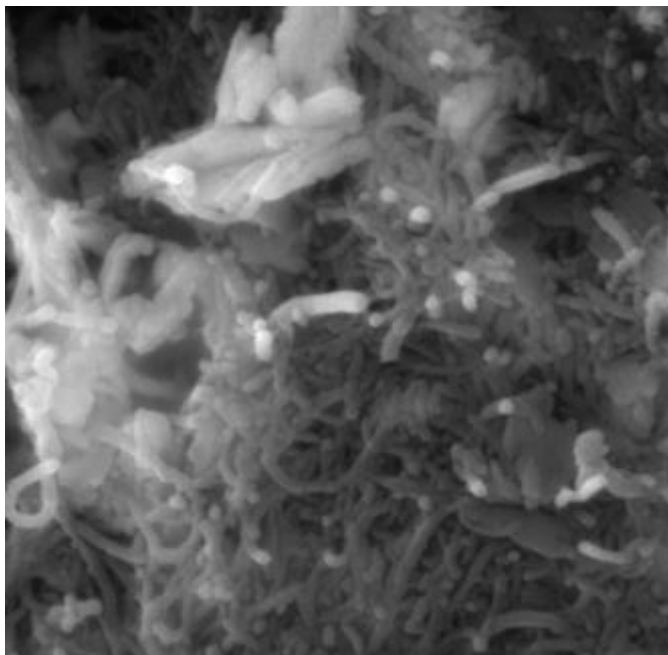


**Figure 4-8: SEM image of 30% Cu<sub>2</sub>O supported CNT catalyst**

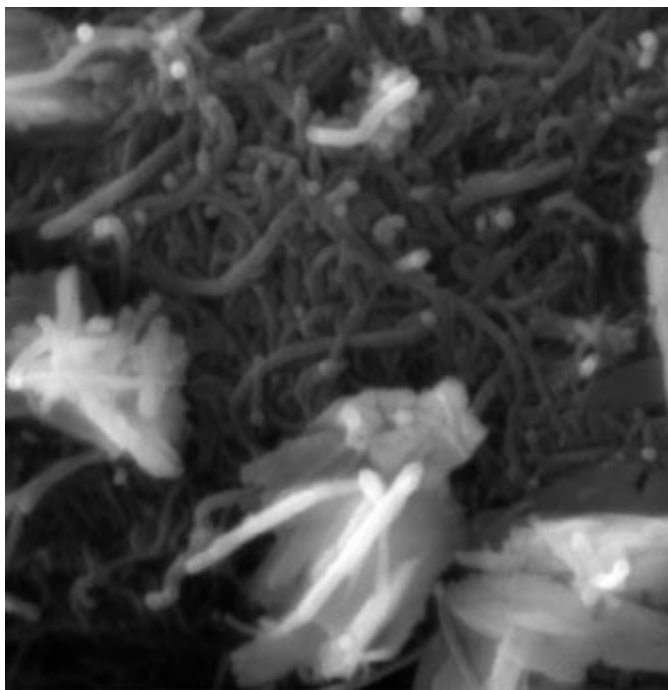


**Figure 4-9: SEM image of 40% Cu<sub>2</sub>O supported CNT catalyst**

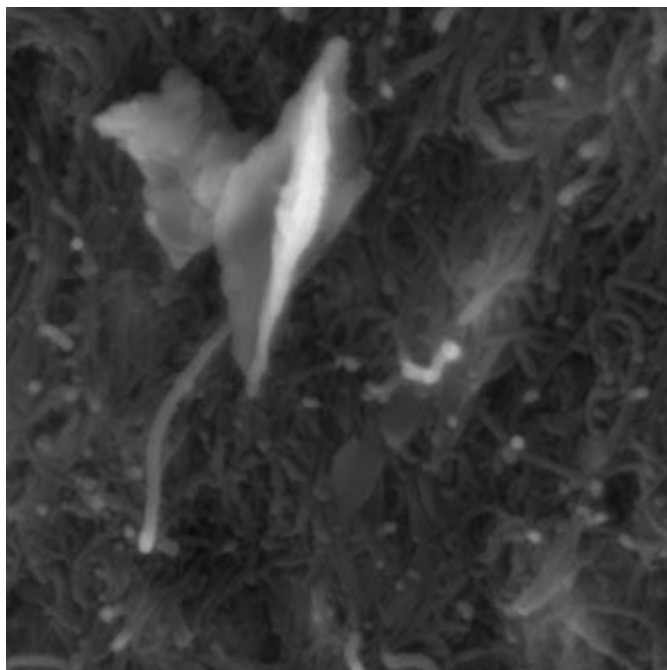


**Figure 4-10: SEM image of 50% Cu<sub>2</sub>O supported CNT catalyst**

#### **4.1.2 Energy dispersive X-ray (EDX) analysis**

EDX is one of the efficient technique used for spot analysis to confirm the existence of different elements in samples. Figure 4-11 to Figure 4-14 clearly indicates the presence of carbon with copper and oxygen to validate effective preparation of electrocatalyst. Carbon peaks in EDX images of Cu<sub>2</sub>O supported CNT in Figure 4-11 and CuO supported CNT in Figure 4-13 comes as a major constituent from carbon nanotubes while copper and oxygen presence in both of these samples clearly confirmed the impregnation of copper oxides on carbon nanotubes. Higher loaded (40%) Cu<sub>2</sub>O and (50%) CuO on CNT image is showed in Figure 4-12 and Figure 4-14 also confirms the presence of carbon, copper and oxygen in electrocatalyst. The intensity of copper peak in both of these higher

loaded copper oxides based electrocatalyst increased due to high percentage of copper content in each samples. In addition to these elements, unknown peaks in all samples is platinum metal that comes from specimen holder.

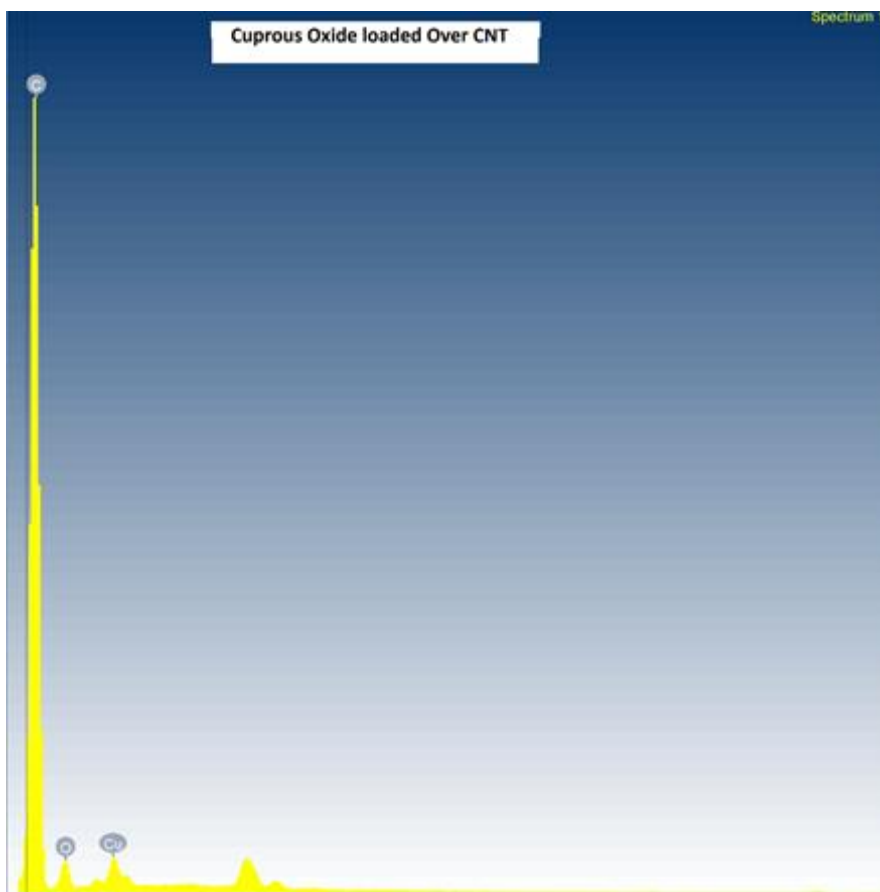
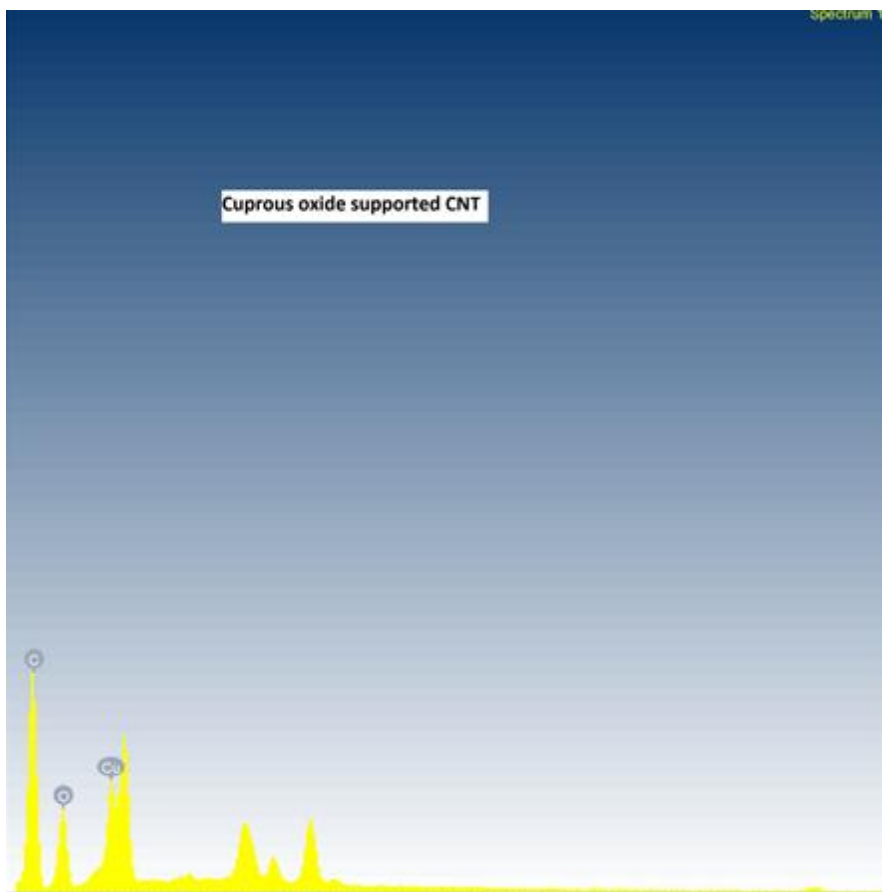
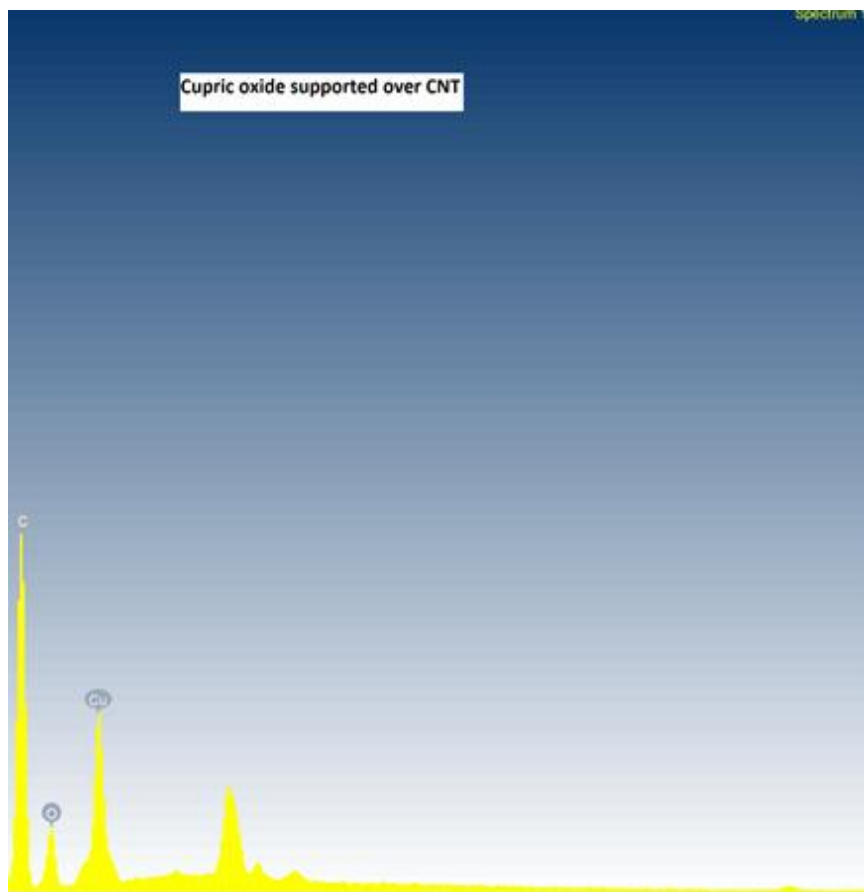


Figure 4-11: EDX image of 10% Cu<sub>2</sub>O supported CNT catalyst



**Figure 4-12: EDX image of 40% Cu<sub>2</sub>O supported CNT catalyst**



**Figure 4-13: EDX image of 20% CuO supported CNT catalyst**

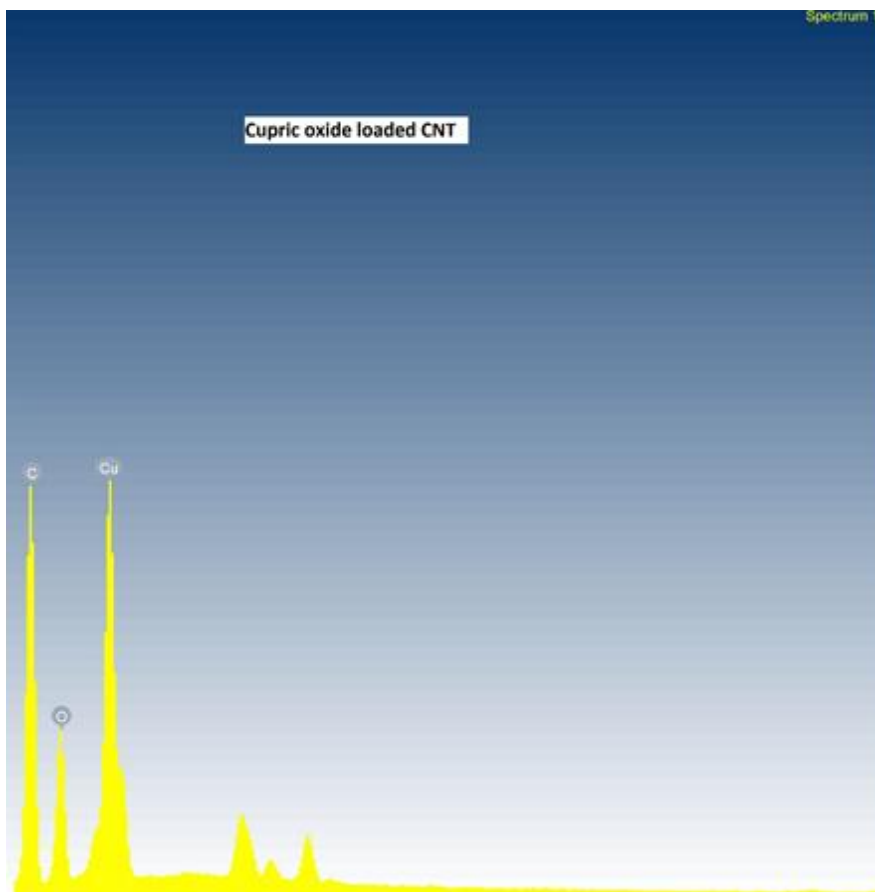


Figure 4-14: EDX image of 50% CuO supported CNT catalyst

### 4.1.3 X-ray diffraction Analysis (XRD Analysis)

XRD analysis was carried out to identify crystals structure and size of the prepared catalyst. Figure 4-15 shows XRD pattern of CNTs- supported cupric oxide (CuO) range from 10% to 50%.

In all prepared samples, diffraction peak at 26 attributes to hexagonal (002) graphite structure which confirmed that CuO is embodied in carbon nanotubes. Other broad peaks at 34 ,38 ,59 and 63.0 show that samples consist CuO divalent nanocrystallites

and exhibit monoclinic symmetry of CuO [98]. Eventually, these results validate successful preparation of CuO supported CNTs. At high loading of CuO supported CNTs, a high peak intensity is experienced. It means that large particle size exhibits strong intensity in XRD pattern.

Similarly, Figure 4-16 shows a broad diffraction peak at  $2\Theta$  26. Which attributed to (002) plane of graphite carbon atoms. Both peak position and its width represents structure order of carbon nanotube[99]. Peak shift of (002) plane of graphite from 25.5 to 26.06 is the result of strong interaction between cuprous oxide and wall of carbon nanotube, thus sufficient peak shift is experienced and interplanar changes in a tube are noticed [100][101]. Other diffraction peaks at angle  $2\Theta=29.7, 36.7, 38.1, 42.5, 49.6, 61.6, 73.9$ .and,  $77.6$  are allocated to the (110), (111), (200), (220), (311), and (222). Lower crystallite size is noted for low loading while high loading exhibits large particles size [102], [103]

The crystalline size of  $\text{Cu}_2\text{O}$  and CuO is calculated by Scherrer's equation

$$d = \frac{0.9\lambda}{\beta \cos\theta} \dots\dots\dots (4.1)$$

Where d is average particle size,  $\Theta$  is diffraction angle of CuO (111) peak,  $\lambda$  is wavelength of X-ray which is 0.154nm and  $\beta$  is peak broadening (FWHM)

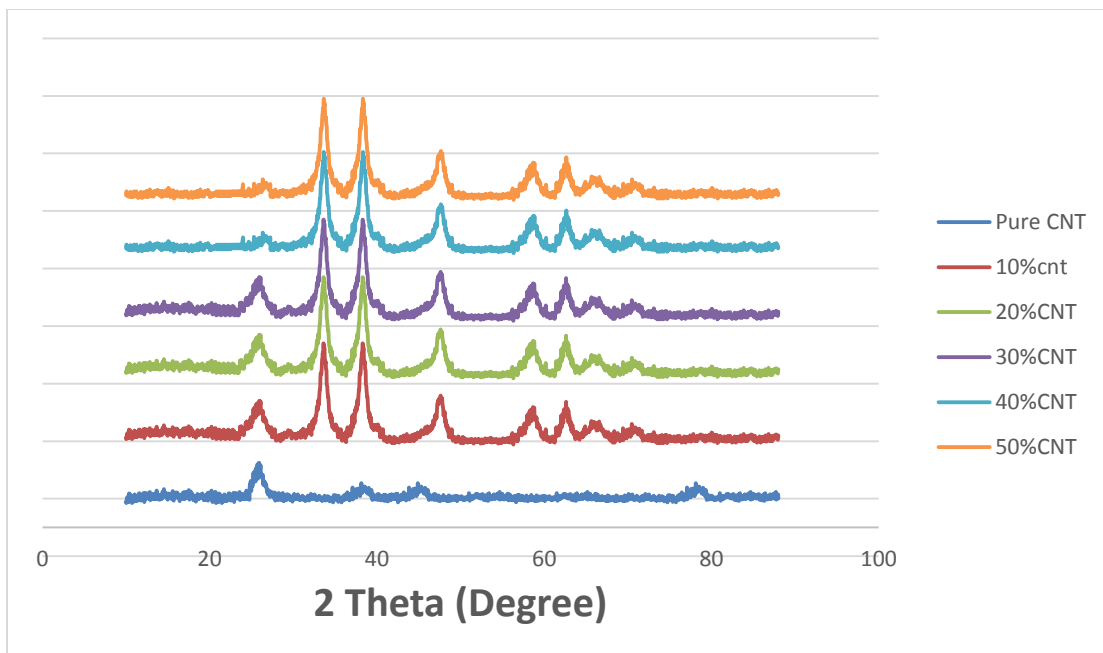


Figure 4-15: XRD pattern for CuO supported CNT catalyst

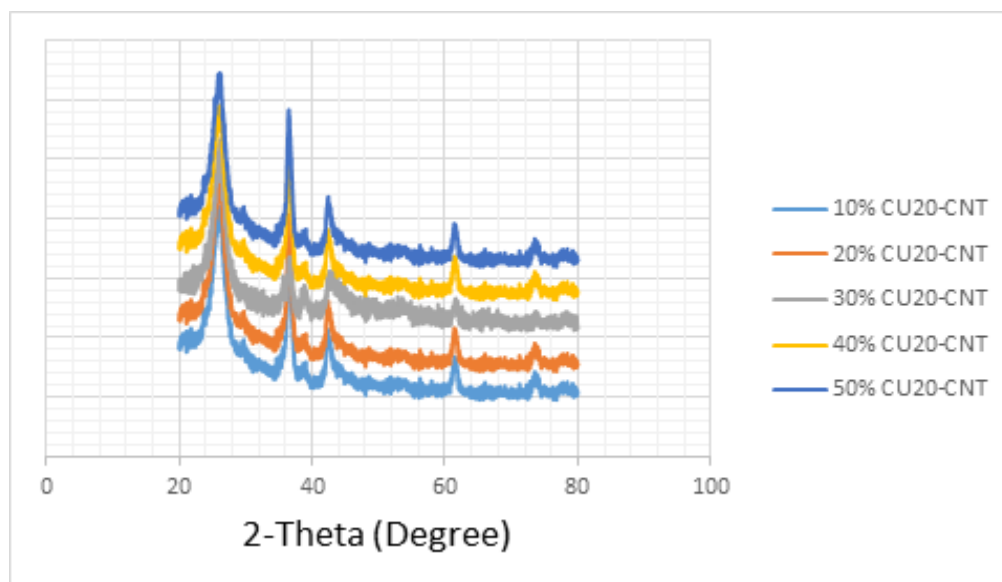


Figure 4-16: XRD pattern for Cu<sub>2</sub>O supported CNT catalyst

#### 4.1.4 Thermogravimetric analysis (TGA)

Thermogravimetric analysis was conducted to investigate thermal degradation temperature and purity of materials. The Thermogravimetric curve show wt% loss vs temperature. The oxidation of carbon took place at the point where a dip in curve occurs. Weight loss in materials would continue to occur till all the carbon is oxidize and left behind a residue of metal catalyst. Figure 4-17 shows the behavior of CNT-supported Cu<sub>2</sub>O loaded nanoparticles. It can be seen that 10%Cu<sub>2</sub>O loaded CNT has a wide decline in weight fraction due to the high percentage of carbon contained in the sample. This decline occurs near dip around 450°C and continue to increase with the rise in temperature. By increasing Cu<sub>2</sub>O loading we experienced less drop in the weight fraction which clearly indicated better encapsulation of Cu<sub>2</sub>O nanoparticles in CNT and also goes to early oxidation of 420°C as compared to 10% Cu<sub>2</sub>O supported catalyst. Early degradation of higher loaded Cu<sub>2</sub>O over CNT has lower stability but better encapsulation as compared to a lower loading of Cu<sub>2</sub>O. Lower loading has more stability but less encapsulation of Cu<sub>2</sub>O in carbon planes.

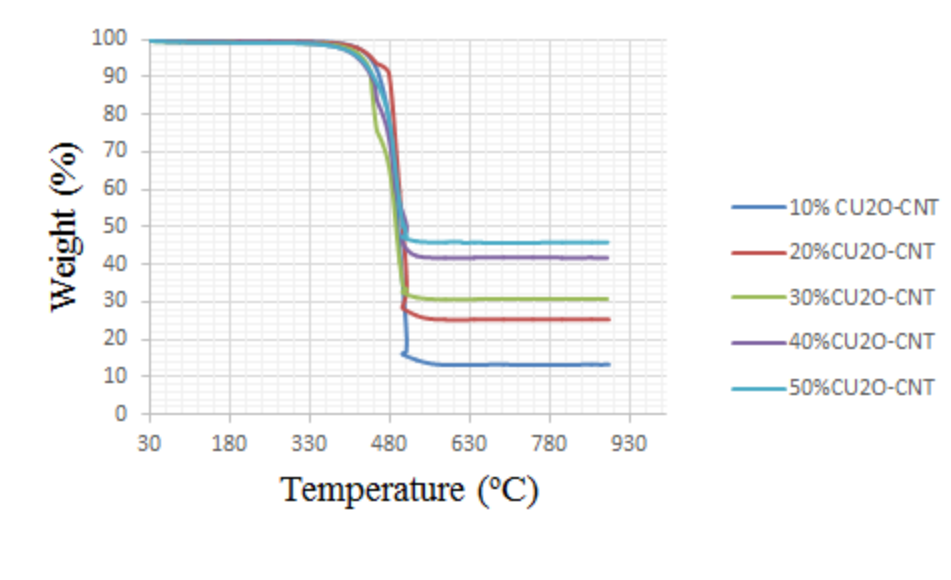


Figure 4-17: Thermogravimetric curves for Cu<sub>2</sub>O supported CNT catalysts

#### 4.1.5 Raman Spectroscopy

It is essential to investigate the location of impregnated metal oxides on carbon nanotubes. Raman spectroscopy is used to identify the site of metal oxide on carbon nanotubes based on the vibrational mode of molecules. We experienced two main peaks in carbon nanotubes sample around  $1350\text{ cm}^{-1}$  and  $1575\text{ cm}^{-1}$ . CuO and Cu<sub>2</sub>O supported carbon nanotube samples also have same peaks around  $1350\text{ cm}^{-1}$  corresponding to the D-band defects on the surface of carbon nanotube. D band represents disorder vibrations on the graphite wall of the carbon nanotube. While another peak around  $1575\text{ cm}^{-1}$  represents G-band, a symmetrical surface on graphite and originates from ordered structure.[104], [105]

CNT supported both cupric oxides and cuprous oxide did not show any peak of impregnated particles in a spectral range which confirms that cupric oxides and cuprous oxide do not have vibrational modes analyzed by Raman spectroscopy.[106]

The ratio of intensity D-band to G-band ( $I_d/I_g$ ) correspond to the defect density on carbon nanotube sample. The ratio of intensity ( $I_d/I_g$ ) for carbon nanotube sample is 1.16 which goes to decrease for impregnated carbon nanotube samples. This decrease in intensity ratio validates anchoring of nanoparticles of CuO and Cu<sub>2</sub>O on defects rather than smooth and order surface of the carbon nanotube.  $I_d/I_g$  ratio of Cu<sub>2</sub>O and CuO loaded CNTs were 0.85 and 0.96 respectively Similar, trends were observed in these studies [107]–[109]

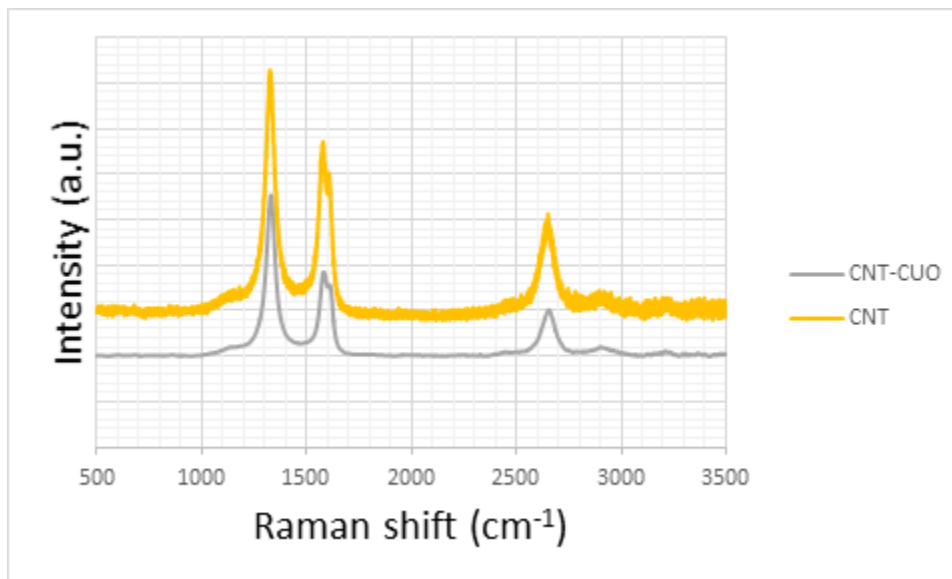


**Figure 4-18: Raman spectra of CuO supported CNT catalysts**

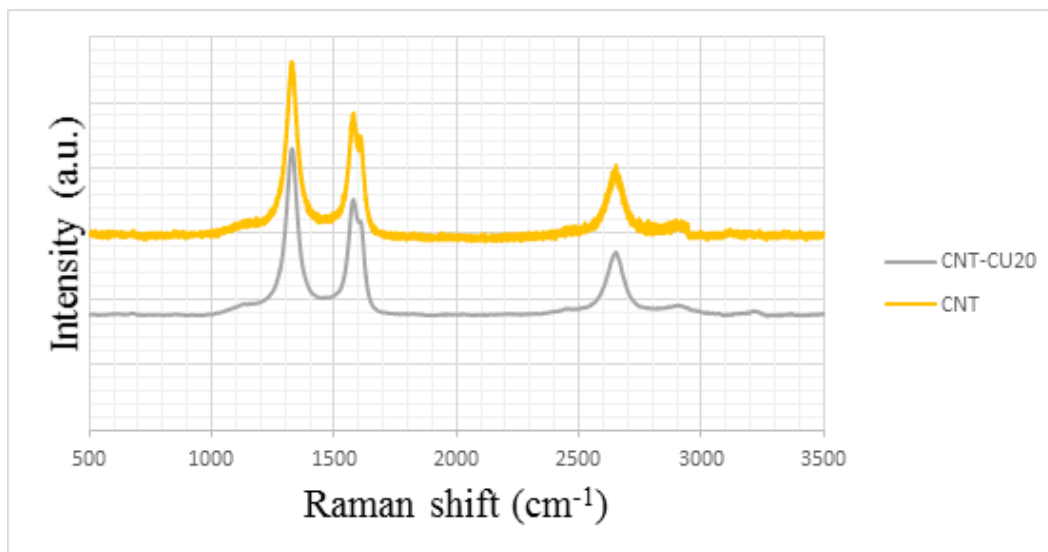


Figure 4-19: Raman spectra of  $\text{Cu}_2\text{O}$  supported CNT catalysts

#### 4.1.6 $\text{N}_2$ adsorption isotherms

Figure 4-20 showed  $\text{N}_2$  adsorption-desorption isotherms for carbon nanotube sample. We recorded isotherms for 10 and 20 % cuprous oxide loaded CNTs. All these isotherms were typical type 3 adsorption model according to IUPAC system. BET surface areas for pure sample and  $\text{Cu}_2\text{O}$  loaded CNT range from 146 to 165 ( $\text{m}^2/\text{g}$ ). The average crystallite size of the  $\text{Cu}_2\text{O}$  particles varied from 10nm to 50 nm depending upon loading of cuprous oxide range i.e. 10 to 50 % on CNT. The particle size measurement by TEM was in agreement with XRD analysis. The increase in  $\text{Cu}_2\text{O}$  loading had increased the particle size and decreased the pore volume and surface area. This increase in particle size reduced catalytic activity. Better trade between optimum loading and particle size would effectively increase surface properties to reduce  $\text{CO}_2$ .

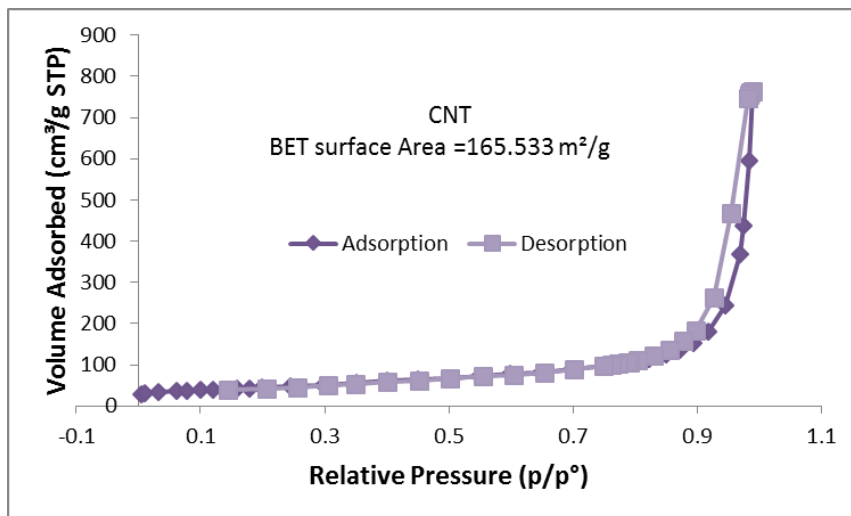
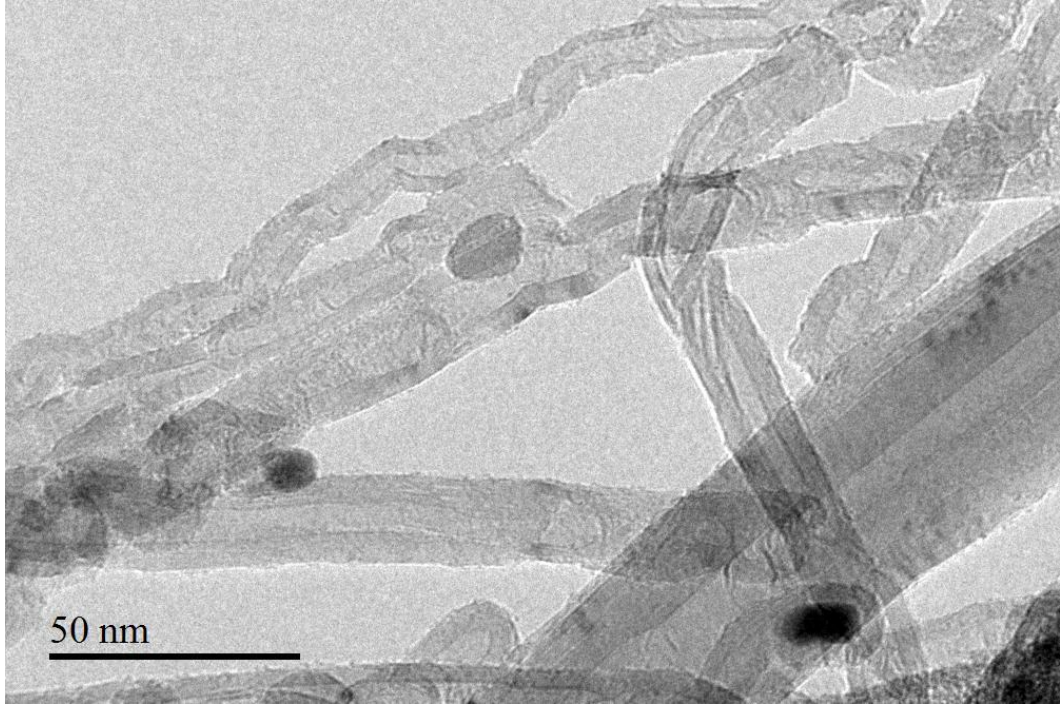


Figure 4-20: Adsorption-desorption isotherm for CNT without loading

#### 4.1.7 Transmission electron microscopy (TEM)

Tubes like structure of carbon nanotubes, 10-20 nm outer diameter (OD) of tube is clearly visible in TEM images of all samples from Figure 4-21 to Figure 4-24. Undoubtedly, nanoparticles of CuO and Cu<sub>2</sub>O is visible and in contact with tubes of carbon nanotubes. Nanoparticles of catalyst are uniformly deposited on carbon nanotubes. Uniformity and firm attachment of copper oxide based particles surrounds CNTs is visible in Figure 4-21 and Figure 4-23. However, on further high loading of copper oxides in Figure 4-22 and Figure 4-24 shows that particles tend to form agglomerates and bigger size of particle with clusters attached with CNTs. These agglomerates decrease reaction activity. Nanoparticles size found in all samples has same conformity with the crystal size investigated in XRD analysis which clearly shows good harmony and accordance in both of these characterizations techniques.



**Figure 4-21: TEM image of 10% CuO supported CNT catalyst**

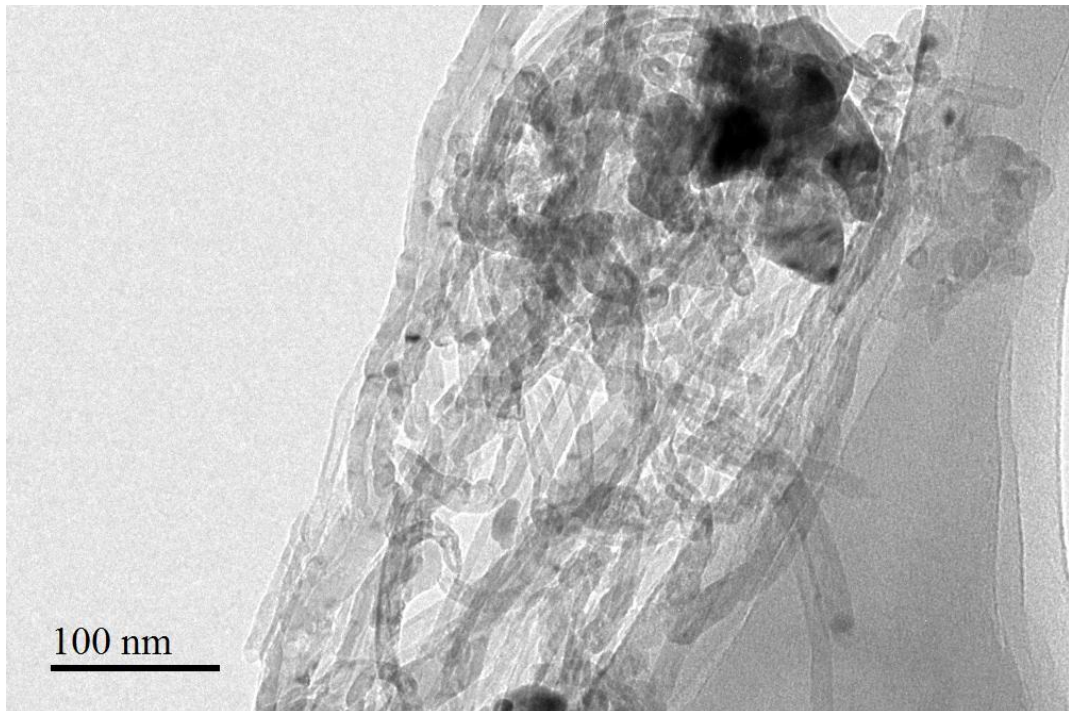


**Figure 4-22: TEM image of 50% CuO supported CNT catalyst**

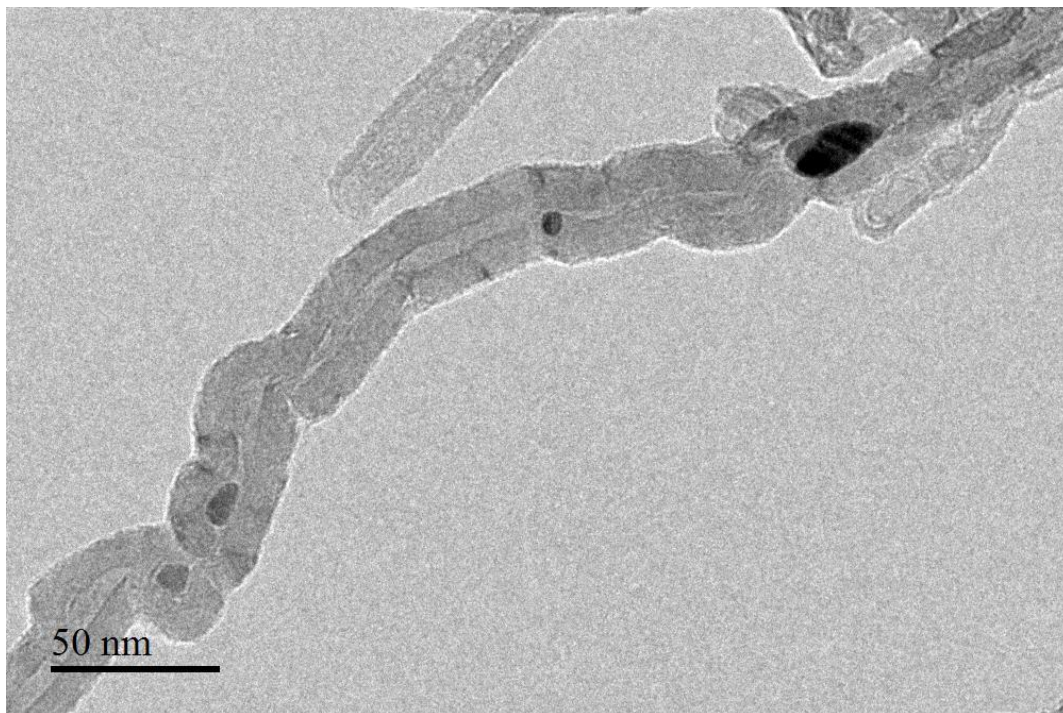


**Figure 4-23: TEM image of 10% Cu<sub>2</sub>O supported CNT catalyst**

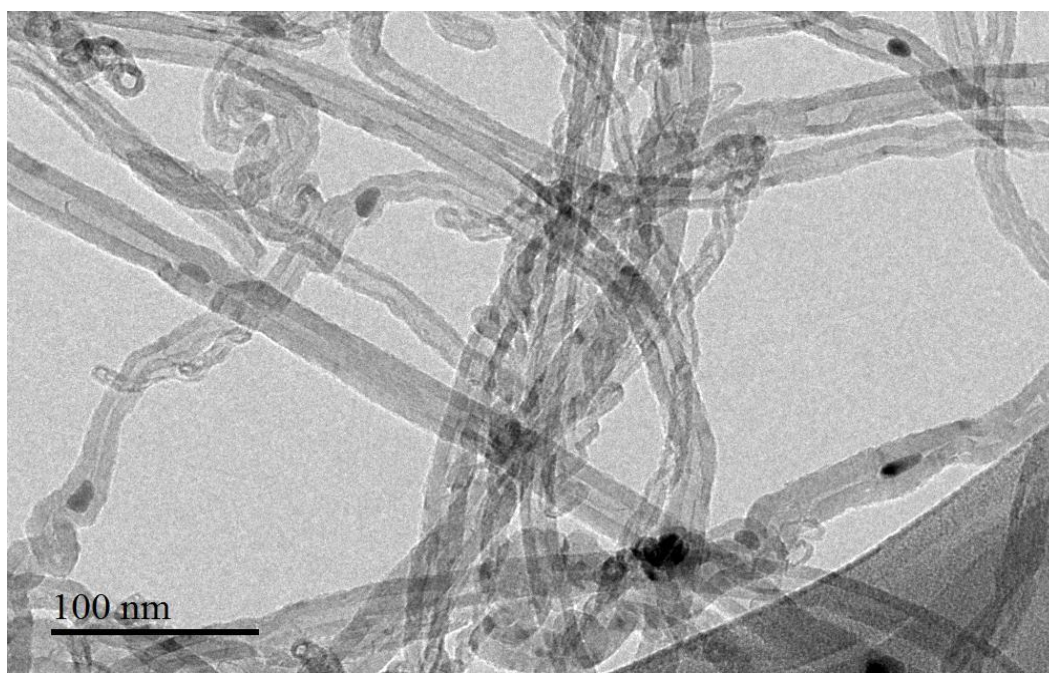


**Figure 4-24: TEM image of 50% Cu<sub>2</sub>O supported CNT catalyst**

## 4.2 Linear sweep voltammetry for carbon nanotubes loaded Cu<sub>2</sub>O based electrocatalyst

Linear sweep voltammetry results show that current density depends upon loading of cuprous oxide catalyst on the surface of CNT. Figure 4-25 shows that 30% Cu<sub>2</sub>O loaded carbon nanotubes displays a significant rise in current density starting at -0.2 V vs. (Ag/AgCl) reference electrode.

Values of current density for different loading of Cu<sub>2</sub>O (10 to 50 %) recorded from -0.2 V to -1.8 V (Ag/AgCl). Highest recorded current density for 30% Cu<sub>2</sub>O loaded CNTs suggest that 30% is the most optimized loading of Cu<sub>2</sub>O over CNT and relatively easily reduced CO<sub>2</sub> to the more positive side of potential. Similarly, an increase of active surface area of the catalyst due to CNTs tend to increase the prospect of reactant to consume into products and we noticed a rise in current density until adequate loading of 30%. The presence of Cu<sub>2</sub>O loaded CNTs on Cu foil not only offered reaction sites for CO<sub>2</sub> but also trapped electrons for intermediate radical CO<sub>2</sub><sup>·-</sup> and turns to increase current density. Similarly, Cu<sup>+</sup> in Cu<sub>2</sub>O was stabilized by incorporation of CNTs as support. CNTs not only stabilized Cu<sup>+</sup> but also protect Cu<sup>+</sup> from disproportionate to Cu<sup>2+</sup> and Cu<sup>0</sup>. The absence of reduction peaks were noted in these experiments. Likewise, trends were also reported in the literature[37], [46].

However, further increased in the loading of the catalyst does not have any consequences on current density. This is because of growth in particle sizes which reduced surface area, explained in TEM, SEM and XRD analysis. Enlargement in particle size causes hindrance for reactants to access active sites of the catalyst. Pore blocking less surface

energy to drive reaction on surface due to less surface area and clusters of particles in the high loading of  $\text{Cu}_2\text{O}$  responsible for the reduction in current density. Similar trends were also reported in this literature[17], [46], [110].

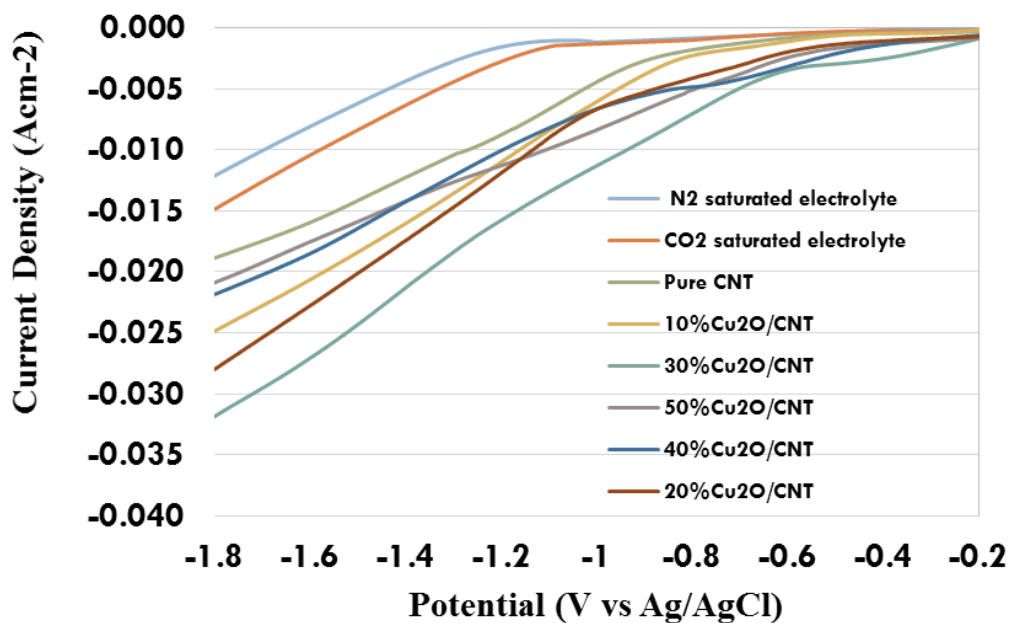


Figure 4-25: LSV profiles for  $\text{Cu}_2\text{O}$  supported CNT in  $\text{CO}_2$  saturated electrolyte

### **4.3 Linear sweep voltammetry for carbon nanotubes loaded CuO based electrocatalyst**

Linear sweep voltammetry analysis recorded for cupric oxide supported CNTs. 20% CuO loaded carbon nanotubes manifested notable rise in current density beginning at -0.2 V (Ag/AgCl). Current density for different loading of CuO (10 to 50 %) achieved from -0.2 V to -1.8 V (Ag/AgCl). Highest accomplished current density for 20% CuO loaded CNT advocate that 20% is the most conducive loading of CuO over CNT and relatively easily reduced CO<sub>2</sub> to the most positive side of potential. Nevertheless, a further degree of loading on catalyst does not have any appreciable current density. This is because large particle sizes which reduced surface area and caused impediment for reactants to access active sites of the catalyst. Pore obstruction and agglomeration of particles in the high loading of CuO are responsible for the reduction in current density. Similar trends were also reported in the literature.[17], [110]

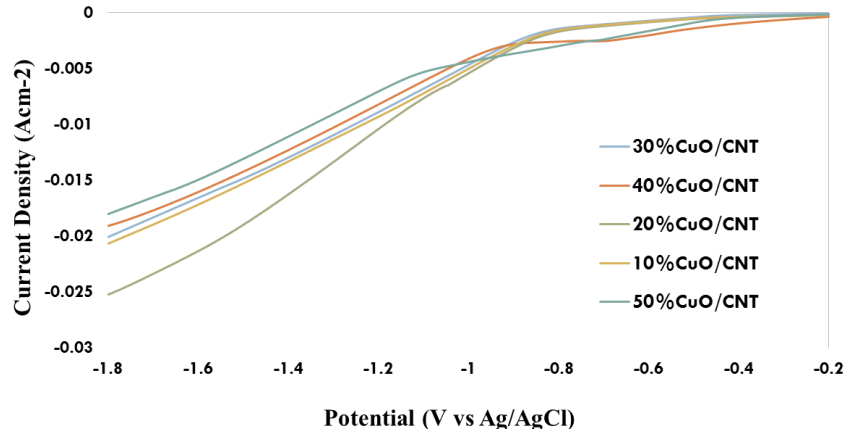


Figure 4-26: LSV profiles for CuO supported CNT in CO<sub>2</sub> saturated electrolyte

### 4.3.1 Comparative analysis of Linear Sweep Voltammetry results based on 30% Copper oxides loading on CNT

Linear sweep voltammetry showed that all tested catalyst have displayed activity to reduce CO<sub>2</sub> efficiently. Loading of catalyst on CNT has a significant influence on the performance of the catalyst. Catalyst formulated with 30 % Cu<sub>2</sub>O loading and 20% CuO are best among all tested catalysts. In Figure 4-27, it is showed that 30% Cu<sub>2</sub>O impregnated CNT have the excellent and most desirable performance to reduce CO<sub>2</sub> as compared to 30% loaded CuO. 30 % Cu<sub>2</sub>O loaded catalyst has highest current density from inception of potential

-0.2 to -1.8 and impart optimum active sites for CO<sub>2</sub> reduction.

Reduction of Cu<sup>+1</sup> to Cu is more difficult than Cu<sup>+2</sup> to Cu [69], [111]. This rise in current density was due to the stability of Cu<sup>+1</sup> with the support of CNT. For example, current

density for 30% Cu<sub>2</sub>O loaded CNT and 20% loaded CuO were 0.032mA/cm<sup>-2</sup> and 0.025 A/cm<sup>-2</sup> at -1.8V respectively. Hence, CNT- loaded - Cu<sub>2</sub>O allow 28% more current density than CNTs loaded with CuO.

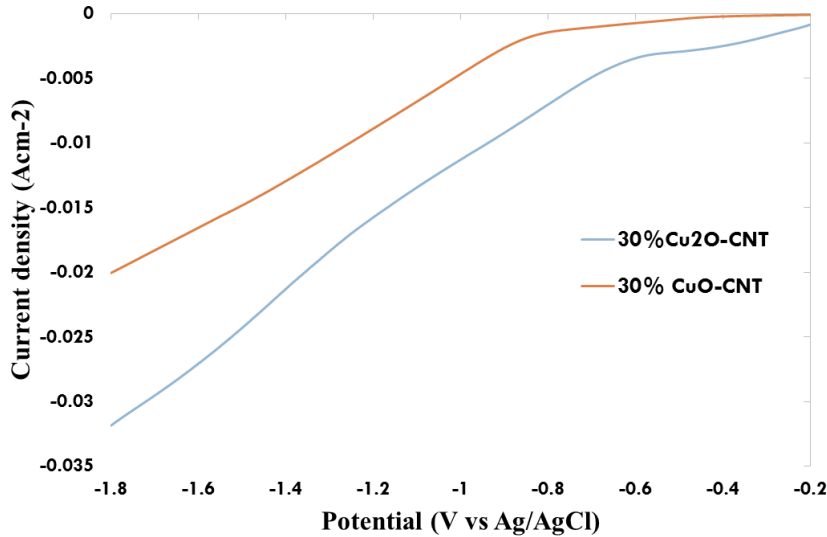


Figure 4-27: LSV profiles for CNT loaded with 30% Cu<sub>2</sub>O and CuO in CO<sub>2</sub> saturated electrolyte

#### 4.4 Faradic Efficiency

CO<sub>2</sub> reduced liquid products were analyzed in GC equipped with FID detector. The internal method of calculation was used to detect the mass of methanol. Later by using formula

$$FE = \frac{n \times F \times m}{I \times t} \dots\dots\dots (4.2)$$

Faradic efficiency was calculated. In above faradic efficiency equation, m is number of moles of methanol formation, F is faraday’s constant, n is number of electrons involved in methanol formation which is 6, I is total current and t is in seconds. FE is actually the

ratio of moles of electron required to form methanol to the total number of moles of electron formed in the process. By multiplying 6 with moles of methanol would give us moles of electron required to produced methanol, while  $\frac{I \times t}{F}$  would give us total number of moles of electron produced in the system.

Figure 4-28 shows that faradic efficiency depends upon potential applied to CO<sub>2</sub> reduction. The highest amount of methanol formation was noticed at the potential of -0.8 V vs Ag/AgCl with the maximum faradic efficiency of 37%. However, faradic efficiency at potentials higher than -1.2 V vs Ag/AgCl was not appreciable. High heat adsorption of faceted Cu<sub>2</sub>O crystal supported CNTs as shown in Figure 4-10, favorably adsorbed intermediates with high active surface area and trapping of electrons in Cu<sub>2</sub>O supported CNTs provides more protons which led the formation of methanol.

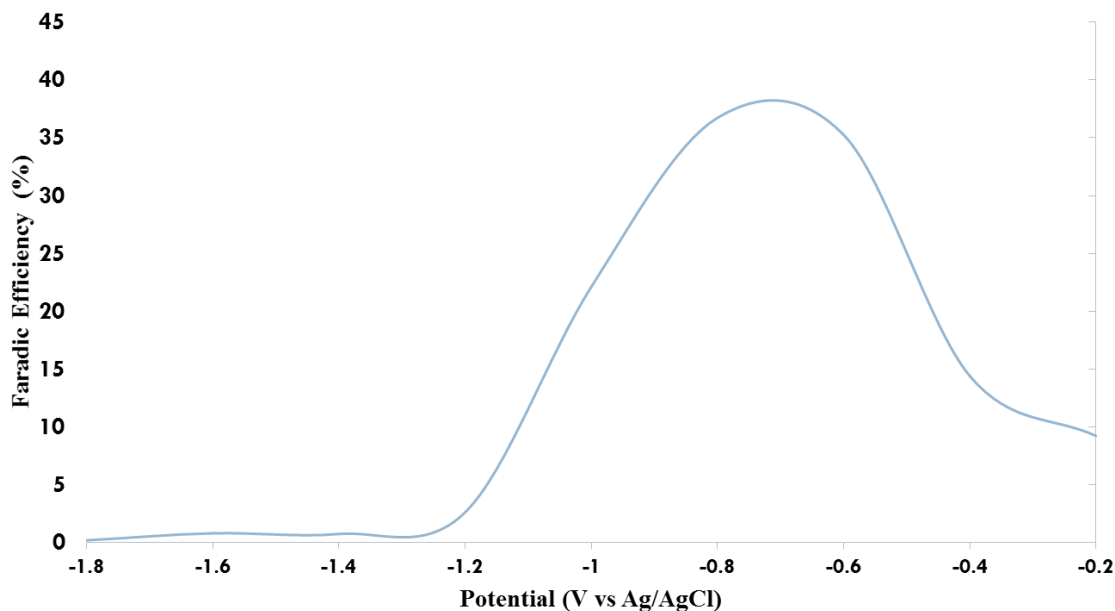


Figure 4-28: Faradic Efficiency of Methanol formation after 1200 seconds

#### 4.4.1 Detailed analysis of Faradic Efficiency results

Cu (I) active sites were proposed by many scientists in electrochemical and photochemical applications. Cuprous oxides in aqueous solution behave in the same way as Cu (I), favorably adsorbed CO and leads to the formation of methanol. Cu(I) species allowed valence band electron to participate in CO adsorption [20], [27], [47], [54], [64], [112].

In the case of the Cu<sub>2</sub>O supported CNTs based electrodes, we can benefit both intermediate stability and coordination of H<sup>+</sup> with surface oxygen defects, which will allow hydrogenation of oxygen in methoxy intermediate rather than carbon of methoxy adsorbate and lead to the formation of methanol. These methoxy intermediates formed by continuous addition of proton and electron to CO<sup>-</sup> species [85]. There is no general understanding on mechanism of methanol formation [27], [33], [35], [113], [114].

A more stable, active and selective catalyst is needed to increase the efficiency of CO<sub>2</sub> reduction process. It has been confirmed that Cu<sub>2</sub>O is the most promising candidate in this regard and Cu (I) species associated with Cu<sub>2</sub>O are active sites for methanol formation. Our first approach was to focus on stabilizing these Cu (I) species on the surface of copper oxides. It is investigated that Cu<sub>2</sub>O supported CNTs have significant performance in hydroxylation and most favorably adsorbed OH<sup>-</sup> [109]. Similarly, the high defect density of CNTs and tight anchoring of Cu<sub>2</sub>O on defects sites of CNTs as showed in Figure 4-19 facilitate electron transferring and protonation on active sites which are responsible for methanol formation.

Numerous properties of CNTs include good compatibility, large surface area, excellent conductivity, modifiable surface, and nanotube structure with the ability to form suspensions in solvents, made CNTs a game changer in a variety of electrochemical applications. CNTs have tubular structure nanomaterials and small diameter with high length to diameter ratio enables them to behave as molecular wire for transferring electron [86].

Higher activity and stability of 30% Cu<sub>2</sub>O supported CNTs are due to the promotion of a large number of electrons on active sites of CNTs. Similarly, the participation of conduction band electrons of Cu<sub>2</sub>O supported CNTs in adsorption of intermediate species also increase current density and favorably increase methanol formation. The hypothesis has been testified by DFT simulation in which we noticed a reduction in band gap of Cu<sub>2</sub>O (2.1 e.V) to 1.78 e.V of Cu<sub>2</sub>O supported CNTs validate involvement of conduction band electrons. Due to the low band gap, electrons jump from valence to the conduction band and actively participate in reactions.

In fact, acceleration of electrons speed up hydrogenation process[115], [116] while at same time favorable adsorption of intermediates leads to the ultimate formation of methanol. Such stable and well-defined structure of CNTs may provide desirable and firm support to cuprous oxide.

#### **4.5 Chronoamperometry Analysis**

To analyze stability of electrode surface, we performed chronoamperometry experiments. Figure 4-29 shows current density vs time response during electrochemical reduction of CO<sub>2</sub> in the presence of different electrocatalysts. In all tested catalysts, fall in current

density was recorded which leads to pseudo steady state values. The reason of early stage fall in current density was unclear, but we reckoned that this early stage degradation of current density is due to physical separation of  $\text{Cu}_2\text{O}$ , which is also reported in the literature.[68]. 30%  $\text{Cu}_2\text{O}$  loaded CNTs exhibit higher activity and stability to reduce  $\text{CO}_2$ . This is in agreement with LSV results, for example, the current density of 30%  $\text{Cu}_2\text{O}$  loaded CNTs starts at  $-0.0075\text{Acm}^{-2}$  and reduce to  $-0.006\text{Acm}^{-2}$ . After that there was negligible change experienced in current density. The electrolyte solution was clear and transparent after 1200 seconds and no insignificant side reactions were occurring in solution. These results show that  $\text{Cu}_2\text{O}$  based catalysts were stable for at least 1200 seconds.

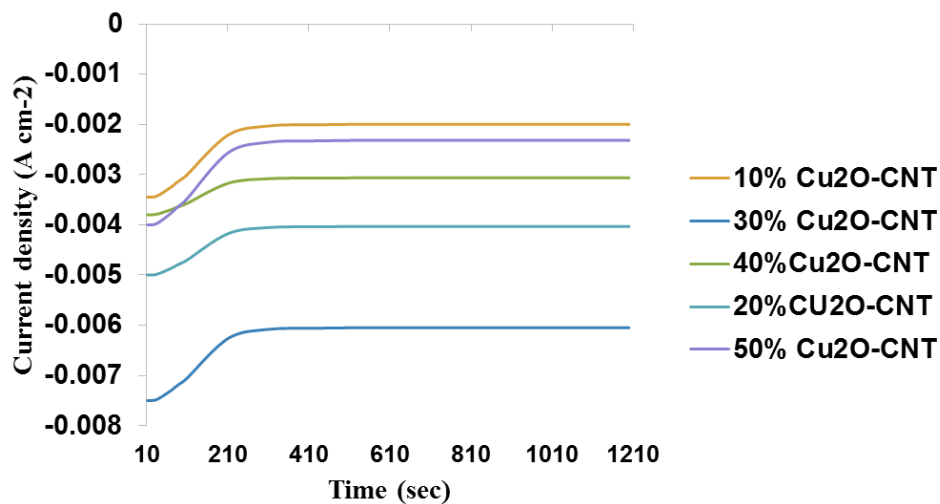


Figure 4-29: Current responses for  $\text{Cu}_2\text{O}$  supported CNTs at constant potential in  $\text{CO}_2$  saturated electrolyte

## CHAPTER 5

### Density Functional Theory

#### 5.1. Quantum Mechanical Modeling

We used density functional theory (DFT) and time dependent DFT quantum mechanical techniques to simulate the complex semiconductor. For the past 30 years, density functional theory has been the principal method for the quantum mechanical simulation of periodic systems. In recent years, it has also been adopted by quantum chemists and is now very extensively used for the simulation of energy surfaces in molecules. The reasons for its admiration and success are:

- 1) The DFT approach is in principle exact.
- 2) It preserves at all levels of approximation the appealing one-electron molecular orbital (MO) view on chemical reactions and properties. The computed orbitals are suitable for the typical MO-theoretical analyses and easy to understand.
- 3) It is a relatively effective computational method, and its fundamental scaling properties do not fail when methodological precision is increased, in particular, when a more accurate XC functional is applied.

## 5.2. The Kohn-Sham molecular orbital (MO) model

The fundamental assumption in Kohn–Sham density functional theory (KS-DFT) is that we can use a single electron calculation to “n” interacting electrons. It can be done by applying appropriate local potential  $V_{XC}(r)$ , external potentials  $V_{ext}(r)$  and the Coulomb potential of the electron cloud  $V_C(r)$ , then using Eq. (1)

$$\left(-\frac{1}{2}\nabla^2 + V_{ext}(r) + V_C(r) + V_{XC}(r)\right)\phi_i(r) = \varepsilon_i\phi_i(r) \quad (5.1)$$

The potential  $V_{XC}$  is the functional derivative with respect to the density ( $\rho$ ) of the exchange–and–correlation energy functional  $E_{XC}[\rho]$ . The one-electron molecular orbitals (MOs)  $\phi_i$  with corresponding orbital energies  $\varepsilon_i$  define the exact electronic charge density and give entree to all properties. The (first) derivatives of the energy with respect to nuclear displacements at the end of the self consistent field (SCF) method are used to find stationary points in the energy surface, particularly for the geometry optimization of molecules.

According to Runge-Gross theorem, the external potential individually finds out the density for a given interaction potential. While according to Kohn-Sham assumption, the density of the non-interacting system is equal to the density of an interacting system. The benefit of this notion is that, the wave function of a non-interacting system can be represented as a Slater determinant of single-particle orbitals, each of which are determined by a single partial differential equation in three variable. Then, the time-dependent (TD) Kohn–Sham equations are:

$$i \frac{\partial}{\partial t} \varphi_i(r, t) = \left( -\frac{\nabla^2}{2} + V[\rho](r, t) \right) \varphi_i(r, t) \quad (5.2)$$

$$\rho(r, t) = \sum n_j |\varphi_i(r, t)|^2 \quad (5.3)$$

The potential (V) includes the  $V_C(r)$ , the nuclear potential,  $V_{ext}(r)$  and  $(X_C)$ , all are functions of time KS-TDDFT technique with solvent effect is used to calculate the excitation energies ( $E_{ex}$ ) in DFT.

### 5.3. Simulation Method

$Cu_2O$  and  $Cu_2O$  loaded CNTs geometries were optimized by considering Hartree fork model and triple- $\zeta$  polarization basis function. In all the calculations, the relativistic effects were taken into account by the zero order regular approximation (ZORA) Hamiltonian in its spin orbit approximation. The optimizer structures of  $Cu_2O$  and  $Cu_2O$ -CNT are shown in Figure 5-1.

**Table 5-1: Calculated Band gaps for  $Cu_2O$  and  $Cu_2O$  supported CNTs**

Sr No	System	Band Gap (eV)
1	$Cu_2O$	2.10
2	$Cu_2O$ -CNT	1.78

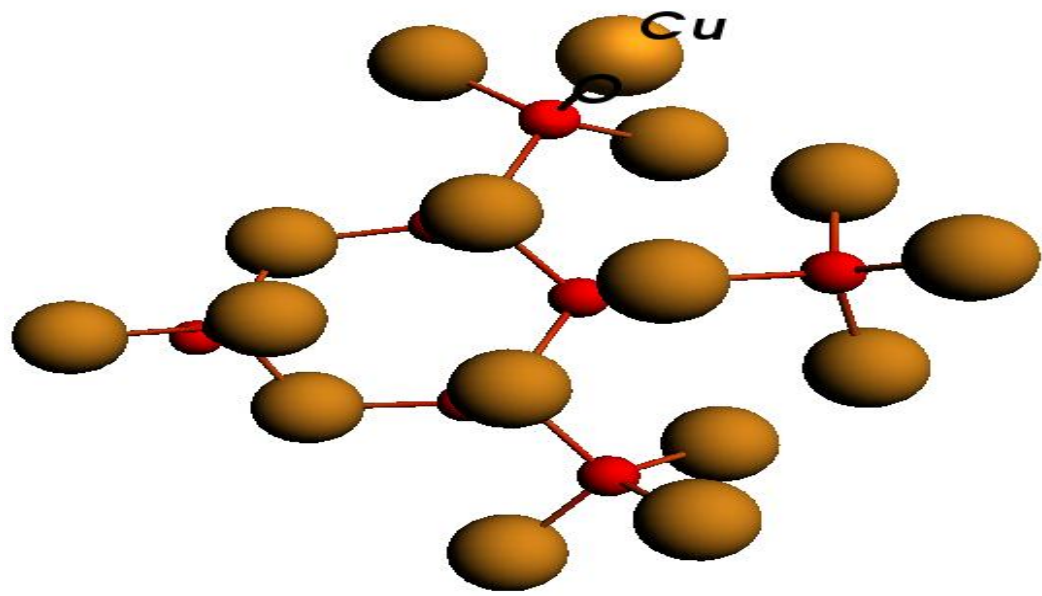


Figure 5-1: Optimized structure of Cuprous oxide (Cu<sub>2</sub>O) P type semiconductor

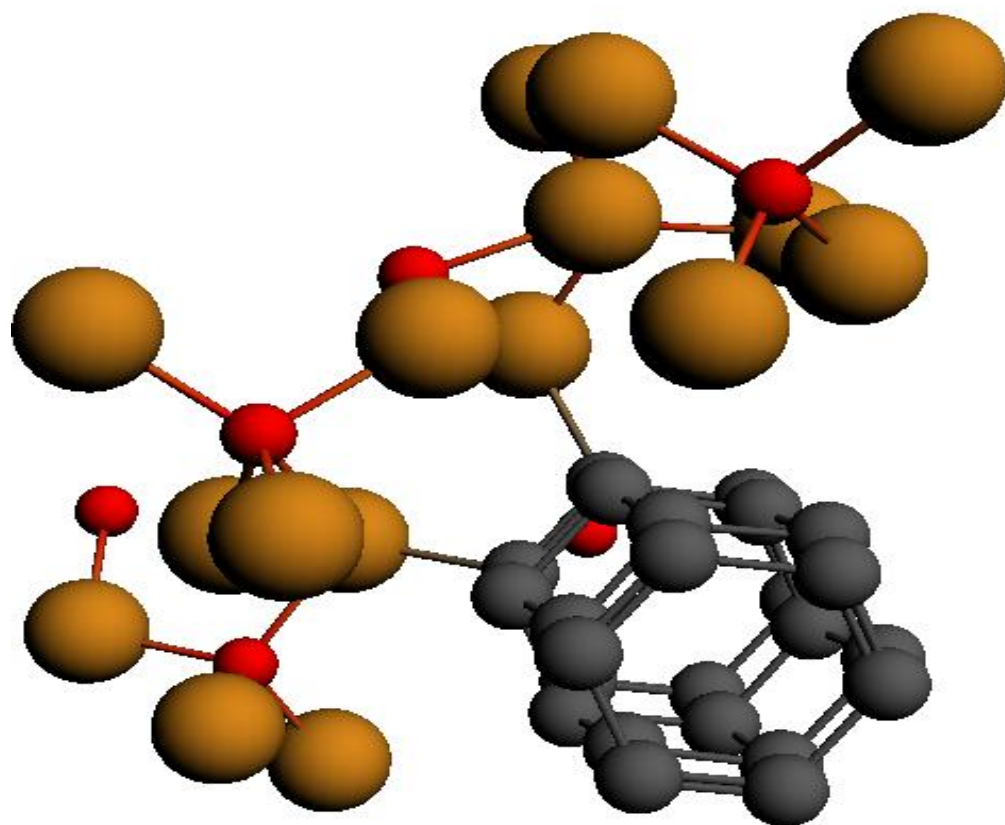


Figure 5-2: Optimized structure of Cu<sub>2</sub>O supported carbon nanotube

## Chapter 6

### Conclusion & Recommendations

#### 6.1 Conclusion

This study discusses the relationship between surface chemistry and catalyst behavior of copper oxides impregnated on carbon nanotubes in CO<sub>2</sub> electrochemical reduction. Linear sweep voltammetry and chronoamperometry results proposed that current density and stability of Cu<sub>2</sub>O loaded carbon nanotubes is remarkably higher. Experimental results also indicate the dynamic role of a carbon nanotubes. Catalyst tested with 30 % cuprous oxide (Cu<sub>2</sub>O) loading CNTs was efficient and has the excellent performance to reduce CO<sub>2</sub>. Loading of copper oxides on carbon nanotubes have the significant influence on the performance of the catalyst. Cuprous oxide (Cu<sub>2</sub>O) supported CNTs enhanced surface area, uniformity and stability of electrode. Firm attachment of cuprous oxide (Cu<sub>2</sub>O) sites on defects of carbon nanotubes facilitated electron transferring on working electrode surface, it also favors adsorption of CO<sub>2</sub> due to the involvement of conduction band electrons. 30% Cu<sub>2</sub>O loaded CNTs is adequate metal oxide loading and provide a tradeoff between active sites to reduce CO<sub>2</sub> efficiently and the size of particle. Higher loading of Cu<sub>2</sub>O reduces activity of catalyst due to agglomeration of a particle. Stability of Cu<sub>2</sub>O loaded CNTs is a key factor to make the process efficient.

## 6.2 Recommendations

A new designed electrochemical cell could be designed for high - pressure reaction condition to increase the solubility of CO<sub>2</sub> in the electrolyte.

Stability and geometry of electrocatalyst strongly affect agglomeration of particle and electron movements on the surface. Therefore, potential support would be required for electrocatalyst.

Density functional theory (DFT) computational chemistry tool can be used to calculate band gap, adsorption energy and binding energy of surface and intermediate.

More advance GC-MS system would be better to analyze all liquid and gas phase products.

## References

- [1] M. Ball and M. Wietschel, “The future of hydrogen – opportunities and challenges☆,” *Int. J. Hydrogen Energy*, vol. 34, no. 2, pp. 615–627, Jan. 2009.
- [2] G. Centi and S. Perathoner, “Opportunities and prospects in the chemical recycling of carbon dioxide to fuels,” *Catal. Today*, vol. 148, no. 3–4, pp. 191–205, Nov. 2009.
- [3] I. Omae, “Recent developments in carbon dioxide utilization for the production of organic chemicals,” *Coord. Chem. Rev.*, vol. 256, no. 13–14, pp. 1384–1405, Jul. 2012.
- [4] M. Conte, “ENERGY | Hydrogen Economy,” in *Encyclopedia of Electrochemical Power Sources*, G. Editor-in-Chief: Jürgen, Ed. Elsevier, 2009, pp. 232–254.
- [5] G. A. Olah, A. Goepfert, and G. K. S. Prakash, *Beyond Oil and Gas: The Methanol Economy: Second Edition*. Wiley-VCH Verlag GmbH & Co. KGaA, 2009.
- [6] P. Sabatier and J. B. Senderens, “New Synthesis of Methane,” *Comptes Rendus l’Académie des Sci. Paris*, vol. 134, p. 1902, 1902.
- [7] W. Paik, T. N. Andersen, and H. Eyring, “Kinetic studies of the electrolytic reduction of carbon dioxide on the mercury electrode,” *Electrochim. Acta*, vol. 14, no. 12, pp. 1217–1232, 1969.
- [8] K. W. Frese and D. Canfield, “Reduction of CO on n-GaAs Electrodes and Selective Methanol Synthesis,” *J. Electrochem. Soc.*, vol. 131, no. 11, pp. 2518–2522, 1984.
- [9] J. J. Kim, D. P. Summers, and K. W. Frese, “Reduction of CO<sub>2</sub> and CO to methane on Cu foil electrodes,” *Journal of Electroanalytical Chemistry and Interfacial Electrochemistry*, vol. 245, pp. 223–244, 1988.
- [10] Y. Hori, K. Kikuchi, and S. Suzuki, “Production of CO and CH<sub>4</sub> in electrochemical reduction of CO<sub>2</sub> at metal electrodes in aqueous hydrogencarbonate solution,” *Chem. Lett.*, vol. 14, no. 11, pp. 1695–1698, 1985.
- [11] Daniel W. Rytz and Alfons Baiker\*, “Partial Oxidation of Methane to Methanol in a Flow Reactor at Elevated Pressure,” *Ind. Eng. Chem.*, pp. 2287–2292, 1991.

- [12] Y. Hori, H. Wakebe, T. Tsukamoto, and O. Koga, "Electrocatalytic process of CO selectivity in electrochemical reduction of CO<sub>2</sub> at metal electrodes in aqueous media," *Electrochim. Acta*, vol. 39, no. 11–12, pp. 1833–1839, Aug. 1994.
- [13] Y. Hori, H. Konishi, T. Futamura, a. Murata, O. Koga, H. Sakurai, and K. Oguma, "'Deactivation of copper electrode' in electrochemical reduction of CO<sub>2</sub>," *Electrochim. Acta*, vol. 50, no. 27, pp. 5354–5369, Sep. 2005.
- [14] D. T. Whipple and P. J. a. Kenis, "Prospects of CO<sub>2</sub> Utilization via Direct Heterogeneous Electrochemical Reduction," *J. Phys. Chem. Lett.*, vol. 1, no. 24, pp. 3451–3458, Dec. 2010.
- [15] Y. Hori and R. Takahashi, "Electrochemical reduction of CO at a copper electrode," *J. Phys. ...*, vol. 5647, no. 97, pp. 7075–7081, 1997.
- [16] M. Le, M. Ren, Z. Zhang, P. T. Sprunger, R. L. Kurtz, and J. C. Flake, "Electrochemical Reduction of CO<sub>2</sub> to CH<sub>3</sub>OH at Copper Oxide Surfaces," *J. Electrochem. Soc.*, vol. 158, no. 5, p. E45, 2011.
- [17] S. Safdar Hossain, S. U. Rahman, and S. Ahmed, "Electrochemical Reduction of Carbon Dioxide over CNT-Supported Nanoscale Copper Electrocatalysts," *J. Nanomater.*, vol. 2014, pp. 1–10, 2014.
- [18] J. Wang, M. Musameh, and Y. Lin, "Solubilization of carbon nanotubes by Nafion toward the preparation of amperometric biosensors.," *J. Am. Chem. Soc.*, vol. 125, no. 9, pp. 2408–9, Mar. 2003.
- [19] G. C. Zhao, L. Zhang, X. W. Wei, and Z. S. Yang, "Myoglobin on multi-walled carbon nanotubes modified electrode: direct electrochemistry and electrocatalysis," *Electrochem. commun.*, vol. 5, pp. 825–829, 2003.
- [20] F. H. Wu, G. C. Zhao, X. W. Wei, and Z. S. Yang, "Electrocatalysis of tryptophan at multi-walled carbon nanotube modified electrode," *Microchim. Acta*, vol. 144, pp. 243–247, 2004.
- [21] C. Cai and J. Chen, "Direct electron transfer of glucose oxidase promoted by carbon nanotubes," *Anal. Biochem.*, vol. 332, pp. 75–83, 2004.
- [22] Y. Y. Sun, K. B. Wu, and S. S. Hu, "Selective determination of dopamine in the presence of high concentration ascorbic acid and uric acid using carbon nanotube modified glassy carbon electrode," *Chem. J. Chinese Univ.*, vol. 23, pp. 2067–2069, 2002.
- [23] M. E. G.-A. Constantinos G.vayenas, Ralph E. white, *Modern Aspects of electrochemistry No 42*. Springer, 2008.

- [24] K. Klier, "Methanol Synthesis," *Adv. Catal.*, vol. 31, no. C, pp. 243–313, 1982.
- [25] Lee et al, "A Comparative study of methanol synthesis from CO<sub>2</sub>/H<sub>2</sub> and CO/H<sub>2</sub> over Cu/ZnO/Al<sub>2</sub>O<sub>3</sub> Catalyst," *J. Catal.*, vol. 144, pp. 414–424, 1993.
- [26] S. T. King, "Reaction mechanism of oxidative carbonylation of methanol to dimethyl carbonate in Cu-Y zeolite," *J. Catal.*, vol. 161, no. 0215, pp. 530–538, 1996.
- [27] X. Liu, G. Lu, Z. Yan, and J. Beltramini, "Recent advances in catalysts for methanol synthesis via hydrogenation of CO and CO<sub>2</sub>," *Ind. Eng. ...*, vol. 42, no. 25, pp. 6518–6530, 2003.
- [28] W. X. Pan, R. Cao, D. L. Roberts, and G. L. Griffin, "Methanol synthesis activity of CuZnO catalysts," *J. Catal.*, vol. 114, no. 2, pp. 440–446, 1988.
- [29] P. Rasmussen, P. Holmblad, and T. Askgaard, "Methanol synthesis on Cu (100) from a binary gas mixture of CO<sub>2</sub> and H<sub>2</sub>," *Catal. Letters*, vol. 26, pp. 373–381, 1994.
- [30] P. S. T.S. Askgaard, J.K. Norskov, C.V. Ovesen, "A kinetic Model of Methanol synthesis," *J. Catal.*, vol. 156, no. 2, pp. 229–242, 1995.
- [31] D. Jingfa, S. Qi, Z. Yulong, C. Songying, and W. Dong, "A novel process for preparation of a Cu/ZnO/Al<sub>2</sub>O<sub>3</sub> ultrafine catalyst for methanol synthesis from CO<sub>2</sub> + H<sub>2</sub>: comparison of various preparation methods," *Appl. Catal. A Gen.*, vol. 139, no. 1–2, pp. 75–85, 1996.
- [32] I. P. Composition, P. Finn, J. B. Bulko, and H. E. T. Al, "Catalytic Synthesis of Methanol from CO / H<sub>2</sub>, of oxygenated products from carbon mon- ponents . The disadvantages of the Cu / significant :," *J. Catal.*, vol. 56, no. 3, pp. 407–429, 1979.
- [33] S. Bailey, G. F. Froment, J. W. Snoeck, and K. C. Waugh, "A DRIFTS study of the morphology and surface adsorbate composition of an operating methanol synthesis catalyst," *Catal. Letters*, vol. 30, no. 1–4, pp. 99–111, 1994.
- [34] K. Klier, V. Chatikavanij, R. G. Herman, and G. W. Simmons, "Catalytic synthesis of methanol from CO/H<sub>2</sub> , The effects of carbon dioxide," *J. Catal.*, vol. 74, no. 2, pp. 343–360, 1982.
- [35] J. Ñ. Nakamura, Y. Choi, and T. Fujitani, "On the issue of the active site and the role of ZnO in Cu / ZnO methanol synthesis catalysts," *Top. Catal.*, vol. 22, no. April, pp. 277–285, 2003.

- [36] M. V. Twigg and M. S. Spencer, "Deactivation of supported copper metal catalysts for hydrogenation reactions," *Appl. Catal. A Gen.*, vol. 212, no. 1–2, pp. 161–174, 2001.
- [37] M. T. S. U. H. Le, "ELECTROCHEMICAL REDUCTION OF CO<sub>2</sub> TO METHANOL," 2011.
- [38] M. Jayamurthy and S. Vasudevan, "Methanol-to-gasoline(MTG)conversion over ZSM-5. A temperature programmed surface reaction study," *Catal. Letters*, vol. 36, no. 1–2, pp. 111–114, 1996.
- [39] K. S. Udupa, G. S. Subramanian, and H. V. K. Udupa, "The electrolytic reduction of carbon dioxide to formic acid," *Electrochim. Acta*, vol. 16, no. 9, pp. 1593–1598, 1971.
- [40] D. P. Summers, S. Leach, and K. W. Frese, "The electrochemical reduction of aqueous carbon dioxide to methanol at molybdenum electrodes with low overpotentials," *J. Electroanal. Chem. Interfacial Electrochem.*, vol. 205, no. 1–2, pp. 219–232, 1986.
- [41] M. Azuma, K. Hashimoto, M. Watanabe, and T. Sakata, "Electrochemical reduction of carbon dioxide to higher hydrocarbons in a KHCO<sub>3</sub> aqueous solution," *J. Electroanal. Chem. Interfacial Electrochem.*, vol. 294, no. 1–2, pp. 299–303, 1990.
- [42] R. L. Cook, "On the Electrochemical Reduction of Carbon Dioxide at In Situ Electrodeposited Copper," *J. Electrochem. Soc.*, vol. 135, no. 6, p. 1320, 1988.
- [43] S. Kaneco, K. Iiba, N. Hiei, K. Ohta, T. Mizuno, and T. Suzuki, "Electrochemical reduction of carbon dioxide to ethylene with high Faradaic efficiency at a Cu electrode in CsOH/methanol," *Electrochim. Acta*, vol. 44, no. 26, pp. 4701–4706, 1999.
- [44] K. O. Satoshi Kaneco, Nobu-hide Hiei, Yue Xing, Hideyuki Katsumata, Hisanori Ohnishi, Tohru Suzuki, "High-efficiency electrochemical CO<sub>2</sub>-to-methane reduction method using aqueous KHCO<sub>3</sub> media at less than 273 K," *J. Solid State Electrochem.*, vol. 7, no. 3, pp. 152–156, 2003.
- [45] Satoshi Kaneco, Kenji Iiba, Kiyohis, "Electrochemical CO<sub>2</sub> Reduction on a Copper Wire Electrode in Tetraethylammonium Perchlorate Methanol at Extremely Low Temperature," *Energy Sources*, vol. 21, no. 7, pp. 643–648, 1999.
- [46] J. C. S. Wu, H. M. Lin, and C. L. Lai, "Photo reduction of CO<sub>2</sub> to methanol using optical-fiber photoreactor," *Appl. Catal. A Gen.*, vol. 296, no. 2, pp. 194–200, 2005.

- [47] K. M. M. Saito, "Development of high performance Cu/ZnO-based catalysts for methanol synthesis and the water-gas shift reaction," *Catal. Surv. Asia*, vol. 8 (4), no. 4, pp. 285–294, 2004.
- [48] K. Kabra, R. Chaudhary, and R. L. Sawhney, "Treatment of Hazardous Organic and Inorganic Compounds through Aqueous-Phase Photocatalysis: A Review," *Ind. Eng. Chem. Res.*, vol. 43, no. 24, pp. 7683–7696, 2004.
- [49] A. Fujishima, "Hydrogen Production under Sunlight with an Electrochemical Photocell," *J. Electrochem. Soc.*, vol. 122, no. 11, p. 1487, 1975.
- [50] B. Aurian-Blajeni, M. Halmann, and J. Manassen, "Electrochemical measurement on the photoelectrochemical reduction of aqueous carbon dioxide on p-Gallium phosphide and p-Gallium arsenide semiconductor electrodes," *Sol. Energy Mater.*, vol. 8, no. 4, pp. 425–440, 1983.
- [51] J. C. Hemminger, R. Carr, and G. a. Somorjai, "The photoassisted reaction of gaseous water and carbon dioxide adsorbed on the SrTiO<sub>3</sub> (111) crystal face to form methane," *Chem. Phys. Lett.*, vol. 57, no. 1, pp. 100–104, 1978.
- [52] T. Inoue, A. Fujishima, S. Konishi, and K. H. Photoelectrocatalytic, "Photoelectrocatalytic reduction of Carbon-Dioxide in aqueous suspensions of semiconductor powders," *Nature*, vol. 277, no. 5698, pp. 637–638, 1979.
- [53] K. Hiranot, K. Inoue, and T. Yatsu, "Photocatalysed reduction of CO<sub>2</sub> in aqueous mixed with copper powder," *J. Photochem. Photobiol.*, vol. 64, no. 2, pp. 255–258, 1992.
- [54] I. H. Tseng, W. C. Chang, and J. C. S. Wu, "Photoreduction of CO<sub>2</sub> using sol-gel derived titania and titania-supported copper catalysts," *Appl. Catal. B Environ.*, vol. 37, no. 1, pp. 37–48, 2002.
- [55] K. Ohkawa, Y. Noguchi, S. Nakayama, K. Hashimoto, and A. Fujishima, "Electrochemical reduction of carbon dioxide on hydrogen-storing materials Part 3 . The effect of the absorption electrodes modified with copper of hydrogen on the palladium," *J. Electroanal. Chem.*, vol. 367, pp. 165–173, 1994.
- [56] M. Jitaru, "Electrochemical Carbon Dioxide Reduction - Fundamental and Applied Topics (Review)," *J. Univ. Chem. Technol. Metall.*, vol. 42, pp. 333–344, 2007.
- [57] H. Noda, S. Ikeda, Y. Oda, and K. Ito, "Potential dependencies of the products on electrochemical reduction of carbon dioxide at a copper electrode.," *Chemistry Letters*, no. 2, pp. 289–292, 1989.

- [58] K. Ohkawa, Y. Noguchi, and S. Nakayama, "Electrochemical reduction of carbon dioxide on hydrogen-storing materials.: Part II. Copper-modified palladium electrode," *J. Electroanal. Chem.*, vol. 348, pp. 459–464, 1993.
- [59] S. Komatsu, M. Tanaka, A. Okumura, and A. Kungi, "PREPARATION OF Cu-SOLID POLYMER ELECTROLYTE COMPOSITE ELECTRODES AND APPLICATION TO GAS-PHASE ELECTROCHEMICAL REDUCTION OF CO<sub>2</sub>," *Electrochim. Acta*, vol. 40, no. 6, pp. 745–753, 1995.
- [60] K. Hara, A. Kudo, and T. Sakata, "Electrochemical reduction of carbon dioxide under high pressure on various electrodes in an aqueous electrolyte," *J. Electroanal. Chem.*, vol. 391, no. 1–2, pp. 141–147, Jul. 1995.
- [61] Y. Nishimura, D. Yoshida, M. Mizuhata, K. Asaka, K. Oguro, and H. Takenaka, "SOLID POLYMER CO<sub>2</sub> REDUCTION," *Energy Convers. Manag.*, vol. 2, pp. 629–632, 1995.
- [62] C. Conversations and M. C. Dioxide, "T. Inui, M. Anpo, K. Izui, S. Yanagida, T. Yamaguchi (Editors)," *Stud. Surf. Sci. Catal.*, vol. 114, pp. 31–42, 1998.
- [63] Y. Terunuma, a. Saitoh, and Y. Momose, "Relationship between hydrocarbon production in the electrochemical reduction of CO<sub>2</sub> and the characteristics of the Cu electrode," *J. Electroanal. Chem.*, vol. 434, no. 1–2, pp. 69–75, 1997.
- [64] K. W. Frese, "Electrochemical Reduction of CO<sub>2</sub> at Intentionally Oxidized Copper Electrodes," *J. Electrochem. Soc.*, vol. 138, no. 11, p. 3338, 1991.
- [65] M. Gattrell, N. Gupta, and a. Co, "A review of the aqueous electrochemical reduction of CO<sub>2</sub> to hydrocarbons at copper," *J. Electroanal. Chem.*, vol. 594, no. 1, pp. 1–19, 2006.
- [66] Y. Hori, "Electrochemical CO<sub>2</sub> Reduction on Metal Electrodes," *Mod. Asp. Electrochem.*, no. 42, pp. 89–189, 2008.
- [67] Y. H. Akira Murata, "Product Selectivity affected by cationic species in Electrochemical reduction of CO<sub>2</sub> and CO at a Cu Electrode," *Chem. Soc. Japan*, vol. 64, no. 1, pp. 123–127, 1991.
- [68] T. Y. Chang, R. M. Liang, P. W. Wu, J. Y. Chen, and Y. C. Hsieh, "Electrochemical reduction of CO<sub>2</sub> by Cu<sub>2</sub>O-catalyzed carbon clothes," *Mater. Lett.*, vol. 63, no. 12, pp. 1001–1003, 2009.
- [69] M. Estrella, L. Barrio, G. Zhou, X. Wang, Q. Wang, W. Wen, J. C. Hanson, A. I. Frenkel, and A. Rodriguez, "In Situ Characterization of CuFe<sub>2</sub>O<sub>4</sub> and Cu / Fe<sub>3</sub>O<sub>4</sub> Water - Gas Shift Catalysts," *J. Phys. Chemistry*, vol. 113, no. C, pp. 14411–14417, 2009.

- [70] Y. Wang, B. Meyer, X. Yin, M. Kunat, D. Langenberg, and F. Traeger, "Hydrogen induced metallicity on the ZnO 10(1)over-bar0) surface," *Phys. Rev. Lett.*, vol. 10, no. 1, p. 2005, 2005.
- [71] K. Ogura, R. Oohara, and Y. Kudo, "Reduction of CO[sub 2] to Ethylene at Three-Phase Interface Effects of Electrode Substrate and Catalytic Coating," *J. Electrochem. Soc.*, vol. 152, no. 12, p. D213, 2005.
- [72] H. Yano, T. Tanaka, M. Nakayama, and K. Ogura, "Selective electrochemical reduction of CO<sub>2</sub> to ethylene at a three-phase interface on copper(I) halide-confined Cu-mesh electrodes in acidic solutions of potassium halides," *J. Electroanal. Chem.*, vol. 565, no. 2, pp. 287–293, 2004.
- [73] K. Ogura, H. Yano, and F. Shirai, "Catalytic Reduction of CO[sub 2] to Ethylene by Electrolysis at a Three-Phase Interface," *J. Electrochem. Soc.*, vol. 150, no. 9, p. D163, 2003.
- [74] S. Ohya, S. Kaneco, H. Katsumata, T. Suzuki, and K. Ohta, "Electrochemical reduction of CO<sub>2</sub> in methanol with aid of CuO and Cu<sub>2</sub>O," *Catal. Today*, vol. 148, no. 3–4, pp. 329–334, 2009.
- [75] Z. Yan, S. Chinta, A. a. Mohamed, J. P. Fackler, and D. W. Goodman, "CO oxidation over Au/TiO<sub>2</sub> prepared from metal-organic gold complexes," *Catal. Letters*, vol. 111, no. 1–2, pp. 15–18, 2006.
- [76] L. C. Grabow and M. Mavrikakis, "Mechanism of Methanol Synthesis on Cu through CO<sub>2</sub> and CO Hydrogenation," *ACS Catal.*, vol. 1, no. 4, pp. 365–384, Apr. 2011.
- [77] J. Horiuti, "Theory of reaction rates as based on the stoichiometric number concept," *Ann. N. Y. Acad. Sci.*, 1973.
- [78] D. J. G. Ives, "Some Abnormal Hydrogen Electrode Reactions," *Can. J. Chem.*, vol. 37, no. 1, pp. 213–221, Jan. 1959.
- [79] A. Takeuchi, "Ethanol Formation Mechanism from CO<sub>2</sub>," *J. phys. Chem.*, vol. 1, no. 6, pp. 2438–2441, 1982.
- [80] E. Andrews, M. Ren, F. Wang, Z. Zhang, P. Sprunger, R. Kurtz, and J. Flake, "Electrochemical Reduction of CO<sub>2</sub> at Cu Nanocluster / (100) ZnO Electrodes," *J. Electrochem. Soc.*, vol. 160, no. 11, pp. H841–H846, Oct. 2013.
- [81] M. Behrens, F. Studt, I. Kasatkin, S. Kuhl, M. Havecker, F. Abild-Pedersen, S. Zander, F. Girgsdies, P. Kurr, B.-L. Kniep, M. Tovar, R. W. Fischer, J. K. Nørskov, and R. Schlogl, "The Active Site of Methanol Synthesis over Cu/ZnO/Al<sub>2</sub>O<sub>3</sub> Industrial Catalysts," *Science*, vol. 336, pp. 893–897, 2012.

- [82] E. Solomon, P. Jones, and J. May, "Electronic structures of active sites on metal oxide surfaces: definition of the copper-zinc oxide methanol synthesis catalyst by photoelectron spectroscopy," *Chem. Rev.*, pp. 2623–2644, 1993.
- [83] Y.-T. Cheng, T.-R. Shan, B. Devine, D. Lee, T. Liang, B. B. Hinojosa, S. R. Phillpot, A. Asthagiri, and S. B. Sinnott, "Atomistic simulations of the adsorption and migration barriers of Cu adatoms on ZnO surfaces using COMB potentials," *Surf. Sci.*, vol. 606, no. 15–16, pp. 1280–1288, Aug. 2012.
- [84] G. Sheffer and T. King, "Potassium's promotional effect of unsupported copper catalysts for methanol synthesis," *J. Catal.*, vol. 387, pp. 376–387, 1989.
- [85] A. a. Peterson, F. Abild-Pedersen, F. Studt, J. Rossmeisl, and J. K. Nørskov, "How copper catalyzes the electroreduction of carbon dioxide into hydrocarbon fuels," *Energy Environ. Sci.*, vol. 3, no. 9, p. 1311, 2010.
- [86] C. Hu and S. Hu, "Carbon Nanotube-Based Electrochemical Sensors: Principles and Applications in Biomedical Systems," *J. Sensors*, vol. 2009, no. iv, pp. 1–40, 2009.
- [87] P. Serp, "Carbon nanotubes and nanofibers in catalysis," *Appl. Catal. A Gen.*, vol. 253, no. 2, pp. 337–358, Oct. 2003.
- [88] A. Khalid, A. A. Al-Juhani, O. C. Al-Hamouz, T. Laoui, Z. Khan, and M. A. Atieh, "Preparation and properties of nanocomposite polysulfone/multi-walled carbon nanotubes membranes for desalination," *Desalination*, vol. 367, pp. 134–144, Jul. 2015.
- [89] F. A. Al-Khalidi, B. Abu-Sharkh, A. M. Abulkibash, M. I. Qureshi, T. Laoui, and M. A. Atieh, "Effect of acid modification on adsorption of hexavalent chromium (Cr(VI)) from aqueous solution by activated carbon and carbon nanotubes," *Desalin. Water Treat.*, pp. 1–13, Mar. 2015.
- [90] L. R. F. Bard, Allen J, "Electrochemical Methods: Fundamentals and Applications, 2nd Edition - Allen J. Bard, Larry R. Faulkner," 2001. [Online]. Available: <http://eu.wiley.com/WileyCDA/WileyTitle/productCd-0471043729.html>. [Accessed: 17-Oct-2015].
- [91] N. Markovic, "Surface science studies of model fuel cell electrocatalysts," *Surf. Sci. Rep.*, vol. 45, no. 4–6, pp. 117–229, Apr. 2002.
- [92] T. J. Schmidt, U. A. Paulus, H. A. Gasteiger, and R. J. Behm, "The oxygen reduction reaction on a Pt/carbon fuel cell catalyst in the presence of chloride anions," *J. Electroanal. Chem.*, vol. 508, no. 1–2, pp. 41–47, Jul. 2001.

- [93] N. Spataru, K. Tokuhira, C. Terashima, T. N. Rao, and A. Fujishima, "Electrochemical reduction of carbon dioxide at ruthenium dioxide deposited on boron-doped diamond," *J. Appl. Electrochem.*, vol. 33, no. 12, pp. 1205–1210, 2003.
- [94] A. Bandi, "Electrochemical Reduction of Carbon Dioxide on Conductive Metallic Oxides," *Journal of The Electrochemical Society*, vol. 137, no. 7. p. 2157, 1990.
- [95] N. Furuya, T. Yamazaki, and M. Shibata, "High performance Ru Pd catalysts for CO<sub>2</sub> reduction at gas-diffusion electrodes," *Journal of Electroanalytical Chemistry*, vol. 431, no. 1. pp. 39–41, 1997.
- [96] K. Hara, a Kudo, and T. Sakata, "Electrochemical CO<sub>2</sub> reduction on a glassy carbon electrode under high pressure," *J. Electroanal. Chem.*, vol. 421, no. 1–2, pp. 1–4, 1997.
- [97] C. H. Kuo, C. H. Chen, and M. H. Huang, "Seed-mediated synthesis of monodispersed Cu<sub>2</sub>O nanocubes with five different size ranges from 40 to 420 nm," *Adv. Funct. Mater.*, vol. 17, no. 18, pp. 3773–3780, 2007.
- [98] S. F. Zheng, J. S. Hu, L. S. Zhong, W. G. Song, L. J. Wan, and Y. G. Guo, "Introducing dual functional CNT networks into CuO nanomicrospheres toward superior electrode materials for lithium-ion batteries," *Chem. Mater.*, vol. 20, no. 11, pp. 3617–3622, 2008.
- [99] S. Gupta and J. Farmer, "Multiwalled carbon nanotubes and dispersed nanodiamond novel hybrids: Microscopic structure evolution, physical properties, and radiation resilience," *J. Appl. Phys.*, vol. 109, no. 1, 2011.
- [100] H. W. Seo, S. Y. Bae, J. Park, H. Yang, K. S. Park, and S. Kim, "Strained gallium nitride nanowires," *J. Chem. Phys.*, vol. 116, no. 21, pp. 9492–9499, 2002.
- [101] J. Hu, Y. Bandog, J. Zhan, C. Zhi, and D. Golberg, "Carbon nanotubes as nanoreactors for fabrication of single-crystalline Mg<sub>3</sub>N<sub>2</sub> nanowires," *Nano Lett.*, vol. 6, no. 6, pp. 1136–1140, 2006.
- [102] L. K. Randeniya, A. Bendavid, P. J. Martin, and C. D. Tran, "Composite yarns of multiwalled carbon nanotubes with metallic electrical conductivity," *Small*, vol. 6, no. 16, pp. 1806–1811, 2010.
- [103] B. Zeng, X. Chen, X. Ning, C. Chen, W. Deng, Q. Huang, and W. Zhong, "Electrostatic-assembly three-dimensional CNTs/rGO implanted Cu<sub>2</sub>O composite spheres and its photocatalytic properties," *Appl. Surf. Sci.*, vol. 276, pp. 482–486, Jul. 2013.

- [104] P. Delhaes, M. Couzi, M. Trinquescoste, J. Dentzer, H. Hamidou, and C. Vix-Guterl, "A comparison between Raman spectroscopy and surface characterizations of multiwall carbon nanotubes," *Carbon N. Y.*, vol. 44, no. 14, pp. 3005–3013, 2006.
- [105] C. A. Cooper, R. J. Young, and M. Halsall, "Investigation into the deformation of carbon nanotubes and their composites through the use of Raman spectroscopy," *Compos. Part A Appl. Sci. Manuf.*, vol. 32, no. 3–4, pp. 401–411, 2001.
- [106] B. H. Lohse, A. Calka, and D. Wexler, "Raman spectroscopy sheds new light on TiC formation during the controlled milling of titanium and carbon," *J. Alloys Compd.*, vol. 434–435, no. SPEC. ISS., pp. 405–409, 2007.
- [107] S. Song and S. Jiang, "Selective catalytic oxidation of ammonia to nitrogen over CuO/CNTs: The promoting effect of the defects of CNTs on the catalytic activity and selectivity," *Appl. Catal. B Environ.*, vol. 117–118, pp. 346–350, 2012.
- [108] S. Ko, J. I. Lee, H. S. Yang, S. Park, and U. Jeong, "Mesoporous CuO particles threaded with CNTs for high-performance lithium-ion battery anodes," *Adv. Mater.*, vol. 24, no. 32, pp. 4451–4456, 2012.
- [109] S. Song, R. Rao, H. Yang, and A. Zhang, "Cu<sub>2</sub>O/MWCNTs Prepared by Spontaneous Redox: Growth Mechanism and Superior Catalytic Activity," *J. Phys. Chem. C*, vol. 114, no. 33, pp. 13998–14003, Aug. 2010.
- [110] K.-R. Lee, J.-H. Lim, J.-K. Lee, and H.-S. Chun, "Reduction of carbon dioxide in 3-dimensional gas diffusion electrodes," *Korean J. Chem. Eng.*, vol. 16, no. 6, pp. 829–836, Nov. 1999.
- [111] X. Wang, J. C. Hanson, A. I. Frenkel, J.-Y. Kim, and J. A. Rodriguez, "Time-resolved Studies for the Mechanism of Reduction of Copper Oxides with Carbon Monoxide: Complex Behavior of Lattice Oxygen and the Formation of Suboxides," *J. Phys. Chem. B*, vol. 108, no. 36, pp. 13667–13673, Sep. 2004.
- [112] H. Slamet and E. Purnama, "Effect of copper species in a photocatalytic synthesis of methanol from carbon dioxide over copper-doped titania catalysts," *World Appl. Sci. ...*, 2009.
- [113] G. R. Sheffer and T. S. King, "Potassium's promotional effect of unsupported copper catalysts for methanol synthesis," *J. Catal.*, vol. 115, pp. 376–387, 1989.
- [114] G. Chinchén and M. Spencer, "Promotion of methanol synthesis and the water-gas shift reactions by adsorbed oxygen on supported copper catalysts," *J. Chem. ...*, 1987.

- [115] H. VU, F. GONCALVES, R. PHILIPPE, E. LAMOUREUX, M. CORRIAS, Y. KIHN, D. PLEE, P. KALCK, and P. SERP, "Bimetallic catalysis on carbon nanotubes for the selective hydrogenation of cinnamaldehyde," *J. Catal.*, vol. 240, no. 1, pp. 18–22, May 2006.
- [116] H. Yang, S. Song, R. Rao, X. Wang, Q. Yu, and A. Zhang, "Enhanced catalytic activity of benzene hydrogenation over nickel confined in carbon nanotubes," *J. Mol. Catal. A Chem.*, vol. 323, no. 1–2, pp. 33–39, May 2010.

## Appendix

### Internal standard method of calibration

The goal of the internal standard method is to accurately investigate the concentration of an analyte in the samples. This method is used for those samples which are not suitable to inject directly into the GC because of below reasons:

- 1) Analytes concentration is too low and they require pre-concentration treatment before injection to the GC.
- 2) When samples are handled and injected into the GC, many losses occurred due to the evaporation.

The internal standard method was used to compensate for these losses. In the internal standard method, a known amount of internal standard is introduced in both standard and in unknown samples. Instead of the base on the absolute response of analyte, calibration uses the ratio of response between the analyte and internal standard.

To construct the calibration curves, a series of standard solutions were prepared. The amount of reference standard with methanol solution at a different concentration ranges were prepared to develop the calibration curve and recorded the response of methanol compared to the internal standard of concentrations. Chromatogram gave us peak area ratios of both methanol and internal standard which helped us to find R (response factor).

R is actually the response of methanol at concentration of internal standard (Cistd). R is the slope of the area ratio of methanol and internal standard to the mass fractions of these samples present in the standard samples. Calibration curve was linear for most of its parts, and its intercept was zero. Investigation of internal standard and methanol in the standard samples were based on retentions times.

After calibration in GC, we analyzed our unknown samples to determine quantity of our analyte (methanol). First the known quantity of internal standard was added in the each unknown samples of 10 ml, then we injected unknown sample by hand syringe in GC and recorded the area ratio of methanol to internal standard.

By comparing the area ratio to mass ratio of each component in unknown sample with R (previously found from calibration curve), we determined mass of methanol in unknown samples.

## Vitae

Name : MUHAMMAD IRFAN MALIK

Nationality : Pakistani

Date of Birth : 09/11/1987

Email : [m.irfanmalik@hotmail.com](mailto:m.irfanmalik@hotmail.com)

Address : Malik Garments, National Hotel Qisa Khawani, P.O. Box  
25000, Peshawar, Pakistan.

Academic Background : BSc Chemical Engineering University of the Punjab  
Pakistan.

M.Sc Chemical Engineering King Fahd University of  
Petroleum and Minerals, Saudi Arabia.

## List of Publications

### Journal Publication:

M. Irfan Malik, B. Abussaud, Z. Malaibari, M. Khalid “Electrochemical reduction of CO<sub>2</sub> under carbon nanotube supported Cu<sub>2</sub>O electrocatalyst”, (underreview) for publication (2015).